

PROCESSING AND CHARACTERIZATION OF
PLASMA SPRAY COATINGS OF
INDUSTRIAL WASTE AND LOW GRADE ORE
MINERAL ON METAL SUBSTRATES

**THESIS SUBMITTED
IN PARTIAL FULFILLMENT OF THE REQUIREMENT FOR THE
DEGREE OF
MASTER OF TECHNOLOGY**

In
Metallurgical & Materials Engineering

By

AJIT BEHERA



**DEPARTMENT OF METALLURGICAL & MATERIALS ENGINEERING
NATIONAL INSTITUTE OF TECHNOLOGY,
ROURKELA, INDIA
MAY, 2012**

PROCESSING AND CHARACTERIZATION OF
PLASMA SPRAY COATINGS OF
INDUSTRIAL WASTE AND LOW GRADE ORE
MINERAL ON METAL SUBSTRATES

**THESIS SUBMITTED
IN PARTIAL FULFILLMENT OF THE REQUIREMENT FOR THE
DEGREE OF
MASTER OF TECHNOLOGY**

In
Metallurgical & Materials Engineering
By
AJIT BEHERA

Under the Guidance of
Prof. S C Mishra



**DEPARTMENT OF METALLURGICAL & MATERIALS ENGINEERING
NATIONAL INSTITUTE OF TECHNOLOGY,
ROURKELA, INDIA
MAY, 2012**

Declaration

I hereby declare that, the work which is being presented in this thesis entitled “Processing And Characterization of Plasma Spray coatings of Industrial Waste and Low Grade Ore mineral on metal substrates” in partial fulfillment of the requirements for the award of M.Tech degree, submitted to the Department of Metallurgical & Materials Engineering, National Institute of Technology, Rourkela, is an authentic record of my own work under the supervision of Prof. S.C. Mishra. I have not submitted the matter embodied in this thesis for the award of any other degree or diploma to any other university or Institute.

Date:22-May-12

Ajit Behera



DEPARTMENT OF METALLURGICAL & MATERIALS ENGINEERING

NATIONAL INSTITUTE OF TECHNOLOGY, ROURKELA

ODISHA, INDIA – 769008.

CERTIFICATE

This is to certify that, the thesis entitled “Processing And Characterization of Plasma Spray coatings of Industrial Waste and Low Grade Ore mineral on metal substrates” being submitted to the National Institute of Technology, Rourkela by Mr. Ajit Behera, Roll no. 210MM1248 for the award of M.Tech degree in Metallurgical & Materials Engineering, is a bonafide record of research work carried out by him under my supervision and guidance.

The candidate has fulfilled all the prescribed requirements. The Thesis which is based on candidate’s own work has not been submitted elsewhere for award of any degree.

In my opinion, the thesis is of standard required for the award of M.Tech degree in Metallurgical & Materials Engineering.

Prof. S.C. Mishra

Supervisor

Department of Metallurgical & Materials Engineering

National Institute of Technology

Rourkela – 769008

Email: subash.mishra@gmail.com

ACKNOWLEDGMENT

I wish to express my sincere gratitude to my supervisor **Prof. S.C. Mishra**, for his guidance, encouragement and support throughout this work and my studies here at N.I.T. Rourkela. His guidance and insight gave me encouragement to proceed with confidence towards the completion of this work. His impressive knowledge, technical skills and human qualities have been a source of inspiration and a model for me to follow.

I am thankful to Prof. B.C. Roy, present Head of the Department of Metallurgical & Materials Engineering Department for providing facilities for smooth conduct of this work. I remain obliged to Dr Alok Satpathy and Dr. S. K. Acharya of Mechanical Engineering Department for their useful suggestions and help rendered to me in carrying out this work. I am also thankful to K. Nayak, of the Mechanical Engineering for the cooperation and help during the time of experimentation.

I am indebted to all my colleagues in the Metallurgy group. Their kindness has made my study in the M.Tech program enjoyable. I would also like to thank the other members of the team, Dr. S.K. Swain (Metallurgical Engg. Dept.), Mr. Ashish Dash (Electrical Engg. Dept.) for extending their technical and personal support. It has been a great pleasure to work with all other talented, creative, helpful and dedicated colleagues.

I am especially grateful to Metallurgical and Mechanical Laboratory supporting staffs without them the work would have not progressed. Thanks are also due to B. Ravi.achari for his help for rapid work.

My heartfelt appreciation goes toward my parents, Mr. Alekha Bihari Behera and Mrs. Urmila Behera who have always provided support and encouragement throughout my education. I would like to thank my younger brother for his friendly support and affection.

Ajit Behera

CONTENTS

	Page No.
CONTENTS	I
ABSTRACT	IV
LIST OF FIGURES	VI
LIST OF TABLES	IX
CHAPTER 1: INTRODUCTION	1
1.1 RESEARCH BACKGROUND	2
1.2 OBJECTIVES OF RESEARCH	6
CHAPTER 2 LITERATURE SURVEY	8
2.1 INTRODUCTORY STATEMENT	9
2.2 SURFACE ENGINEERING	9
2.3 TECHNIQUES OF SURFACE MODIFICATION	10
2.4 THERMAL SPRAYING	11
2.5 PLASMA SPRAYING	14
2.5.1 Requirements for Plasma Spraying	18
2.5.2 Process Parameters in Plasma Spraying	19
2.5.3 Mechanism of Coating Formation in Plasma Spraying Process	22
2.6 INDUSTRIAL APPLICATIONS OF PLASMA SPRAYING	24
2.7 WEAR	26
2.8 TYPES OF WEAR	27
2.8.1 Abrasive wear	27
2.8.2 Adhesive wear	28
2.8.3 Erosive wear	28
2.8.4 Surface fatigue wear	29
2.8.5 Corrosive wear	29
2.9 SYMPTOMS OF WEAR	29
2.10 RECENT TRENDS IN METAL WEAR RESEARCH	30

2.11 WEAR RESISTANT COATINGS	30
2.11.1 Carbide Coatings	31
2.11.2 Oxide Coatings	31
2.11.3 Metallic Coatings	32
2.11.4 Dimond Coatings	32
2.12 UTILIZATION OF FLYASH AS WEAR RESISTANCE COATINGS	33
2.13 EROSION WEAR OF CERAMIC COATINGS	33
CHAPTER 3 EXPERIMENTAL SET UP & METHODOLOGY	35
3.1 INTRODUCTION	36
3.2 DEVELOPMENT OF COATINGS	36
3.2.1 Preparation of Powder	36
3.2.2 Preparation of Substrate	36
3.2.3 Plasma Spray Coating Deposition	36
3.3 CHARACTERIZATION OF FEEDSTOCK	38
3.3.1 Particle Size Analysis	38
3.3.2 Compositional Analysis	38
3.4 CHARACTERIZATION OF COATINGS	38
3.4.1 Scanning Electron Microscopic Studies	38
3.4.2 X-Ray Diffraction Studies	38
3.4.3 Evaluation of Coating Interface Bond Strength	39
3.4.4 Evaluation of Coating Deposition Efficiency	40
3.4.5 Coating Thickness Measurement	40
3.4.6 Hardness Measurement	40
3.4.7 Porosity Measurement	40
3.5 EROSION WEAR BEHAVIOUR OF COATINGS	40
CHAPTER 4 RESULTS AND DISCUSSION	43
4.1 INTRODUCTION	44
4.2 CHARACTERIZATION OF COATING MATERIAL:	44
4.2.1 Particle Size Analysis	44
4.2.2 Chemical Composition Analysis	44

4.2.3 Morphology of powder/raw material for coating	45
4.3 CHARACTERIZATION OF COATINGS	45
4.3.1 Microstructural Study of the Coatings	46
4.3.2 XRD ANALYSIS	48
4.3.5 Coating Adhesion Strength	51
4.3.1 Coating Deposition Efficiency	52
4.3.2 Coating Thickness	54
4.3.3 Hardness of the Coatings	56
4.3.4 Coating Porosity	57
4.3.4 Surface Roughness	58
4.3.6 ANN Prediction of Adhesion Strength	59
4.4 EVALUATION OF COATING PERFORMANCE	65
4.4.1 Erosion Wear Behavior of Coatings	65
4.4.2 Taguchi Experimental Design	65
4.4.5 Microstructural Investigation of Erodants and Eroded Surfaces.	70
4.5 DISCUSSION	72
CHAPTER 5 CONCLUSIONS	73
Scope for Future Work	75
REFERENCES	76
LIST OF PUBLICATIONS	92

Abstract

Emerging portable applications and the rapid advancement of technology have posed rigorous challenges to Metallurgical engineers for development of an efficient material which can sustain for long period at any type of environment. The foremost objectives are to develop required surface properties with economical process. Now-a-days the investigation explores the coating potential of industrial wastes. Fly-ash emerges as a major waste of thermal power plants. It mainly comprises of oxides of silicon, iron, aluminium, and titanium along with some other minor constituents. Fly-ash premixed with quartz and illmenite which are low cost minerals available in plenty are excellent candidates for providing protection against abrasive wear and resistant to erosion.

Plasma spraying is gaining acceptance for development of quality coatings of various materials on a wide range of substrates. Utilization of such kind of industrial waste as coating material minimizes the cost of plasma spray coating deposition, which posed to be the major hindrance to its wide spread application due to high cost of the spray grade powders.

Fly-ash+quartz+illmenite (weight percentage ratio: 60:20:20) is deposited on mild steel and copper substrates by atmospheric plasma spraying, at various operating power levels ranging from 11 to 21kW and then characterization of the coatings is carried out. The properties of the coatings depend on the materials used, operating condition and the process parameters. The plasma spraying process is controlled by the parameter interdependencies, co-relations and individual effect on coating characteristics. The particle sizes of the raw materials used for coating are characterized using Laser particle size analyzer of Malvern Instruments. Coating interface adhesion strength is evaluated using coating pull out method, confirming to ASTM C-633 standard. Deposition efficiency is an important factor that determines the techno economics of the process. It is evaluated for the deposited coatings. In view of tribological applications, hardness is one of the most required mechanical properties. Hardness measurement is done on the polished cross section of the samples using Leitz Micro-Hardness Tester. Coating porosity is measured by image analysis technique. Coating thickness is measured on the polished cross-sections of the samples, using an optical microscope. To ascertain the phases present and phase changes/transformation taking place during plasma

spraying, XRD analysis is made. The coating quality and behavior depends on Coating surface & interface morphology are studied with Scanning Electron Microscope. For wear resistance application, wear properties of these coatings are studied by “Air Jet Erosion Test Rig”. The erosion wear behaviour of these coatings is evaluated with angular solid particle erosion tests under various operating conditions.

In order to optimize the surface property for different application, one of the challenges is to recognize parameter interdependencies; correlations and their individual effects on process so that the coating can be useful for a specific application. This challenge can be analysed/predicted by Artificial Intelligence Methods. Statistical analysis of the experimental results using Artificial Neural Network and Taguchi experimental design is been made. Spraying parameters such as impact angle, size of the erodent, standoff distance and impact velocity are identified as the significant factors affecting the coating tribological property.

This work establishes that fly-ash+quartz+illmenite composite mixture can be used as a potential coating material suitable for depositing plasma spray coating. It also opens up a new pathway for value added utilization of this industrial waste and low-grade ore mineral.

List of figures

Figure 2.1 Summery plot of surface modification techniques.

Figure 2.2 (a) Schematic diagram showing plasma spraying and **(b)** Schematic physical-thermomechanical description of plasma spray process.

Figure 2.3 conventional plasma spray process.

Figure 2.4 Temperature Distribution and geometry of the plasma jet.

Figure 2.5 plasma spraying arrangement.

Figure 2.6 Carrier Gas Flow Rate a) too low b) correct c) too high [35].

Figure 2.7 schematic presentation of electrode arrangement and spraying distance.

Figure 2.8 SEM examination of splat morphologies obtained from impacting droplets at substrate inclinations of (a) 0°, (b) 10°, (c) 20°, (d) 30°, (e) 40°, (f) 50°, (g) 60° [41].

Figure 2.9 Schematic of the (a) physical plasma spray process and (b) its idealization for modeling [51].

Figure 2.10 Splat formation after the impact of the spherical powder during spraying.

Figure 3.1 General arrangement of plasma spraying equipment.

Figure 3.2 Jig under the test.

Figure 3.3 Specimen under tension

Figure 3.4 Adhesion test with Instron 1195 UTM.

Figure 3.5 Erosion test set up.

Figure 3.6 Schematic diagram of erosion test rig.

Figure 4.1 Particle size analysis of fly-ash+quartz+illmenite spray coating feedstock.

Figure 4.2 SEM micrographs of fly ash+quartz+illmenite raw powder prior to coating.

Figure 4.3 Surface morphology of fly ash+quartz+illmenite coatings deposited on mild steel Substrates, at (a) 11kW (b) 15kW (c) 18 kW (d) 21kW power level.

Figure 4.4 Interface morphology of fly ash+quartz+illmenite coatings deposited on mild steel Substrates, at (a) 11kW (b) 15kW (c) 18 kW (d) 21kW power level.

Figure 4.5 X-Ray diffractogram of fly ash+quartz+illmenite feedstock.

Figure 4.6 X-Ray diffractogram of fly ash+quartz+illmenite coating deposited at 11kW.

Figure 4.7 X-Ray diffractogram of fly ash+quartz+illmenite coating deposited at 15kW.

Figure 4.8 X-Ray diffractogram of fly ash+quartz+illmenite coating deposited at 18kW.

Figure 4.9 X-Ray diffractogram of fly ash+quartz+illmenite coating deposited at 21kW.

Figure 4.10 Comparison of adhesion strength of mild steel and copper with respect to power level.

Figure 4.11 Variation of deposition efficiency of fly-ash+quartz+illmenite coatings at different power levels.

Figure 4.12 Variation of coating thickness of fly ash+quartz+illmenite coatings at different power levels.

Figure 4.13 Variation of coating hardness of fly ash+quartz+illmenite coatings at different power levels.

Figure 4.14 Variation of coating porosity of fly ash+quartz+illmenite coating with torch power.

Figure 4.15 Variation of coating surface roughness of fly ash+quartz+illmenite coating with torch power.

Figure 4.16 The three layer neural network for adhesion strength

Figure 4.17 Comparative plot of experimental and ANN predicted values of adhesion strength of fly-ash+quartz+illuminite on Cupper & Mild Steel substrate (Plasma spray at 12 gm/min feed rate and 100 mm torch to base distance)

Figure 4.18 Comparative plot of experimental and ANN predicted values of adhesion strength of fly-ash+quartz+illuminite on Cupper & Mild Steel substrate (Plasma spray at 18 gm/min feed rate and 140 mm torch to base distance).

Figure 4.19. Predicted adhesion strength of Cupper & Mild Steel substrate with respect to different power level (Plasma spray of fly-ash+quartz+illuminite at 12 gm/min feed rate and 40 μ m powder size, 100mm torch to base distance).

Figure 4.20 Predicted adhesion strength Vs Power level for Cupper by change in size of powder (Plasma spray of fly-ash+quartz+illuminite at 12 gm/min feed rate and 100mm torch to base distance).

Figure 4.21 Predicted adhesion strength vs Power level for Mild Steel by change in size of powder (Plasma spray of fly-ash+quartz+illuminite at 12 gm/min feed rate and torch to base distance 100mm).

Figure 4.22 Predicted adhesion strength vs torch to base distance for Cupper by change in size of powder (Plasma spray of fly-ash+quartz+illuminite at 18kW power level and 12 gm/min feed rate).

Figure 4.23. Predicted Adhesion strength vs torch to base distance for Mild Steel by change in size of powder (Plasma spray of fly-ash+quartz+illuminite at 15kW power level and 12 gm/min feed rate and).

Figure 4.24 Residual plots for mean on erosion rate of fly-ash+quartz+illmenite coatings.

Figure 4.25 Residual plots for S/N ratio on erosion rate of fly-ash+quartz+illmenite coatings.

Figure 4.26 Main effect of plots for means on erosion rate of fly-ash+quartz+illmenite coatings.

Figure 4.27 Main effects of plots for S/N ratios on erosion rate of fly-ash+quartz+illmenite coatings.

Figure 4.28 cumulative mass loss of coating Vs time for 18kW coating substrate at erodent impact pressure of (a) 1 bar (b) 2 bar.

Figure 4.29 Cumulative mass loss of coating Vs time for 21kW coating substrate at erodent impact pressure of (a) 1 bar (b) 2 bar.

Figure 4.30 Surface morphology of SiC particles

Figure 4.31 SEM micrographs of eroded surfaces of coatings deposited at 18 kW at angle of impact (a) 60° and (b) 90° using SiC as the erodent..

List of tables

Table 2.1 basic way to generate heat for melting spray powder.

Table 2.2 Thermal spraying processes.

Table 2.3 Different wear mechanism, symptoms and surface appearance

Table 3.1 Operating parameters during coating deposition.

Table 4.1 Chemical composition of fly-ash.

Table 4.2 Deposition efficiency of fly-ash+quartz+illmenite coatings.

Table 4.3 Thickness values of fly ash+quartz+illmenite coatings on mild steel substrates.

Table 4.4 Hardness on the coating cross section for the coatings deposited at different power levels.

Table 4.5 Coating porosity of mild steel and copper at different power levels.

Table 4.6 Coating porosity of mild steel and copper at different power levels.

Table 4.7 Input parameters selected for training (Coating adhesion strength).

Table 4.8 Variables used in the experiment as per Taguchi L8 method

Chapter 1

INTRODUCTION

- Research Background
- Objectives of Research

Chapter 1

Introduction

1.1 RESEARCH BACKGROUND

Currently emerging technologies contains some of the most prominent ongoing developments, advances, and innovations in various engineering field to improve surface property by using different type of modern technology. Because for higher efficiency and productivity across the entire spectrum of engineering and manufacturing industries has ensured that most modern day components are subjected to increasingly harsh environments during routine operation. Critical industrial components are, therefore, prone to more rapid degradation as the parts fail to withstand the rigors of aggressive operating conditions and this has been taking a heavy toll of industry's economy. In large number of cases i.e. by hostile environments and also by high relative motion between mating surfaces, corrosive media, extreme temperatures and cyclic stresses, the accelerated deterioration of parts and their eventual failure has been traced to material damage. So it became necessary to develop research on new materials for fabrication. So this division's mission is to develop quality assurance in coating systems and surfaces. Furthermore, the division is concerned with the enhancement of the life time and the quality of products as well as with failure analysis and damage prevention of new coating materials and components. As a result of the above, the concept of incorporating engineered surfaces by various surface modification techniques, capable of combating the accompanying degradation phenomena like wear, corrosion and fatigue to improve component performance, reliability and durability has gained increasing acceptance in recent years.

Treatment of Surface is an established provider of advanced materials processing and coating technologies for a wide range of applications in the automotive, Aerospace, Oil & Gas, Semiconductor, missile, power, electronic, biomedical, textile, petroleum, petrochemical, chemical, steel, power, cement, machine tools, construction industries. The development of a suitable high performance coating on a component fabricated using an appropriate higher mechanical strength metal/alloy, offers a promising method of meeting both the bulk and surface property requirements of virtually all imagined applications. A protective coating is deposited as a barrier between component's surfaces and the aggressive environment that it is exposed to during operation is now globally acknowledged to be an attractive means to significantly hinder damage to the actual component by acting as the first line of defense. Along with the traditional one, the newer surfacing techniques are eminently suited to modify a wide range of engineering properties. There are several properties that can be modified by adopting the surface engineering approach include tribological, mechanical, thermo-mechanical, electrochemical, electrical, electronic, magnetic/acoustic and biocompatible, optical properties.

Surface treatments typically are removing material, adding material or chemically altering the surface. Surface treatments are widely used in most industries to provide improved surface properties of a machine component. Different categorized surface treatments are:

a) Anodizing

Anodizing is an electrolytic passivation process used to increase the thickness of the natural oxide layer on the surface of metal parts. In this process the part to be treated forms the anode electrode of an electrical circuit. Some typical anodizing processes are Chromic acid anodizing, Sulfuric acid anodizing, Organic acid anodizing, Phosphoric acid anodizing, etc. Aluminum metal is on the anodic side of the galvanic series. Its position is similar to zinc and magnesium, i.e. it is readily oxidized. The oxide on aluminum is naturally corrosion resistant, very hard, abrasion resistant, an insulator and very tenacious. In its natural form the oxide film on aluminum is less than 0.50 microns thick.

b) Electroplating (galvanizing)

Electroplating is often also called electro-deposition. Electro-deposition is the process of producing a coating, usually metallic, on a surface by the action of electric current. The deposition of a metallic coating onto an object is achieved by putting a negative charge on the object to be coated and immersing it into a solution which contains a salt of the metal to be deposited (in other words, the object to be plated is made the cathode of an electrolytic cell). The metallic ions of the salt carry a positive charge and are thus attracted to the object. When they reach the negatively charged object (that is to be electroplated).

c) Cladding

This is the application of one material over another to provide a skin or layer intended to control the infiltration of weather elements or for aesthetic purposes. Cladding does not necessarily have to provide a waterproof condition but is instead a control element. This control element may only serve to safely direct water or wind in order to control run-off and prevent infiltration into the main structure.

d) Diffusion coating (Nitriding, Phosphating, carburizing, cyaniding, boronizing, chromizing etc.)

The Diffusion Coating Process is a thermally activated high temperature oxidation / corrosion / wear resistance coating for iron, nickel, and cobalt based metals with severe operating conditions. It provides a chemically bonded, tenacious coating which acts as a diffusion barrier against oxygen and other elements into the substrate.

e) Polymer film

Among wide range of insulating material with embedded metal nanoparticles, thick or thin insulating layers have raised special interest. Polymer thin films are especially suitable as host materials for nanoparticles, while their chemical structure and physical properties can be very different.

f) Shot peening

Shot peening is a cold working process used to produce a compressive residual stress layer and modify mechanical properties of metals. It entails impacting a surface with shot (round metallic, glass, or ceramic particles) with force sufficient to create plastic deformation. Peening a surface spreads it plastically, causing changes in the mechanical properties of the surface. Shot peening is often called for in aircraft repairs to relieve tensile stresses built up in the grinding

process and replace them with beneficial compressive stresses. Depending on the part geometry, part material, shot material, shot quality, shot intensity, shot coverage, shot peening can increase fatigue life up to 1000%.

g) Lubricants

Failure mechanisms include high contact resistance, high adhesion, melting/shorting, and contact erosion. But by addition of lubricant these failure mechanism can be hinder much more time. e.g. It was found that the rollers with lubricating coating resulted in lowest boundary friction closely followed by the rollers with the hardest DLC coatings.

h) Flame hardening

In this process heat is applied by a high temperature flame followed by quenching jets of water. It is usually applied to medium to large size components such as large gears, sprockets, slide ways of machine tools, bearing surfaces of shafts and axles, etc. In flame hardening a defined surface area directly impings by an oxy-gas flame. The result of the hardening process is controlled by four factors, i.e. i) the design of the flame head; ii) the duration of heating; iii) the target temperature to be reached; and iv) the composition of the metal being treated.

i) Thermal spraying

Thermal Spray Technologies are specializes coating solutions using leading edge technology and equipment for Electric Arc Spraying, Flame Sprayed Coatings, Plasma Spraying, and High Velocity Oxy Fuel Coatings.

j) Induction hardening

This process is a non contact heating technique which utilizes the principle of electromagnetic induction to produce heat inside the surface layer of a work-piece. By placing a conductive material into a strong alternating magnetic field electrical current can be made to flow in the steel thereby creating heat due to the I^2R losses in the material. The current generated flows predominantly in the surface layer, the depth of this layer being dictated by the frequency of the alternating field, the permeability of the material, the surface power density, the heat time and the diameter of the bar or material thickness.

From all of the above techniques, thermal spraying is popular for its wide range of applicability, adhesion of coating with the substrate and durability. Surface modification technologies have grown rapidly, both in terms of finding better solutions and in the number of technology variants available, to offer a wide range of quality and cost.

Surface engineering has been developed largely on account of the fact that it is a discipline of science and technology that is being increasingly relied upon to meet all the key modern day technological requirements: enhanced efficiencies, material savings, environmental friendliness etc [1]. The selection of coating material is a crucial factor which needs to be considered carefully and in relation to the substrate and application method. The wrong selection can not only affect the long term reliability but can cause massive difficulties with both processing and costs. While the ‘Material Considerations’ section below is very important to finding the correct coating and is also important to find a coating chemistry which meets specific application needs. Selection of the correct choice of coating material (lacquer) is one of the process engineer's most

critical decisions. Criteria for selection must be based on answering many questions, which will include:

- What is being protected against ? (e.g. moisture/chemicals/wear)
- What temperature range will the equipment/parts are operated?
- What are the physical, chemical and electrical requirements for the coating material itself ?
- On which substrate, material to be coated ? (In account of range of adhesion strength/coating deposition/coating thickness etc.)
- Electrical, chemical, and mechanical compatibility with the parts and substances to be coated.
- For instance, does it need to match the coefficient of expansion of component ?
- How much coating material resist to the attack expected ?
- How easily can the material be reworked once applied ?
- How fast can the material be applied and dried ?
- What type of procedure and equipments are necessary to achieve the required coating quality (uniformity and repeatability) ?
- Price of the coating material and process.
- Quality of the material supplier (different fly-ash composite material manufacturers will not make equal quality of material).

Answers will determine the suitability of a particular material, Process, production and commercial issues.

Thermal spraying techniques are surface modification process in which melted (or heated) materials are sprayed onto a substrate surface. The feedstock (coating precursor) is heated by electrical (plasma or arc) or chemical means (combustion flame). Plasma spraying process is a thermal spraying technique, which is a relatively specialized high temperature industrial process that utilizes electrically generated plasma to heat and melt the feedstock material. The process is capital intensive and requires significant electrical power. It offers a method of depositing a feedstock material over an underlying target material as a solid coating layer. Deposition thickness gives a wide range from a few micrometers (μm) up to several millimeters by use of a variety of feedstock materials, including metals and ceramics. The feedstock material is normally presented to the plasma torch typically, in the form of a powder or wire. This feedstock melts rapidly within the plasma gun, where the typical operating temperature is $\sim 10,000^{\circ}\text{C}$ ($18,000^{\circ}\text{F}$). Powdered materials are injected within the plasma (RF discharges) or the plasma jet (dc arcs) where particles are accelerated and melted, or partially melted, before they flatten and solidify onto the substrate (forming lamellae or splats), the coating being built by the layering of splats [2]. This technique is mostly used to produce coatings on different structural materials and provides protection against corrosion, erosion and wear, high temperatures, to change the appearance and also improves electrical properties of the surface. Plasma spraying is extensively used in a wide range of industries like aerospace, nuclear energy as well as conventional industries like chemicals, textiles, plastics and paper to develop a suitable surface coating to

improve the component life span at operating environment mainly wear resistant coatings in crucial components.

During the last decade, a large number of investigations have been carried out for new development of plasma spray coating material by using industrial waste and low-grade ore [3]. Flyash is a finely divided powder generated as a solid waste in huge quantities in thermal power plants. A small fraction of flyash is used in the development of high value products. New ways of utilizing flyash are being explored in order to minimize the plant wastage and provide a safeguard to the environment. Flyash is a fine powder which can be used as refractory material in industry. Now-a-days flyash composite has a number of useful applications [4]. However, increase in the demand of its applications; have led to the development of new fly-ash composite coatings. Fly-ash composite coatings, such as fly-ash+redmud [5] and fly-ash+zinc coatings [6], fly-ash+jute-polymer [7], fly-ash+ Na-geopolymer [8], flyash+illmenite [9], fly-ash+quartz [10], have been studied. According to recent investigations composite fly-ash coatings can obtain high corrosion resistant, in addition to increased wear resistance. Some of these recent reports concerning the development and surface properties of this type of fly-ash composite coatings are presented below.

This investigation describes about processing of plasma spray coatings and characterization/evaluation of substrate surface properties i.e. microstructure, adhesion strength, deposition efficiency, thickness, hardness, porosity and wear resistance. Fly-ash+quartz+illmenite with weight percentage ratio: 60:20:20 is deposited on mild steel and copper substrates by atmospheric plasma spraying. Spraying carried out at various operating power levels ranging from 11 to 21kW. Coating-substrate interface adherence strength is evaluated using coating pull out method. Deposition efficiency is an important factor that determines the techno economics of the process which is evaluated for the deposited coatings. Hardness measurement is done on the polished cross section of the samples using Leitz Micro-Hardness Tester. Coating porosity is measured by image analysis technique. Coating thickness is measured on the polished cross-sections of the samples, using an optical microscope. XRD analysis is made to ascertain the phases present and phase changes/transformation taking place during plasma spraying. Coating surface & interface morphology is studied with Scanning Electron Microscope. Erosion wear behaviors of these coatings are studied by “Air Jet Erosion Test Rig”.

1.2 OBJECTIVES OF RESEARCH

The objective of the present investigation is as follows:

- To explore the coating potential of fly ash+quartz+illmenite on metal substrates by plasma spraying.
- To develop a series of plasma sprayed coatings from fly ash+quartz+illmenite on metal substrates and to find out deposition efficiency, porosity, surface roughness, thickness and wear properties etc.
- X-ray diffraction studies to find out the presence/formation of different phases.

- Micro-structural characterization (surface and interface morphology) to evaluate the soundness of the coatings.
- Measurement of hardness and adhesion strength of the coatings.
- Sustainability of the coatings against wear with solid particle erosion test.
- To analyze the experimental results using statistical techniques so as to identify the significant factors/interaction parameter set by which one can get better plasma surface property.

Chapter 2

Literature Survey

- Introductory Statement
 - Surface engineering
- Techniques of surface modification
 - Thermal spraying
 - Plasma spraying
- Industrial applications of plasma spraying
 - Wear
 - Types of wear
 - Symptoms of wear
- Recent trends in material wear research
 - Wear resistant coatings
- Utilization of fly ash as wear resistant coatings
 - Erosion wear of ceramic coatings

Chapter 2

Literature Survey

2.1 INTRODUCTORY STATEMENT

This chapter describes the literature survey of the broad topic of interest namely the development of surface modification technology. This explains various coating techniques with a special reference to plasma spraying, the raw spray materials and their characteristics. It gives a brief description of the coating deposition process by plasma spray technique. The performances of wear resistant coatings under various conditions have been reviewed critically along with the corresponding failure mechanisms. It also presents a review of the wear i.e. types of wear, symptoms of wear and recent trends in metal wear research along with erosion wear behavior of ceramic coatings, which is the material of interest in this work.

2.2 SURFACE ENGINEERING

In a wide variety of industry the role of surface coating have been imparted its increasingly importance because higher energy efficiency and longer service life are expected more strongly for various plants and industries. Thermal spraying holds a unique position in the spectra of surface modification technologies because it can provide thick coatings over $\sim 100\mu\text{m}$ over a large area at a very high application rate compared with other coating processes such as PVD, CVD and electroplating [11]. Surface engineering can defined as: “treatment of the surface and near surface regions of a material to allow the surface to perform functions that are distinct from those functions demanded from the bulk of the material” [12]. Engineers have always been faced with difficult decision when selecting materials for the structural components in the modern high technology field such as nuclear, space power, oil exploration etc. operating in the extremely hostile environment of temperature, gas flow, pressure and corrosion media. The properties desired at the surface are different from those at the bulk of the components. This is the reason for the use of surface coating. Wear, corrosion, erosion, fatigue and creep can cause environmental degradation of the surface over time. Surface engineering involves altering the properties of the surface in order to reduce the degradation over time. This is accomplished by making the surface robust to the environment in which it will be used [13]. Surface Engineering is the name of the discipline - surface modification technique is the philosophy behind it.

Surface treatment for engineering material may be necessary to:

- Improve resistance to wear, erosion, and indentation (wear surfaces of machinery, and shafts, rolls, cams, and gears slideways in machine tools).
- Control friction (sliding surfaces on tools, dies, bearings, and machine ways).
- Reduce adhesion (electrical contacts).
- Improve thermal insulation.

- Improve corrosion & oxidation resistance (sheet metals for automotive or other outdoor uses, gas turbine components, and medical devices).
- Improve stiffness and fatigue resistance (bearings and multiple-diameter shafts with fillets).
- Improve lubrication (surface modification to retain lubricants).
- Rebuild surfaces on worn components (worn tools, dies, and machine components).
- Improve surface roughness (appearance, dimensional accuracy, and frictional characteristics).
- Impart decorative features, color, or special surface texture.
- Increase product life span.

By fulfilling the above criteria, surface engineering techniques are being used in the steel, power, aerospace, missile, automotive, power, electronic, biomedical, textile, petroleum, petrochemical, chemical, cement, machine tools, construction industries. Almost all types of materials, including metals, ceramics, polymers, and composites can be coated on similar or dissimilar materials. To elucidate the matter some example can be taken. A) The surface of erritic stainless steel modified with Mo by laser treatment. It is found that, pitting potential increased by approximately 150 mV than that of unprocessed stainless steel [14], B) Tungsten carbide cobalt composite is a very popular cutting tool material, and is well known for its high hardness and wear resistance. If a thin coating of TiN is applied on to the WC-Co insert, its capabilities increase considerably [15]. Actually a cutting tool, in action, is subjected to a high degree of abrasion, and TiN is more capable of combating abrasion. On the other hand, TiN is extremely brittle, but the relatively tough core of WC-Co composite protects it from fracture. Thus, through a surface modification process we assemble two (or more) materials by the appropriate method and exploit the qualities of both [16].

2.3 TECHNIQUES OF SURFACE MODIFICATION

Today a large number of commercially available technologies are present in the industrial scenario. An overview of such technologies is presented below (Fig 2.1):

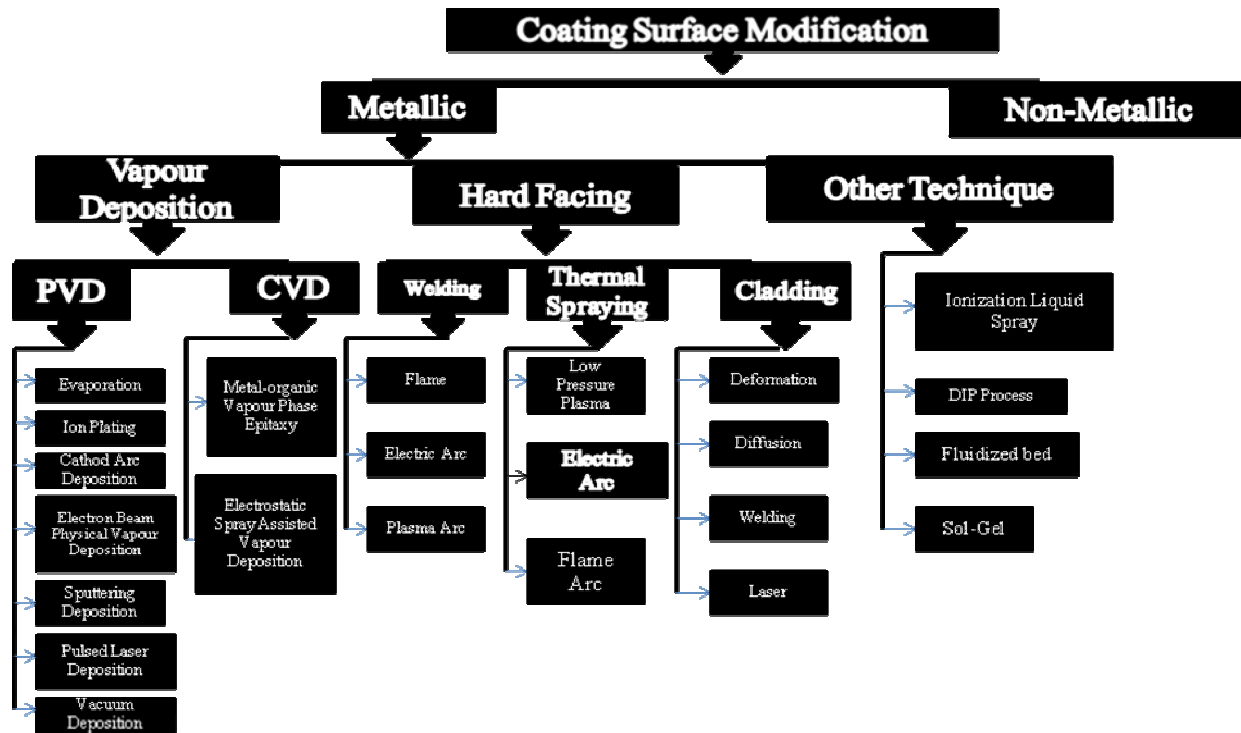


Figure 2.1 Sumnerized plot of surface modification techniques.

2.4 THERMAL SPRAYING

In the early 1900s, M.U. Schoop was the first scientist to explore the possibility that a stream of metallic particles formed from molten metal might be used to produce coatings. But the thermal spraying technologies expanded in the 1970s due to development of thermal plasmas, and the increasing demand of high temperature and wear resistant materials and coating systems [17]. In the 1990s thermal spraying was demandingly available and had become a standard tool for improving surfaces in about all industries. Thermal spraying is the application of a material (consumable) to a substrate by melting into droplets and impinging the softened or molten droplets on a substrate to form a continuous/ pulsed coating [18]. Thermal spray consumables can be metallic, ceramic, alloys or polymeric substances. Any material can be sprayed as long as it can be melted by the heat source employed and does not undergo degradation during heating [19]. The spray techniques that have been used to deposit coatings for protection against hostile atmosphere are enlisted below, as summarised by Heath et al. [20]:

- Flame spraying with a powder particle or wire
- Electric arc wire spraying
- Plasma spraying
- High Velocity Oxy-Fuel (HVOF) spraying
- Spray and fuse

These processes are basically differentiated from each other on the basis of particle speed, flame temperature and spray atmosphere [21]. Thermal spray technology is uniquely important

to an ever-increasing engineering community, for its (i) improved spray footprint definition versus wide spray beam; (ii) high throughput versus competitive techniques; (iii) significantly improved process control; (iv) lower cost-per-mass of applied material, together with overall competitive economics. Thermal spray coatings have been produced for at least 50 years, but the last decade has seen a virtual revolution in the capability of the technology to produce truly high performance coatings of a great range of materials on many different substrates [22].

The various advantages of thermal spraying technology are listed as:

- Choice of wide variety coating materials; metals, alloys, ceramics, cermets and carbides.
- Thick coatings can be applied at high deposition rates.
- Coatings are mechanically bonded to the substrate - can often spray coating materials which are metallurgically incompatible with the substrate, e.g. materials with high melting point than the substrate.
- Components can be sprayed with little or no pre- and post- heat treatment and component distortion is minimal.
- Parts can be rebuilt quickly and at low cost and usually at a fraction of price of a replacement.
- By using a premium material for the thermal spray coating, coated components can outlive new parts.
- Thermal spray coatings can be applied both manually and automatically.

The main principle behind thermal spraying is to melt material feedstock (wire or powder) to accelerate the melt to impact on a substrate where rapid solidification and deposit build up occur. Thus, a heat source and a means of accelerating the material are required. This is pictured schematically in Fig 2.2 [23].

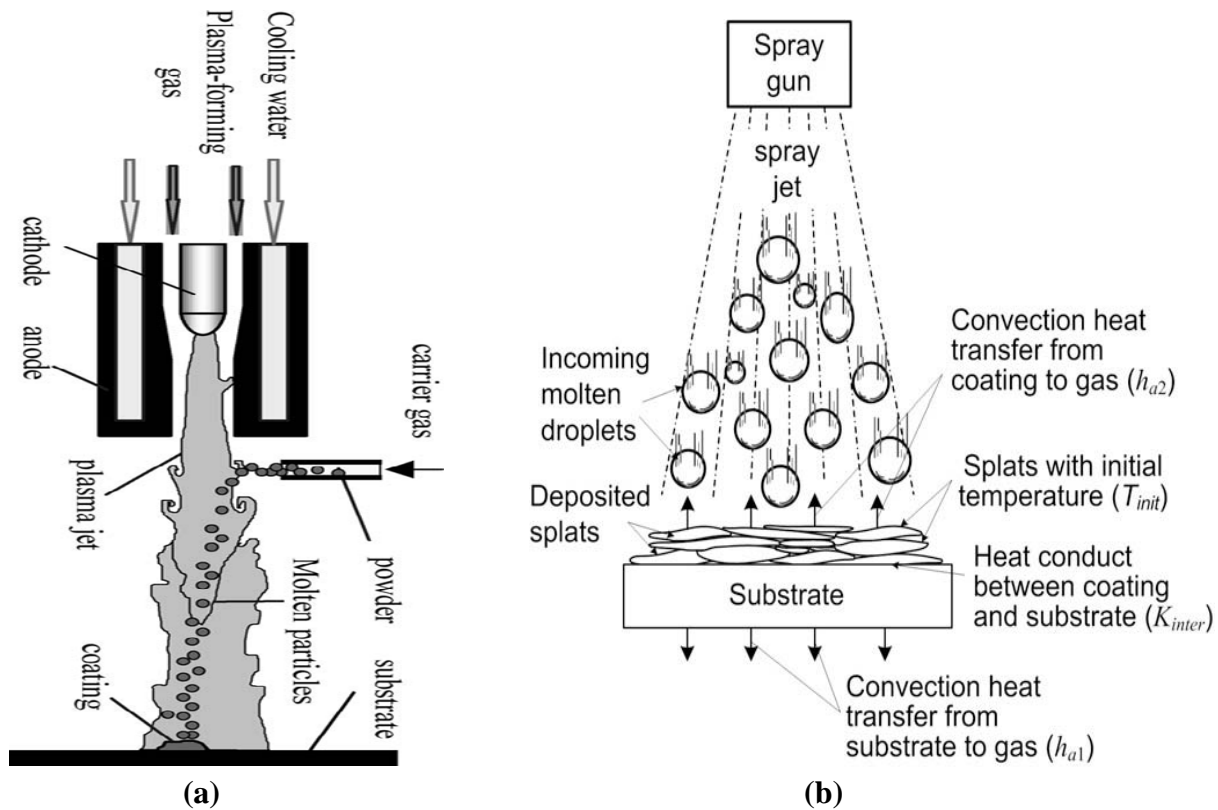


Figure 2.2 (a) Schematic diagram showing plasma spraying and (b) Schematic physical-thermomechanical description of plasma spray process.

The nature of bonding at the coating-substrate interface depends on mechanical/metallurgical bonding. This is one extremely significant feature of thermal spraying. Another aspect of thermal spraying is that the substrate surface temperature seldom exceeds 2000C. Stress related distortion problems are also not so significant. The spraying action is achieved by the rapid energy transfer of combustion gases to the molten droplets or by a separate supply of compressed air. There are two basic ways of generating heat required for melting the consumables. They are (i) combustion of a fuel gas and (ii) high energy arc processes [24, 25], categorize in Table 2.1. Processes available for thermal spraying have been developed specifically for a purpose and fall into two categories-high and low energy processes. The key processes and their energy sources are summarized in Table 2.2 [26].

Table 2.1 basic way to generate heat for melting spray powder.

Thermal Spray Process	Gas combustion process	Oxy-fuel/wire
		Oxy-fuel/powder
		Detonation gun
		HVOF
	Arc process	Electric Arc
		Plasma Arc

Table 2.2 Thermal spraying processes.

Processes		Energy sources	Different Nomenclature
Low energy process	Flame spraying	Chemical	Oxyfuel gas-powder spraying
			Oxyfuel gas-wire spraying
			metallizing
	Arc spraying	Electrical	Electric arc spraying
			Twin-wire arc spraying
			metallizing
High energy process	Plasma spraying	Electrical	Atmospheric plasma spraying
			Vacuum plasma spraying
			Low pressure plasma spraying
			Water stabilized plasma spraying
			Inductive plasma spraying
	Detonation flame spraying	Chemical	D-gun
	High velocity oxyfuel spraying	Chemical	HVOF spraying
			High velocity oxygen fuel spraying
			High velocity flame spraying
			High velocity air fuel

2.5 PLASMA SPRAYING

Plasma spraying is one of the most widely used thermal spraying technique which finds a lot of applications due to its versatility of spraying a wide range of materials from metallic to non metallic and hence more suitable for spraying of high melting point materials like refractory ceramics material, cermets etc [27,28]. A schematic diagram of plasma spray process is shown in Fig 2.3. This process is part of thermal spraying, in which finely divided metallic and non-metallic materials are deposited in a molten or semi-molten state on a prepared substrate [29]. In the fifties, the plasma torches were developed to test materials at high enthalpies for simulated re-entry vehicles. Then in the late fifties and early sixties, the first attempts were reported using plasma torches for spraying of primarily refractory materials. Almost any material can be used for plasma spraying on almost any type of substrate. This flexibility is probably one of the major reasons for the rapid development of this technology [30]. The high temperatures enable the use of coating materials with very high melting points such as alloys, ceramics, cermets and refractory. Materials can be processed as long as there is a temperature difference of at least 300K between the melting temperature and decomposition or evaporation temperature [31]. Among other key features of plasma spraying are the formation of microstructures with fine, noncolumnar and equiaxed grains, the ability to produce homogeneous coatings that do not

change in composition with thickness and length of deposition time, the ability to process materials in virtually any environment (e.g., air, reduced-pressure inert gas, high pressure, under water) [32]. Applications for plasma spraying include corrosion, erosion, temperature and abrasion resistant coatings and production of monolithic and near net shapes, which at the same time take advantage of the rapid solidification process. Powder of glassy metals can be plasma sprayed without changing their amorphous characteristics. High temperature superconductive materials have also been deposited by the plasma spray technique. A new application of plasma spraying is in producing hydroxyapatite coatings onto the stems of orthopaedic endoprostheses [33].

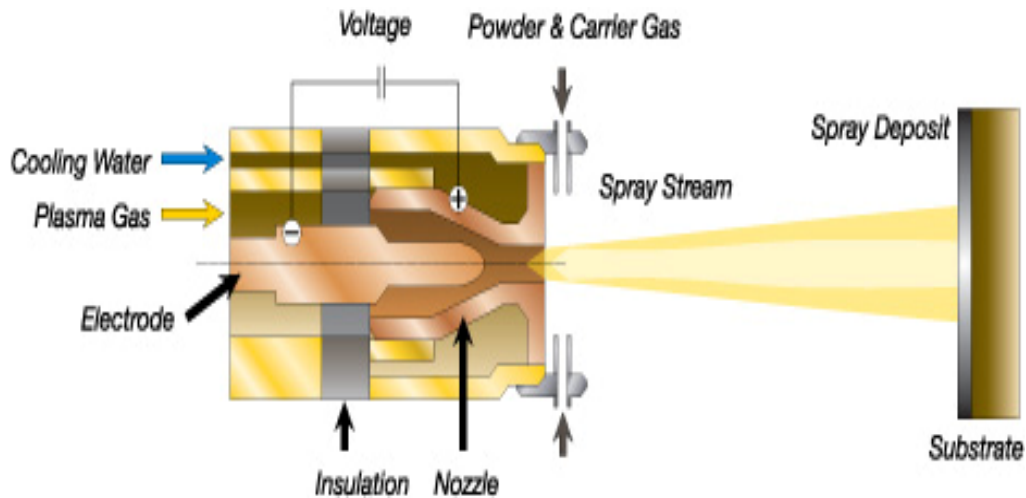


Figure 2.3 conventional plasma spray process.

In this technique an arc is created between tungsten cathode and an copper anode. Generated plasma gas is is forced to pass through the annular space between the electrodes. the gas undergoes ionization in the high temperature environment resulting plasma, While passing through the arc. Temperature in the plasma arc can be as high as 2,000°C to 20,000°C (as shown in Fig 2.4) and is capable of melting anything.

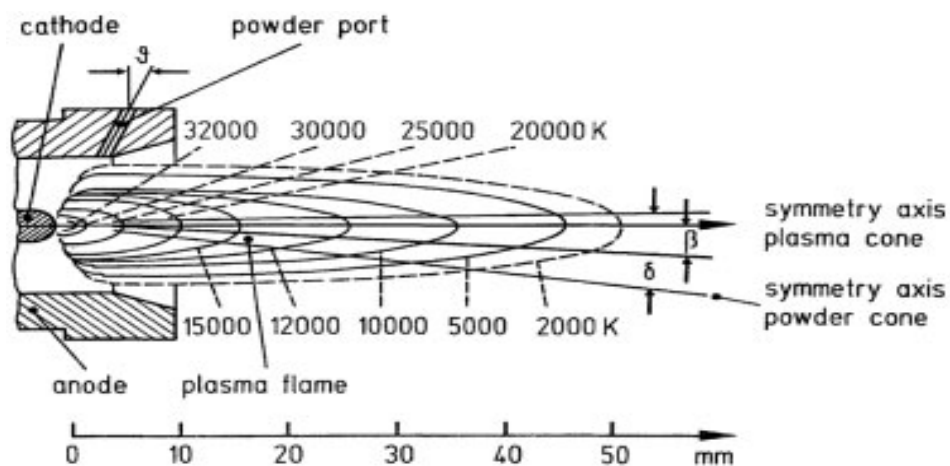


Figure 2.4 Temperature Distribution and geometry of the plasma jet.

The ionization is achieved by collisions of electrons of the arc with the neutral molecules of the gas. The plasma protrudes out of the electrode encasement in the form of a flame. Electrodes are water cooled. The raw coating material in the powdered form is poured into the flame with required feed rate. The powders melt immediately by gain of plasma energy and momentum and then rush towards the target to form a thin deposited layer. In this way the coating builds up layer by layer [34]. Elaborate cooling arrangement is required to protect the spray system from excess heating. The equipment consists of the following modules [35]:

- ❖ **The plasmatron:** It is the device which houses the electrodes and in which the plasma reaction takes place. It has the shape of a gun and it is connected to the water cooled power supply cables, powder supply hose and gas supply hose.
- ❖ **The power supply unit:** Normally plasma arc works in a low voltage (30-60 Volts) and high current (300-700 Amps), DC ambient. The available AC power of 3 phase, 440Volts must be transformed and rectified to suit the reactor. This is taken care of by the power supply unit.
- ❖ **The powder feeder:** The powder is kept inside a hopper. A separate gas line directs the carrier gas that fluidizes the powder and carries it to the plasma arc. The flow rate of the powder can be controlled precisely.
- ❖ **The coolant and water supply unit:** It circulates water into the plasmatron, the power supply unit and the power cables. Units capable of supplying refrigerated water are also available.
- ❖ **The control unit:** Important functions (current control, gas flow rate control etc.) are performed by the control unit. It also consists of relays and solenoid valves and other interlocking arrangements essential for safe running of the equipment. For e.g. an arc can only be started if the coolant supply is on and water pressure and flow rate is adequate.

An arrangement of plasma spraying equipment is shown in Fig 2.5.

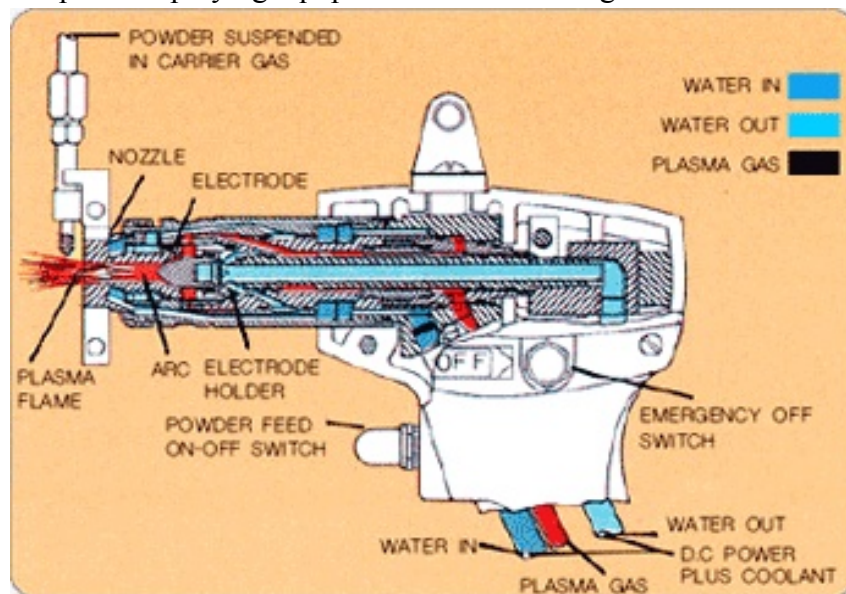


Figure 2.5 plasma spraying arrangement.

The main advantages of the plasma spraying process have been presented by Heath et al. [36] and others as follows:

1. Very flexible in coating material selection and optimization for specific resistance to corrosive environments and particle abrasion/erosion.
2. Coating systems (multi-layer or functionally graded) can be used.
3. Unique alloys and microstructures can be obtained with thermal spraying which are not possible with a wrought material. These include continuously graded composites and corrosion resistant amorphous phases.
4. Costs of the coating solution are normally significantly lower than those of a highly alloyed bulk material; thermal spray coatings are especially interesting for their cost/performance ratio.
5. Thermal spray coatings additionally offer the possibilities of on-site application and repair of components, given a sufficient accessibility for the sprayer and his equipment.
6. Forms microstructure with fine, equiaxed grains and without columnar boundaries.
7. Produces deposits that do not change in composition with thickness (length of deposition time).
8. Can change from depositing a metal to a continuously varying mixture of metals ceramics (i.e. functionally graded materials).
9. High deposition rates (>4kg/h).
10. Fabricates freestanding forms of virtually any material or any materials combination.
11. Process materials in virtually any environment e.g. air, reduced pressure inert gas, high pressure etc.

However, thermal spraying in the work shop is preferred, whenever possible, to achieve optimum results. Among the thermal spray coating processes, plasma spraying is reported to be a versatile technology that has been successful as a reliable cost-effective solution for many industrial problems by Fauchais et al. [37]. Plasma spraying is the most flexible thermal spray process with respect to the sprayed materials. The high temperatures of plasma spray processes permit the deposition of coatings for applications in areas of liquid and high temperature corrosion and wear protection and also special applications for thermal, electrical and biomedical purposes. Plasma-sprayed metallic coatings are used in high-temperature applications e.g. in diesel engines, aircraft engines and land-based gas turbines to protect the component from oxidation and corrosion [38].

2.5.1 Requirements for Plasma Spraying

Roughness of the substrate surface:

Surface roughness of substrate provides anchorages for better mechanical interlocking. Better is the surface roughness, better is the adhesion strength. A rough surface is generally created by grit blasting technique. The grits are kept inside a hopper, and compressed air is supplied at the bottom of the hopper. The grits are taken a float by the compressed air stream into a hose and ultimately directed to an object kept in front of the exit nozzle of the hose. The grits used for this purpose are irregular in shape, highly angular in nature, and made up of hard material like alumina, silicon carbide, etc. Upon impact they create small craters on the surface by localized plastic deformation, and finally yield a very rough and highly worked surface. The roughness obtained is determined by shot blasting parameters, i.e., shot size, shape and material, air pressure, angle of impact, stand-off-distance between nozzle and the job, substrate material etc [39]. The effect of shot blasting parameters on the adhesion of plasma sprayed alumina has been studied [40]. Mild steel serves as the substrate material. The adhesion increases proportionally with surface roughness and the parameters listed above are of importance. A significant time lapse between shot blasting and plasma spraying causes a marked decrease in bond strength [41].

Cleanliness of the substrate surfaces:

The substrate to be sprayed must be free from any dirt or grease or any other material that might prevent intimate contact of the splat and the substrate. For this purpose the substrate must be thoroughly cleaned by acetone (ultrasonically, if possible) before spraying. Spraying must be conducted immediately after grit blasting and cleaning. Otherwise on the nascent surfaces, oxide layers tend to grow quickly and moisture may also affect the surface. These factors deteriorate the coating quality drastically [41].

Bond coat:

Materials like ceramic cannot be sprayed directly onto metals, owing to a large difference between their thermal expansion coefficients (α). Ceramics have a much lower value of " α " and hence undergo much less shrinkage as compared to the metallic base to form a surface in compression. If the compressive stress exceeds a certain limit, the coating gets peeled off. To alleviate this problem a suitable material, usually metallic of intermediate a value is plasma sprayed onto the substrate followed by the plasma spraying of ceramics. Bond coat may render itself useful for metallic topcoats as well. Molybdenum is a classic example of bond coat for metallic topcoats. Molybdenum adheres very well to the steel substrate and develops a somewhat rough top surface ideal for the topcoat spraying. The choice of bond coats depends upon the application. For example, in wear application, an alumina and Ni-Al top and bond coats combination can be used [42]. In thermal barrier application, CoCrAlY or Ni-Al bond coat [43] and zirconia topcoat are popular. Ceramic coatings when subjected to hertzian loading deform elastically and the metallic substrate deforms plastically. During unloading, elastic recovery of the coating takes place, whereas for the metallic substrate a permanent set has already taken

place. Owing to this elastoplastic mismatch the coating tends to spall off at the interface. A bond coat can reduce this mismatch as well.

Cooling water:

Distilled water was used for cooling purpose. Normally a small volume of distilled water is recirculated into the gun and it is cooled by an external water supply from a large tank. Sometime water from a large external tank is pumped directly into the gun [44].

2.5.2 Process Parameters in Plasma Spraying

In plasma spraying parameters are interrelated with each other, which determine the degree of particle melting, adhesion strength and deposition efficiency of the powder. Deposition efficiency is the ratio of amount of powder deposited on substrate to the amount fed to the gun as raw material. An elaborate listing of these parameters and their effects are reported in the literature [45]. Some important parameters and their roles are listed below:

Arc power:

It is the electrical power drawn by the consumable/non-consumable arc. The power is injected into the plasma gas, which in turn gain energy from plasma stream. Part of the energy of power is dissipated as radiation and also by the gun cooling water. Arc power determines the mass flow rate of a given powder that can be effectively melted by the arc with a appropriate contact time. Deposition efficiency improves to a certain extent with an increase in arc power, since it is associated with an enhanced particle melting [46]. However, increasing power beyond a certain limit may not cause a significant improvement. On the contrary, once a complete particle melting is achieved, a higher gas temperature may prove to be harmful. Because at some point vaporization may take place, which is responsible for lowering the deposition efficiency.

Plasma gas:

Generally Nitrogen or Argon doped with about 10% Hydrogen or Helium is used as a plasma gas. The major constituent of the gas mixture is known as primary gas and the minor is known as the secondary gas. The neutral molecules are subjected to the electron bombardment resulting in their ionization. Both temperature and enthalpy of the gas increase as it absorbs energy. Since nitrogen and hydrogen are diatomic gases, they first undergo dissociation followed by ionization. Thus they need higher energy input to enter the plasma state. This extra energy increases the enthalpy of the plasma. On the other hand, the mono-atomic plasma gases, i.e. argon or helium, approach a much higher temperature in the normal enthalpy range. Good heating ability is expected from them for such high temperature [47]. In addition, hydrogen followed by helium has a very high specific heat, and therefore is capable of acquiring very high enthalpy. When argon is doped with helium the spray cone becomes quite narrow which is especially useful for spraying on small targets.

Carrier gas:

Usually the primary gas itself is used as a carrier gas. The flow rate of the carrier gas is an important factor. If the flow rate is very high then the powders might escape the hottest region of the jet and a very low flow rate cannot convey the powder effectively to the plasma jet (as shown in Fig 2.6) [45]. There is an optimum flow rate for each powder at which the fraction of unmelted powder is minimum and hence the deposition efficiency is maximum.

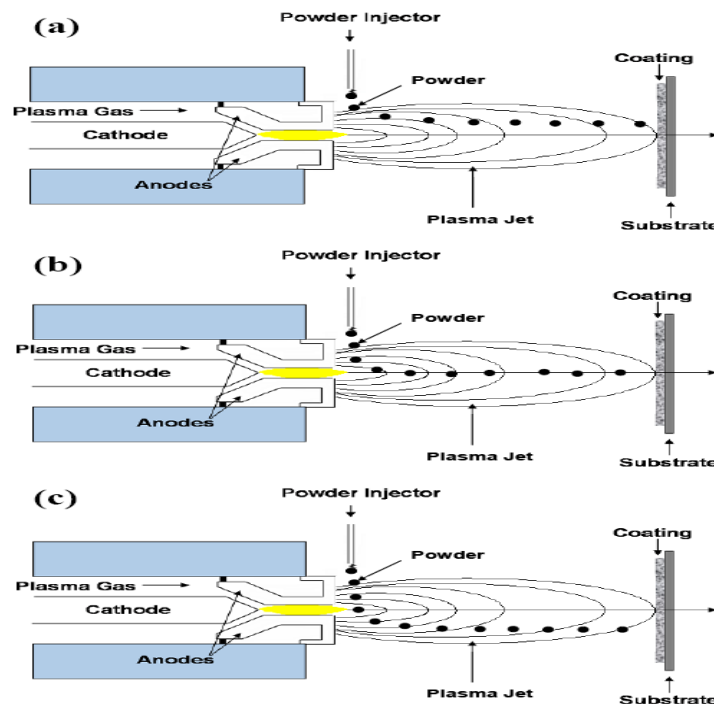


Figure 2.6 Carrier Gas Flow Rate a) too low b) correct c) too high [35].

Mass flow rate of powder:

Ideal mass flow rate for each powder has to be determined. Spraying with a lower mass flow rate keeping all other conditions constant results in under utilization and slow coating buildup. On the other hand, a very high mass flow rate may give rise to an incomplete melting resulting in a high amount of porosity in the coating. The un-melted powders may bounce off from the substrate surface as well keeping the deposition efficiency low [45].

Powder related variables:

These variables are powder size, shape and size distribution, phase composition, processing history etc. They constitute a set of extremely important parameters. For example, in a given situation if the powder size is too small it might get vaporized. On the other hand a very large particle may not melt substantially and therefore will not deposit. The shape of the powder is also quite important. A spherical powder will not have the same characteristics as the angular ones, and hence both could not be sprayed' using the same set of parameters [48].

Stand-off-distance (Spray Distance):

It is the distance between the tip of the gun and the substrate surface (shown in Fig 2.7). A long distance may result in freezing of the melted particles before they reach the target, whereas a short standoff distance may not provide sufficient time for the particles in flight to melt and may erode the substrate surface [41, 45]. A larger fraction of the un-melted particles go in the coating owing to an increase in stand-off-distance.

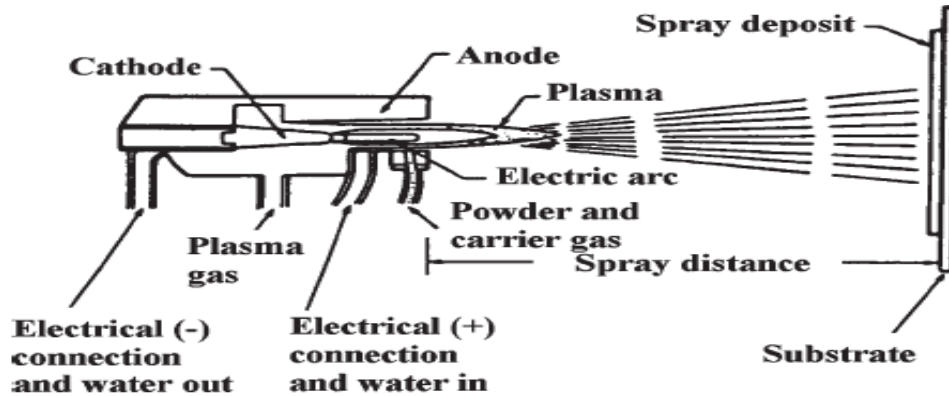


Figure 2.7 schematic presentation of electrode arrangement and spraying distance.

Spraying angle:

Angle is one of an important factor during spraying. It is responsible for splat formation. Different angle chosen by considering different material (ductile/ brittle substrate). The influence of spraying angle on the cohesive strength of chromia, zirconia 8wt% yttria and molybdenum has been investigated, and it has been found that the spraying angle does not have much influence on the cohesive strength of the coatings [49]. SEM examination of splat morphologies obtained from impacting droplets at substrate with different angle of (a) 0°, (b) 10°, (c) 20°, (d) 30°, (e) 40°, (f) 50°, (g) 60° are shown in Fig 2.8.

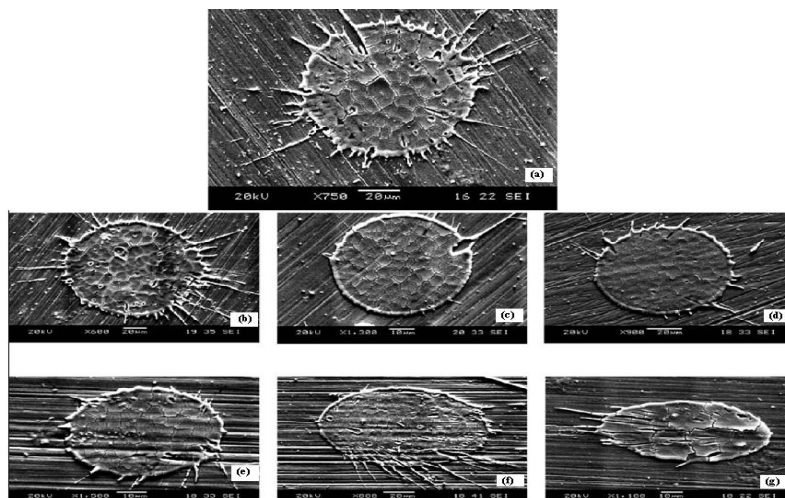


Figure 2.8 SEM examination of splat morphologies obtained from impacting droplets at substrate inclinations of (a) 0°, (b) 10°, (c) 20°, (d) 30°, (e) 40°, (f) 50°, (g) 60° [41].

Substrate cooling:

During a continuous spraying, the substrate might get heated up and may develop thermal stresses related distortion accompanied by a coating peel-off. This is especially true in situations where thick deposits are to be applied. To reduce the substrate temperature, it is kept cool by an auxiliary air supply system. In addition, the cooling air jet removes the unmelted particles from the coated surface and helps to reduce the porosity.

Angle of power injection:

Coating Powders can be injected perpendicularly, coaxially or obliquely in to the plasma jet. The residence time of the powders material will vary with injection angle for a given carrier gas flow rate. The residence time will influence the degree of melting of a given powder. For example, to melt high melting point materials a long residence time needed and hence oblique injection may prove to be better. The angle of injection is found to influence the cohesive strength and adhesion strength of the coatings [19].

2.5.3 Mechanism of Coating Formation in Plasma Spraying Process

Plasma spray is formed by the impact of a stream of particles from nozzle striking the substrate surface, the major controlling factors which influenced by the structure of a particular coating are the velocity, temperature and size distribution of the incident particles. Ideally all the surface striking particles would be completely molten. Unmolten particles may bounce off reducing the deposition efficiency and partly melted particles are incorporated within the deposit modifying its microstructure and properties [50]. Coatings are formed by the build up of successive layers of molten droplets which flatten and solidify on impact to give lamellar microstructure. When a liquid droplet strikes the surface at low velocity, it flattens to a disc (shown in Fig 2.9) [51] which then come to the equilibrium shape of spherical cap to form a cone and the spreads again to the final equilibrium shape determined by the static surface tension forces (shown in Fig 2.10). At high impact velocities the thin sheet of liquid becomes unstable and disintegrates at the edge into many small droplets i.e. splashing occurs. Its cooling rate then rapidly increases by conduction from molten particle to surface of the substrate. The cooling rates achieved are of the order of 10^6 - 10^7 Ksec⁻¹ [52]. P. Fauchais and co-worker also investigated on coating generation and predicted a model for calculating the splat-quenching rate [28]. It was observed that some metastable phases are formed during cooling, like γ -alumina rather than α -alumina which was explained on the basis of nucleation kinetics, i.e. γ - alumina was easily nucleated because of lower interfacial energy between crystal and the liquid and at sufficiently rapid cooling rates, the metastable form is retained at room temperature [53, 54]. Mechanical behavior of the coatings is limited to the degree of contact between the lamellae within the coatings (cohesion strength) and between the lamellae and the substrate (adhesion strength) rather than the nature of bonds in regions of good contact. This study was made on alumina coatings. The low apparent area of contact may be due to entrapped gases and other asperities between the impinging droplet and the substrate [55]. So surface grit blasting and cleaning of the substrates is necessary for better bonding between coating and the substrate [56].

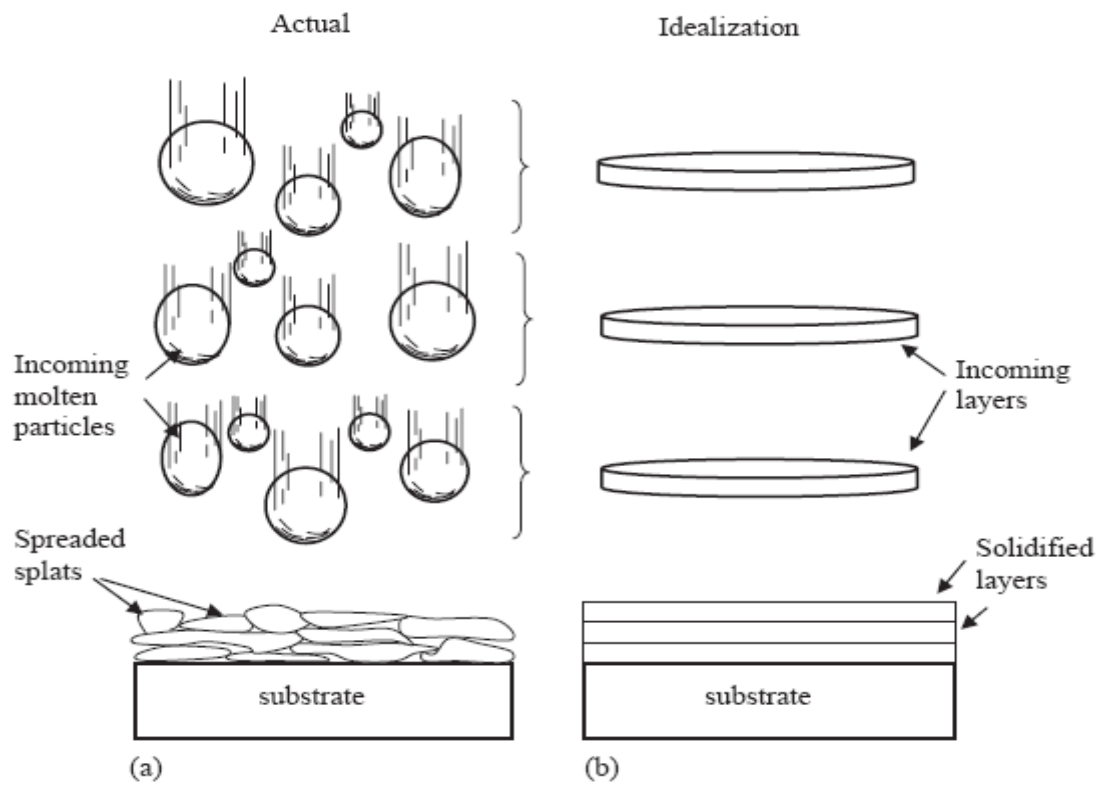


Figure 2.9 Schematic of the (a) physical plasma spray process and (b) its idealization for modeling [51].

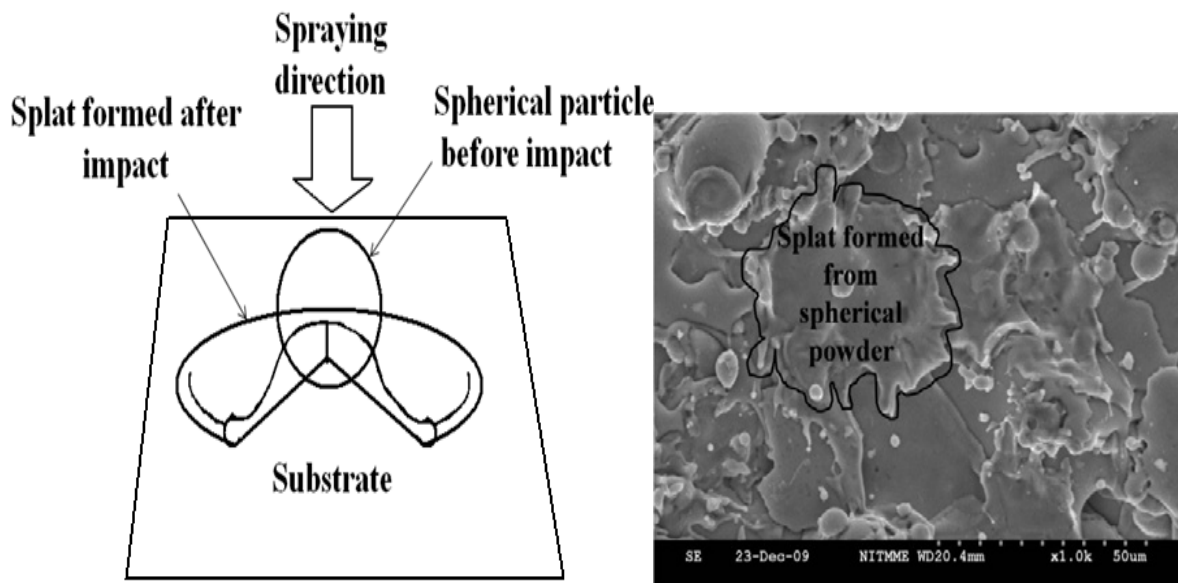


Figure 2.10 Splat formations after the impact of the spherical powder during spraying.

2.6 INDUSTRIAL APPLICATIONS OF PLASMA SPRAYING

There has been a gradual increasing in the number of applications of plasma sprayed coatings. Availability of hardware and adaptability of the technique are the main cause of this growth. This technique has been successfully applied to a wide range of industrial technologies from aerospace industry to biomedical industry [57]. Some of the typical applications are given below:

Steel Industry

In the steel working industry plasma surfacing roller used to handle very heavy thermal loads of hot steel. In addition, slag from steel production must be reckoned with, and in zinc production, corrosive attack from the molten zinc. Plasma coating have been qualified for use on both new parts and repair applications in steel production equipments [58, 59].

Aircraft Industry

Aircraft jet engine parts are subjected to serve mechanical, thermal stresses and chemical. A jet engine has a number of construction nodes where plasma coating is employed with much success in order to protect them. Some typical plasma sprayed parts are face of the blower box, compressor box and disc, fuel nozzles, guide bearing, blades, combustion chambers etc. [60]. plasma spray is used to replace hard chromium plate is that of aircraft landing gear components.

Automotive industry and the production of combustion engines:

Plasma sprayed coatings used in automotive industries endure higher working pressure and temperature with improve in good friction properties, wear resistance, resistance against burn-off and corrosion due to hot combustion products and resistance against thermal loading. Some of the several applications developed for the automotive industry at the Slovak Academy of Sciences (SAV) in Bratislava are spraying torsion bars with aluminium coatings against corrosion. The plasma spraying technology is introduced in the production of gearshift forks for gearboxes in fiat car factory and on the critical parts of big Diesel engines [58]. The cylinder bores of the engines are coated by means of a special rotating plasma gun manipulator, which can apply the coating to the interior of the small bores with a wear resistant surface.

Medical Industry

For strong and durable anchoring of orthopedic implants such as artificial hip joints, surface finish is of great importance. Plasma spray coatings applied using the vacuum, are purposely sprayed with a much fissured surface that allows the bone to grow into it. There are plasma coatings that act as a biocompatible titanium coating or bioactive hydroxy apatite coatings, which actively accelerates the growth of the natural bone into the surface of the prosthesis [61, 62].

Gas Turbine industry

sprayed coatings are used In both stationary and flight gas turbines in many different places and for many different functions [63].

Electrochemical industry:

In the electromechanical and computer industries the electrically conductive Al, Cu, W and the semi-conductive and insulating ceramic layers are widely used. Some contacts of electrodes, e.g. the spark gaps of nuclear research equipment, are produced of massive tungsten. Modern electrodes can replace such electrodes with a sprayed tungsten coating about 0.5mm thick. This electrode ensures short- time passages of 300,000A current with a life of several hundred switching [64, 65].

Hydraulic industry

The range of possible applications in this field of Hydraulic machines is very extensive, mainly in water power plants, in production and work of pumps, where many parts are subjected to combined effects of wear, corrosion, erosion and cavitations [66].

Rolling mills

The wear resistant coatings are used in Rolling mills and pressing shops to renovate the heavy parts of heavy-duty machines whose replacement would be very costly [67]. Several applications in this field are presented herewith:

- Rolling strand journals being repaired by giving a coating layer of stainless steel. Blooming roll mill journal renovated with a NiCrBSi layer.
- Gears of rolling mill gearbox being renovated by a wear resistance coating.
- Conveyer rollers in plate production with zirconia based refractory coatings.
- To repair a rolling mill slide and the plungers of a forging press a hard wear resistance is applied.

Foundry mills

Heat resistant plasma coating is widely used for foundry and metallurgical equipment where molten metal or very high temperatures are encountered. This equipment includes the sliding plugs of steel ladles with alumina or zirconia coatings. Oxygen tubes, cast iron moulds in continuous casting of metals are also employed plasma spraying [68].

Chemical plants:

The base metal of machine parts is subjected to different kind of wear and corrosion continuously in contact with chemical reagents. In these cases plasma coatings are applied to protect the base metal. They can be used for various bearing surfaces, tubes, burners, blades, shafts, parts of cooling equipments etc [69].

Textile industry:

For the first time, Czechoslovakia textile industry employed Plasma spraying technique. Plasma spraying has replaced the conventional technologies of anodization, chrome plating and chemical surface hardening. Advantages of this technique are for different critical machinery parts: Different thread guiding & distribution rollers, distribution plates, ridge thread brakes, driving & driven rollers, tension rollers, thread brake caps, gallets, lead-in bars etc. High wear

resistance coatings are required on machinery parts which are in contact with synthetic fibers. For this purpose especially $\text{Al}_2\text{O}_3 + 3\% \text{TiO}_2$, Cr_2O_3 , $\text{WC} + \text{Co}$, $\text{Al}_2\text{O}_3 + 13\% \text{TiO}_2$ are applied [70, 71]. These coatings with hardness ranging from 1800 - 2600 HRV are extraordinarily dense, have high wear resistance and provide excellent bonding with the substrate. Plasma spraying has following advantages in textile industries:

- Replacement of worn out parts is minimized and hence reduces the idle times.
- Physical and mechanical properties of fibers are improved.
- Revolution speed of these lighter parts can be increased.
- Shelf life of the textile machinery parts with plasma sprayed coating last 5 to 20 times longer than parts coated by chrome plating or another classical technique.
- Economic savings are realized considerably by substituting heavy steel or cast iron parts with aluminum or durable ones with wear- resistant coatings.

Paper and printing industry:

The machinery in the paper and printing industry is usually quite large and is subjected to considerable wear from the sliding and friction contact with the paper products. Affected machinery parts are typically Paper drying rolls, filters, sieves, roll pins, printing rolls, tension rolls and other parts of printing machines. Spraying of oxide layers carried out for its economical solution.

Here oxide layers composed of Al_2O_3 with 3 to 13 % additions of TiO_2 , Cr_2O_3 or MnO_2 are applied. Cast iron rolls are typically first sprayed with NiCr 80/20, 50 μm thick and then over it 0.2mm thick $\text{Al}_2\text{O}_3 + 13\% \text{TiO}_2$ layer is coated [72]. The special advantages are mentioned below:

- Ensures corrosion resistance of rolls i.e. the base metal
- Resistance of oxide layers against printing inks extends the life of machine parts
- Production cost is reduced considerably
- Coating resulted to the so-called “orange peel” phenomena, surface finishing obtainable that prevents paper foil, dyes etc. from sticking and allows their proper stretching.

Glass industry:

Molten glass rapidly wears the surface of metal when that comes in contact with it. In order to protect the metal tools, plasma sprayed coatings are made on to it [73].

2.7 WEAR

Wear is a natural process of a material in which damage/deterioration of its surface occurs. Wear may be defined as damage to the solid surface caused by the removal or displacement of material by the mechanical action of a contacting solid, liquid or gas which occurs as a natural consequence when two surfaces in relative motion interact with each other. Widely varied wearing conditions causes wear of materials. It may be due to surface damage or

removal of material from one or both of two solid surfaces in a sliding, rolling or impact motion relative to one another. In 1940 Holm [74] starting from the atomic mechanism of wear, calculated the volume of substance worn over unit sliding path. different types of wear (Tribology) have been investigated by different researcher by taking different materials [75-86]. In these investigation various wear theories are taken in which Physico-Mechanical characteristics of the materials and the physical conditions (i.e. the resistance of the rubbing body and the stress state at the contact area) are taken in to consideration. Wear of metals depends on many variables for which wear investigation programs must be planned systematically. It should be understood that the real area of contact between two solid surfaces compared with the apparent area of contact is invariably very small, being limited to points of contact between surface asperities. The load applied to the surfaces will be transferred through these points of contact and the localized forces can be very large. wear is not an intrinsic material property but characteristics of the engineering system which depend on load, temperature, speed, hardness, the environmental conditions and presence of foreign material [87]. During relative motion, material on contacting surface may be removed from a surface, may result in the transfer to the mating surface, or may break loose as a wear particle. The wear resistance of materials is related to its microstructural characteristics may take place during the wear process and hence it seems that in wear research emphasis is placed on microstructure [88].

2.8 TYPES OF WEAR

In most basic wear studies dry friction has been investigated where the problems of wear have been a primary concern to avoid the influences of fluid lubricants. Dry friction is defined as friction under not intentionally lubricated conditions but it is well known that it is friction under lubrication by atmospheric gases, especially by oxygen [89]. A fundamental scheme to classify wear was outlined by Burwell [90], include five distinct types of wear, namely (1) Abrasive (2) Adhesive (3) Erosive (4) Surface fatigue (5) Corrosive.

2.8.1 Abrasive Wear

Abrasive wear or abrasion account for most failures in any industrial equipment, which can originate from of the two rubbing surfaces, rubbing against each other. It can defined as the wear that is caused by the displacement of material from a solid surface due to hard particles or protuberances sliding along the surface and cutting grooves on the softer surfaces. In sliding mechanisms, abrasion can arise from the existing asperities on one surface (if it is harder than the other), from the generation of wear fragments which are repeatedly deformed and hence get work hardened for oxidized until they became harder than either or both of the sliding surfaces, or from the adventitious entry of hard particles, such as dirt from outside the system. Two body abrasive wear occurs when one of the harder surface cuts material away from the second of less harder. Abrasives can act as in grinding where the abrasive is fixed relative to one surface or as in lapping where the abrasive tumbles producing a series of indentations as opposed to a scratch. According to the recent tribological survey, abrasive wear is responsible for the largest amount of material loss in industrial practice [91].

2.8.2 Adhesive Wear

Adhesive wear can be defined as wear due to localized bonding between contacting solid surfaces leading to material transfer between the two surfaces or the loss from either surface [92]. In this wear it is necessary for the surfaces to be in intimate contact with each other. To obstruct for adhesion wear it is necessary for two surface to held apart by lubricating films, oxide films etc. Fretting wear is also this type of wear mechanism.

2.8.3 Erosive Wear

Erosive wear can be defined as the progressive loss of original material from a solid surface due to mechanical interaction between that surface and a fluid, a multi-component fluid, or impinging liquid or solid particles [ASTM G40-99] [93]. When the angle of impingement is small, the wear produced is closely similar to abrasion. When the angle of impact is normal to the surface, more loss of material occurs. The erosion mechanism depends on the material (brittle / ductile). So erosion has been divided into brittle and ductile erosion. Ductile materials fail as a result of impacting particles causing localized plastic flow that exceeds the critical strain to failure in the local areas. When the erodent particles in either gas or liquid carrier fluid strikes the surface of a ductile material, they initially extrude thin microplatelates of the base material from craters which are formed at the sites of impacts and then the platelates are then further flattened. After a small number of particles have impacted the same localized area, the extruded platelates would have been strained to their critical strain and fracture of portions of the platelate will occur [94]. The mechanism of erosion of brittle materials (i.e. ceramic type materials) is considerably different. Brittle materials are removed by a cracking and chipping mechanism. Here erosion occurs by the propagation and intersection of cracks produced by the impacting particles. The dense, columnar grain, outer scale cracks are chipped away, while the small equiaxed grains of the inner scale initially form hertzian cone cracks or ring cracks. Subsequently, at latter times, increased loading leads to increasing number of ring cracks leading to chipping away of the inner scales [94, 95].

Erosion modes can be subdivided according to the erosive medium as:

- ❖ **Solid particle erosion:** It is the removal of material by repeated impact of tiny solid particles in gaseous or liquid medium [96]. In this erosion, a series of particles strike and rebound from the surface and cause a force on the material due to their deceleration. This erosion depend on velocity, size, amount of erodent particle
- ❖ **Liquid impingement erosion:** When small drops of liquid are striking on the surface of a solid at a high speed (~1000m/s) and very high pressures are experienced, exceeding the yield strength of most materials, this erosion occurs. Thus plastic deformation or fracture may result from a single impact and repeated impacts may lead to pitting and erosive wear. Here liquids need not contain particles to damage to a solid surface [97].

- ❖ **Cavitation erosion:** Cavitation is defined as the formation and subsequent collapse of cavities or bubbles within liquid. Cavitation erosion is the mechanical damage of a solid surface caused by the cavities or bubbles collapsing either at or near the surface [98].
- ❖ **Slurry erosion: when erosion occurs by** a mixture of solid particles in a liquid with a high velocity, then it can be called as slurry erosion [99].
- ❖ **Erosion-Corrosion:** This is basically erosion enforced by corrosion mechanism. Corrosion may enhance the erosion rate through preferential dissolution or it may inhibit erosion through the formation of a passive film. Erosion-corrosion interaction is the potential synergy between the two processes. When metal alloys are exposed to the combined degradation mechanisms of corrosion and small solid particle erosion, combinations of the loss mechanisms of ductile and brittle materials occur, but primarily the brittle behavior [94].

2.8.4 Surface Fatigue Wear

Wear arises from material fatigue is called as surface Fatigue Wear. This wear became dominant, when a solid is subjected to cyclic loading involving tension and compression above a certain critical stress. Repeated loading causes the generation of micro cracks at the site of a pre-existing point of weakness and leads to join of micro-void and form the crack. When crack reaches the critical size, it changes its direction to emerge at the surface, and thus flat sheet like particles is detached during wearing. The number of stress cycles required to cause such failure decreases as the corresponding magnitude of stress increases [100].

2.8.5 Corrosive Wear

Thermodynamically unstable metals with oxygen to form an oxide and gradually develop scales or layers on the surface. These layers are very weak or unprotected which allows gradual degradation of metal on the surface. Deterioration also cause by the effects of the atmosphere, acids, gases, alkalis, etc. This type of wear creates pits and perforations and may eventually dissolve metal parts [101].

2.9 SYMPTOMS OF WEAR

Wear is a characteristic of the system & its surrounding and is influenced by many parameters. So it is necessary to understand the wear mechanism to protect the metal. In Laboratory scale investigations, individuals of tribo-systems are carefully control and study the effects of different variables on the wear behaviour of the coating. The data generated through such research under controlled conditions may help in correct interpretation of the results. A summary of the appearance and symptoms of different wear mechanism is indicated in Table 2.3 [102] and the same is a systematic approach to diagnose the wear mechanisms.

Table 2.3 Different wear mechanism, symptoms and surface appearance.

Type of wear	symptoms	Appearance of worn out surface
Abrasive	Presence of chip-out of surface	Grooves
Adhesive	Metal transfer s prime symptoms	Seizure, catering rough and torn-out surfaces
Erosion	Presence of abrasives in the fast moving fluid and short abrasion furrows	Waves & Troughs
Fatigue	Presence of surface or subsurface cracks accompanied by pits and spalls	Sharp and angular edges around pits
Corrosion	Presence of metal corrosion products	Rough pits and depressions
Delamination	Presence of subsurface cracks parallel to the surface with semi-dislodge or loose flakes	Loose, long and thin sheet like particle
Impacts	Surface fatigue, small sub-micron particles or formation of spalls	Fragmentation, peeling and pitting
Fretting	Production of voluminous amount of loose debris	Roughening, seizure and development of oxide ridges
Electric attack	Presence of micro-craters or a track with evidence of smooth molten metal	Smooth holes

2.10 RECENT TRENDS IN MATERIAL WEAR RESEARCH

Most of wear researches carried out in the 1940's and 1950's were conducted by metallurgical and mechanical engineers to generate data for the protective structural materials of different motor drive, trains, bearings, brakes, bushings and other types of moving mechanical assemblies [103]. It became apparent during the survey that wear of metals was a prominent topic in a large number of the responses regarding some future priorities for research in tribology. Much of the wear research conducted over more than past 50 years is in ceramics, polymers, composite materials and coatings [104]. Now-a-days this type of research are in rapid progress in different country in different part of the world.

2.11 WEAR RESISTANT COATINGS

Today a variety of materials, e.g., carbides, oxides, metallic, etc. are available commercially for protecting the metal surface. The wear resistant coatings can be classified into the following categories: [12]

(i) Carbides: WC, TiC, ZrC, Cr_2C_3 , SiC, etc.

(ii) Oxides: Cr_2O_3 , Al_2O_3 , TiO_2 , ZrO_2 etc.

(iii) Metallic: NiCrAlY, Triballoy etc.

(iv) Diamond

The choice of a material depends on the application. However, the ceramic coatings are very hard and hence can provide more abrasion resistance than their metallic counterparts.

2.11.1 Carbide Coatings

For wear and corrosion applications WC is very popular among all carbides [105]. The WC powders are clad with a cobalt layer. During spraying the cobalt layer undergoes melting and upon solidification form a metallic matrix in which the hard WC particles remain embedded. Spraying of WC-Co involves a close control of the process parameters such that only the cobalt phase melts without degrading the WC particles. Such degradation may occur in two ways: one is Oxidation of WC leading to the formation of CoWO_4 and WC_2 [106] and another one is dissolution of WC in the cobalt matrix leading to a formation of brittle phases like CoW_3C which embrittles the coating [107]. An increase in the spraying distance and associated increase of time in flight leads to a loss of carbon and a pickup of oxygen. As a result the hardness of the coating decreases [108]. An increase in plasma gas flow rate reduces the dwell time and hence can control the oxidation to some extent. However, it increases the possibility of cobalt dissolution in the matrix [109]. The other option to improve the quality of such coating is to conduct the spraying procedure in vacuum [107]. some carbides like TiC, TaC and NbC are provided along with WC in the cermet to improve upon the oxidation resistance, hot strength, and hardness. A coating of Cr_3C_2 with Ni-Cr alloy cladding is known for its excellent sliding wear resistance, superior oxidation and erosion resistance, but its hardness is lower than that of WC. After spraying in air, Cr_3C_2 loses carbon and transforms to Cr_7C_3 . Such transformation generally improves hardness and erosion resistance of the coating [110].

2.11.2 Oxide Coatings

Metallic coatings and metal containing carbide coatings sometime are not suitable in high temperature environments in both wear and corrosion applications due to formation of oxidation or decarburization. In such case the material of choice can be an oxide ceramic coating, e.g., Al_2O_3 , Cr_2O_3 , ZrO_2 , TiO_2 or their combinations [111]. However, a high wear resistance, and chemical and thermal stability of these materials are counterbalanced by the disadvantages of low values of thermal expansion coefficient, thermal conductivity, mechanical strength, fracture toughness and somewhat weaker adhesion to substrate material. The thickness of these coatings is also limited by the residual stress that grows with thickness. Therefore, to obtain a good quality coating it is essential to exercise proper choice of bond coat, spray parameters and reinforcing additives.

2.11.3 Metallic Coatings

Metallic coatings can be easily applied by flame/plasma spraying or welding techniques making the process very economical. Metallic wear resistant materials are classified into three categories:

- (i) Cobalt based alloys
- (ii) Nickel based alloys
- (iii) Iron based alloys

The common alloying elements in a cobalt-based alloy are Cr, Mo, W and Si. The microstructure is constituted by dispersed carbides of M₇C₃ type in a cobalt rich FCC matrix. The carbides provide the necessary abrasion resistance and corrosion resistance. Hardness at elevated temperatures is retained by the matrix [112, 113]. The principal alloying elements in Ni-based alloys are Si, B, C and Cr. The abrasion resistance can be attributed to the formation of extremely hard chromium borides. Besides carbides, Laves phase is also present in the matrix [112]. Iron based alloys are classified into pearlitic steels, austenitic steels, martensitic steels and high alloy irons. The principal alloying elements used are Mo, Ni, Cr and C. The softer materials, e.g., ferritic, are for rebuilding purpose. The harder materials, e.g., martensitic, on the other hand provide wear resistance. Such alloys do not possess much corrosion, oxidation or creep resistance. Nickel aluminide is another example of coating material for wear purpose. The prealloyed Ni-Al powders, when sprayed, react exothermically to form nickel aluminide. This reaction improves the coating substrate adhesion. In addition to wear application, it is also used as bond coat for ceramic materials. NiCoCrAlY is an example of plasma sprayable superalloy. It shows an excellent high temperature corrosion resistance and hence finds application in gas turbine blades. In addition, it serves as a bond coat for zirconia based thermal barrier coatings [114].

2.11.4 Diamond Coatings

In some industrial application diamond films are commonly produced by CVD, plasma assisted CVD, laser ablation technique and ion beam deposition [115, 116]. Such coatings are used in electronic devices and ultra wear resistant overlays. The limitation of the aforesaid methods is their slow deposition rates. The DIA-JET process involving DC Ar/H₂ plasma with methane gas supplied at the plasma jet is capable of depositing diamond films at a high rate [117]. However, the process is extremely sensitive to the process parameters. Deposition of diamond film is also possible using an oxy-acetylene torch [118]. One significant limitation of a diamond coating is that it cannot be rubbed against ferrous materials, owing to a phase transformation leading to the formation of other carbon allotropes [119]. Diamond films are tested for the sliding wear against abrasive papers, where wear progresses by micro fracturing of protruding diamond grits. The process continues till the surfaces becomes flat and thereafter wear progresses by an interfacial spalling. Therefore, the life of the coating is limited by its thickness [120].

2.12 UTILIZATION OF FLY ASH AS WEAR RESISTANT COATINGS

Fly ash is the industrial waste in all iron and steel industries. Fly ash is a finely divided by-product with particle size varying from 0.5 to 100 μm . It is refractory and abrasive in nature as it contains hard oxide materials. The effective utilization of these wastes not only decreases environmental pollution, but also produces high value-added products [121, 122]. The chemical composition of fly ash is not constant everywhere due to the nature of different product in different industries. However, its main constituents are silicon dioxide (SiO_2), aluminium oxide (Al_2O_3) and iron oxide (Fe_2O_3), and are hence a suitable source of aluminum and silicon. In previous time, silica and alumino-silicate bricks have been preferred as refractory materials in many industrial applications due to their high wear resistance and high load bearing capacity at high temperatures. During the last decade, although a large number of investigations have been carried out for development of plasma spray ceramic coatings. Fly ash is a substitute for high cost conventional spray powder in high performance industrial coatings [123]. It can be utilized to develop ceramic coatings on metal substrate. In this context, Mishra et al. has been investigated some experiments on fly-ash composite to spray on different type of metal by plasma spraying [124-128]. Buta singh et.al have investigated the fly ash coating obtained by shrouded plasma spray process on carbon steel and found it to be effective to increase the oxidation and salt corrosion resistance of the given carbon steel [129]. Fly-ash composite coatings, such as fly-ash+zinc coatings [130] and fly-ash+ Na-geopolymer [131] have been extensively studied. The properties of fly ash has been studied by Tiwari and Saxena and coatings that were developed have shown improved corrosion and abrasion resistance and also better resistance to chemicals (5% Na_2CO_3 , 1% NaOH , and 2% H_2O [132].

2.13 EROSION WEAR OF CERAMIC COATINGS

When equipments/ parts are operated in industrial hostile environment involving two or more damage modes such as corrosion-erosion or corrosion-wear; many coatings perform poorly due to the synergistic action of wear and corrosion [133]. Considerable efforts have been continuously made to develop high-performance coatings that can resist corrosive wear encountered in various industries such as oil, petroleum, mining, sand and chemical industries [134]. Now-a-days Plasma sprayed coatings (one of a Thermal spray technique) are used as thermal barriers and abrasion, erosion or corrosion resistant coatings in a wide variety of applications owing to their high hardness and high temperature performance [135]. Almost any material can be used for plasma spraying on almost any type of substrate. The high temperatures of plasma spray processes permit the deposition of coatings for applications in areas of liquid and high temperature corrosion and wear protection and also special applications for thermal, electrical and biomedical purposes [136, 137]. Superalloys can be used as protective coatings [138, 139]. Lee et al. investigated the liquid impact erosion resistance of 12Cr steel and stellite 6B coated with TiN by reactive magnetron sputter ion plating [140]. The erosion wear behaviour and mechanism of several kinds of middle temperature seal coatings were investigated by Yi Maozhong et al. [141]. The results show that the relationship between the erosion mass loss and

the erosion time is linear, the coatings hold a maximum erosion rate at 60° impact angle, and the relation between the erosion rate and the impact speed is an exponential function. Branco et al. examined room temperature solid particle erosion of zirconia and alumina-based ceramic coatings, with different levels of porosity and varying microstructure and mechanical properties [142]. The erosion tests were carried out by a stream of alumina particles with an average size of 50µm at 70 m/s, carried by an air jet with impingement angle of 90°. The results indicate that there is a strong relationship between the erosion rate and the coating porosity.

Chapter 3

Experimental set up and Methodology

- Introduction
 - Development of coatings
- Characterization of feedstock
 - Characterization of coatings
- Erosion wear behavior of coatings

Chapter 3

Experimental set up and Methodology

3.1 INTRODUCTION

This chapter explains about procedure of different experimental processes used to prepare the coatings and to characterize. Before preparation of coating, some basic process required for substrate material i.e. size measurement of coating powder, Grit blasting & cleaning of substrate. After plasma spraying, the coated materials have been subjected to a series of characterization test i.e. microstructural characterization of the surfaces, and microstructural characterization of substrate-coating interface, X - ray diffraction studies, adhesion test, surface roughness test, porosity measurement, micro-hardness measurement, erosion wear test etc. Each process are briefly described here.

3.2 DEVELOPMENT OF COATINGS

3.2.1 Preparation of Powder

Fly ash of 60 weight percentage premixed with 20 weight percentage of quartz and 20 weight percentage of illmenite are mechanically milled in a FRITSCH-Planetary ball mill for 3 hours to get a homogenized product. There are 4 numbers of zirconia balls of 20gm and 20 numbers of zirconium balls of 2gm present in the planetary ball mill. The powders obtained were sieved by the help of a Roto-Tap Sieve Shaker Machine by using Laboratory test sieves (ISO R565). Required size of powder mixture for spraying are collected.

3.2.2 Preparation of Substrate

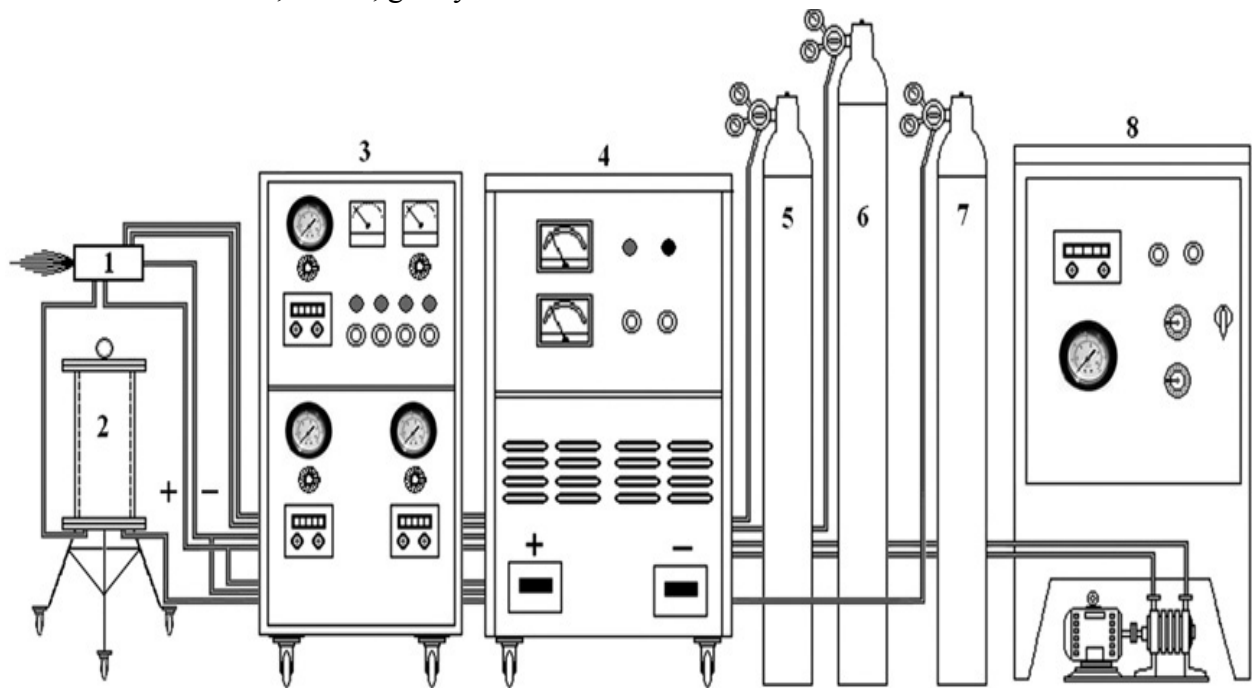
Two Commercially available metal: Mild Steel and Copper have been chosen as substrate materials. These substrates were circular disc having dimension of 1 inch diameter and 3mm thickness. The specimens were grit blasted at a pressure of 3 kg/cm² using alumina grits (grit size of 60). Stand-off-distance was kept between 120-150 mm for blasting. Surface roughness of the substrates was approximately 5 Ra. The grit blasted specimen surface was cleaned with acetone in an ultrasonic cleaning unit. Plasma spraying was immediately carried out after cleaning.

3.2.3 Plasma Spray Coating Deposition

The plasma spray deposition was done at the Laser and Plasma Technology Division, Bhaba Atomic Research Center, Mumbai. 40kW DC non-transferred arc mode Conventional atmospheric plasma spraying (APS) set up was used. In plasma torch input power level was varied from 11kW to 21 kW, by controlling the gas flow rate, voltage and the arc current. The powder injection was external from the nozzle and directed towards the plasma. Argon and hydrogen plasma mixture gas used as carrier gas. The powder feed rate of 15 gm/min was kept constant, using a turntable type volumetric powder feeder. A four stage closed-looped centrifugal

pump (water cooling) used for cooling the system, regulated at a pressure of 10kg/cm² supply. The typical arrangement of the plasma spray equipment and schematic diagram of the plasma spraying process are shown in Fig 3.1. The equipment consists of the following units:

- ✓ Plasma spraying equipment
- ✓ Control console
- ✓ Powder feeder
- ✓ Power supply
- ✓ stand-off-distance of torch
- ✓ Torch cooling system (water)
- ✓ carrier gas supply
- ✓ Hoses, cables, gas cylinders and accessories



1. Plasma torch 2. Powder feeder 3. Control console 4. Plasma power source
5. Ar gas cylinder 6. H₂ gas cylinder 7. N₂ gas cylinder 8. Cooling tower

Figure 3.1 General arrangement of plasma spraying equipment.

Argon is taken as the primary plasmagen gas and nitrogen as the secondary gas. The powder mixture are deposited at a spraying angle of 90°. The properties of the coating products are dependent on the spray process parameters. The operating parameters during coating deposition are listed in Table 3.1.

Table 3.1 Operating parameters during coating deposition.

Operating parameters	values
Plasma arc current(amp)	260-500
Arc voltage (volt)	40-44
Torch input power(kW)	11,15,18,21
Plasma gas(argon) flow rate(IPM)	28
Secondary gas(N2) flow rate(IPM)	3
Carrier gas(Ar) flow rate(IPM)	12
Powder feed rate (gm/min)	15
Torch to base distance(TBD)(mm)	100

3.3 CHARACTERIZATION OF FEEDSTOCK

3.3.1 Particle Size Analysis

The particle sizes of the raw materials used for coating (fly ash+quartz+illmenite powder) were characterized using Laser particle size analyzer of Malvern Instrument (PSA).

3.3.2 Compositional Analysis

The compositional analysis of fly-ash was done by wet chemical analysis method [143].

3.4 CHARACTERIZATION OF COATINGS

3.4.1 Scanning Electron Microscopic Studies

By using JEOL JSM-6480 LV scanning electron microscope (SEM), microstructure of raw powder and plasma sprayed coated specimens were studied. The surface morphology as well as the coating-substrate interface morphology of all coatings was observed under the microscope. Here SEM mostly using the secondary electron imaging.

3.4.2 X-Ray Diffraction Studies

X-ray diffraction technique was used to identify the different phases (elemental phase/ intermetallic phase/ crystalline phase/ non-crystalline phase) presents in the coating. XRD analysis was done by using X-Pert MPD system (PAN Analytical). Here Ni-filtered Cu-K α radiation used in X-ray diffractometer. d-values obtained from XRD patterns were compared with the characteristic d-spacing of all possible values from JCPDS cards to obtained the various X-ray peaks. Obtained d-spacing based on the equation:

$$\lambda = 2d\sin\theta$$

3.4.3 Evaluation of Coating Interface Bond Strength

Coating adhesion strength measure by using a special type jig (Fig 3.2) which was fabricated. Cylindrical mild steel dummy samples (length 25 mm, top and bottom diameter 12 mm) were prepared. By punching the surfaces of the dummies were roughened. These dummies were then fixed on top of the coating with the help of a polymeric adhesive. After mounting the dummy on the jig, ultimate tensile stress has been measured by pull-out method (Fig 3.3). This coating pullout test was carried out using the Instron 1195 set up at a crosshead speed of 1 mm/minute. the reading (of the load) at the time of the torn-off moment of coating from the specimen corresponds to coating adhesive strength, was recorded. A typical test set up during testing is shown in Fig 3.4. The test was performed as per ASTM C-633 [144].



Figure 3.2 Jig under the test.



Figure 3.3 Specimen under tension.



Figure 3.4 Adhesion test with Instron 1195 UTM.

3.4.4 Evaluation of Coating Deposition Efficiency

Deposition efficiency can be defined as the ratio of the weight of coating deposited on the substrate to the weight of the expended feedstock [145]. Weighing method is used to measure this. Specimen weighing was done by using a precision electronic balance with ± 0.1 mg accuracy [146]. Each specimen have been weighed before and after coating deposition. G_c known as the difference is the weight of coating deposited on the substrate. G_p is the weight of expended feedstock which can be calculated from the powder feed rate and time of deposition. The deposition efficiency (η) is then calculated using the equation:

$$\eta = \left(\frac{G_c}{G_p} \times 100 \right) \%$$

3.4.5 Coating Thickness Measurement

To measure the thickness of coated material on the substrate, specimen cross section was polished and measured using an optical microscope. Five readings were taken on each specimen and the average value is reported as the (mean) coating thickness.

3.4.6 Hardness Measurement

The coated samples were transversally sliced to form small specimens which containing coating deposition. Coating cross-sections were mounted and polished. Vickers hardness measurement was made using Leitz Micro hardness Tester equipped with a monitor and a microprocessor based controller, with a load of 50 Pa (0.419N) and a loading time of 20 seconds. About four or more readings were taken on each sample and the average value is reported as the data point.

3.4.7 Porosity Measurement

Porosity measurement was done by using the image analysis technique. In this technique, cross section was polished and placed under a microscope (Neomate) equipped with a CCD camera (JVC, TK 870E) [147]. The digitized image is transmitted to a computer equipped with VOIS image analysis software. The total area captured by the objective of the microscope or a fraction can be accurately measured by the software. Hence the total area and the area covered by the pores are separately measured and the surface porosity determined.

3.5 EROSION WEAR BEHAVIOUR OF COATINGS

Solid particle erosion is usually simulated in laboratory by one of two methods: one is “sand blast” method, where particles are carried in an air flow and impacted onto a stationary target and the second one is “whirling arm” method, where the target is spun through a chamber of falling particles. In the present investigation, sand blast type erosion apparatus with angular erodent is used (Fig 3.5). The test is conducted as per ASTM G76 standards [148]. Erosion Test carried out with varying particle sizes, velocities, incidence angles, and particles fluxes in order to generate quantitative data on materials and to study the mechanisms of damage.



(a)

(b)

Figure 3.5 Erosion test set up.

In this work, the jet erosion test rig used whose schematic diagram shown in Fig 3.6 employs a 300 mm long nozzle of 300 mm long and 3 mm bore. The mass flow rate was measured by conventional method. Particles were fed from a simple hopper under gravity into the groove. Velocity of impact is measured using double disc method [149]. This nozzle size permits a wider range of particle types to be used in the testing, allowing better simulations of real erosion conditions.

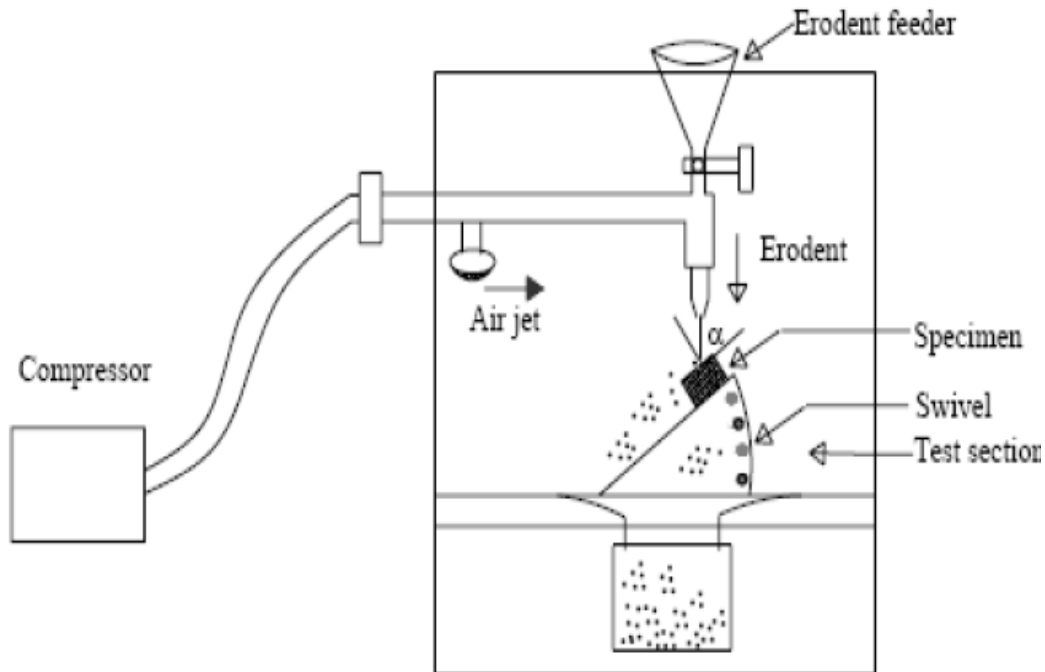


Figure 3.6 Schematic diagram of erosion test rig.

Some of the features of this test set up are:

- Vertical traverse for the nozzle: provides variable nozzle to target stand-off-distance, which influences the size of the eroded area.
- Different nozzles may be accommodated: provides stability to change the particle plume dimensions and velocity range.
- Large test chamber with sample mount (typical sample size 25mm X 25mm) can be angled to the flow direction: by tilting the sample stage, the angle of impact of the particles can be changed in the range of 0°-90° and this will influence the erosion process.

The erosion wear test were carrying out by varying angles (i.e. at 30°, 45°, 60°, 90°), standoff distance (100 mm to 140 mm), pressure (1 bar to 3 bar), time (60 sec to 180 sec). The erosion wear rates were obtained with silicon carbide erodent of 150 μm size. Amount of wear is determined on “mass loss” basis [150, 151]. It was done by measuring the weight change of the samples at regular intervals of time during the test. A precision electronic balance with 0.001 mg accuracy was used for weighing. Erosion rate defined as the coating mass loss per unit erodent mass was calculated.

Chapter 4

Results and Discussion

- Introduction
- Characterization of Coating Material
 - Characterization of coatings
 - Coating performance
 - Discussion

4.1 INTRODUCTION

Thermal plasma spray coatings are deposited on two different metal substrates i.e. Mild Steel and Copper, using fly-ash+quartz+illmenite as the coating material. Characterizations of the coatings were done and the tribological performances of the coating were investigated. The results of various tests are presented and discussed in this chapter.

4.2 CHARACTERIZATION OF COATING MATERIAL

4.2.1 Particle Size Analysis

The particle size distribution of fly ash+quartz+illmenite powder just before spraying was characterized by using Laser particle size analyzer of Malvern Instruments. The particle size distribution of the feedstock is represented in Fig 4.1. The particles are found to be in the range of 40 to 100 micron. Maximum volume fractions of the particles are in the range of 50 micron.

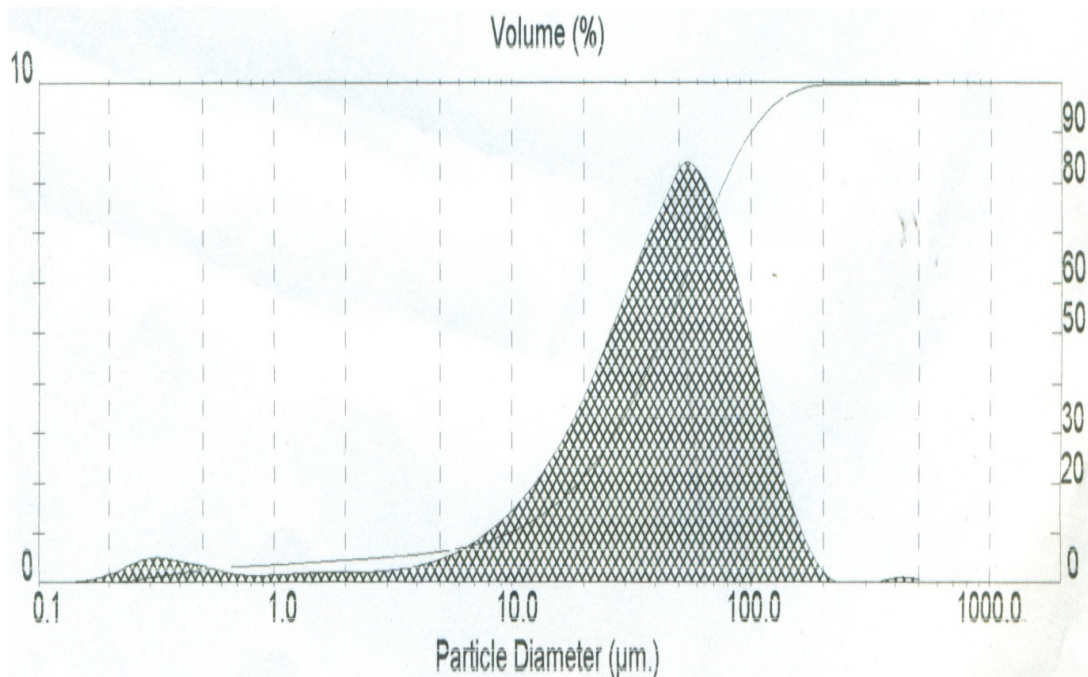


Figure 4.1 Particle size analysis of fly-ash+quartz+illmenite spray coating feedstock.

4.2.2 Chemical Composition Analysis

Fly-ash is collected from Rourkela Steel Plant (CPP-1), Rourkela. The chemical composition analysis of major constituents of fly ash is given in Table 4.1. To this material, quartz powder (SiO_2) and illmenite (FeTi_2O_3) has been added (20 wt% each) to prepare the feedstock.

Table 4.1 Chemical composition of fly-ash.

Compounds	Percentage
SiO ₂	58.00
Al ₂ O ₃	29.30
Fe ₂ O ₃	5.60
CaO	1.05
TiO ₂	1.70
MgO	1.25
P ₂ O ₅	0.25
K ₂ O	0.84
Na ₂ O	0.61
SO ₃	0.41
H ₂ O	0.20

4.2.3 Morphology of powder/raw material for coating

SEM micrographs of fly ash+quartz+illmenite feedstock prior to coating are shown in Fig 4.2. It is observed that the Particles are of irregular in shape and of varied sizes. Some particles are elongated type and some are multifaceted.

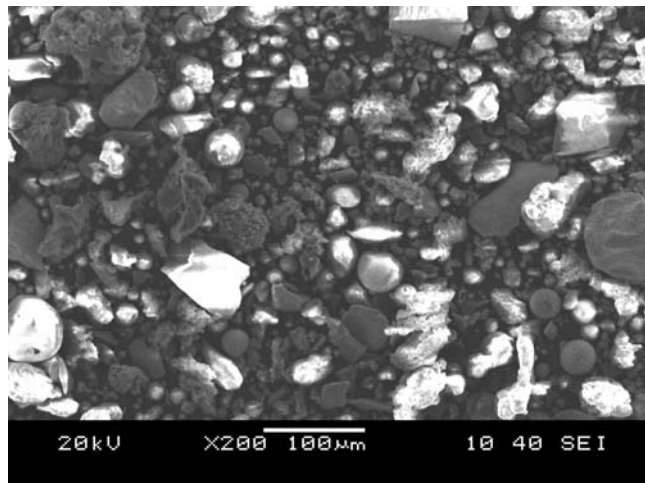


Figure 4.2 SEM micrographs of fly ash+quartz+illmenite raw powder prior to coating.

4.3 CHARACTERIZATION OF COATINGS

The coatings are deposited with atmospheric plasma spraying and the following characterizations are carried out.

4.3.1 Microstructural Study of the Coatings

Surface Morphology:

The interface adhesion of the coatings depends on the coating morphology and inter-particle bonding of the sprayed powders. SEM micrographs of fly ash+quartz+illmenite coating surfaces are shown in Fig 4.3.

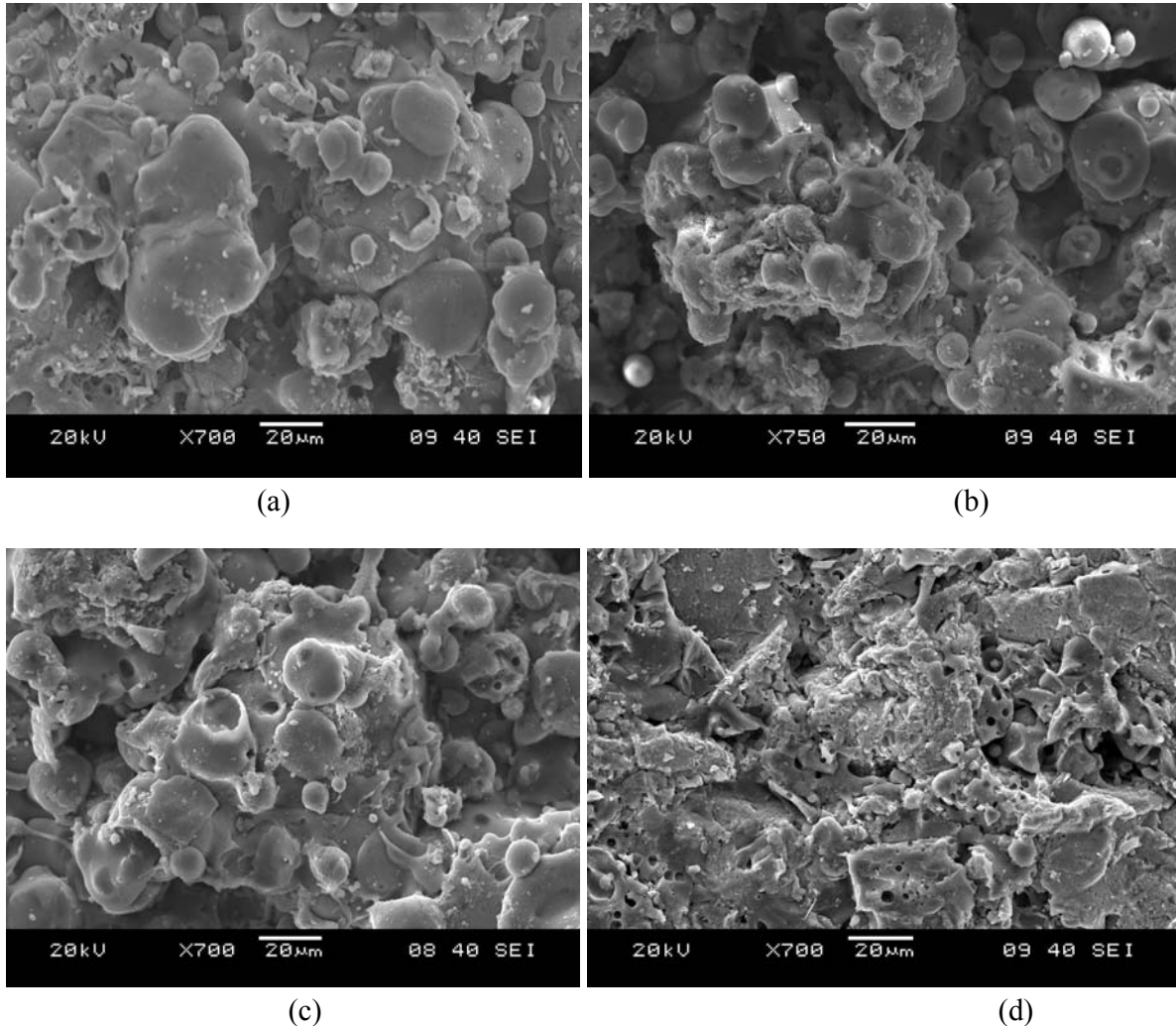


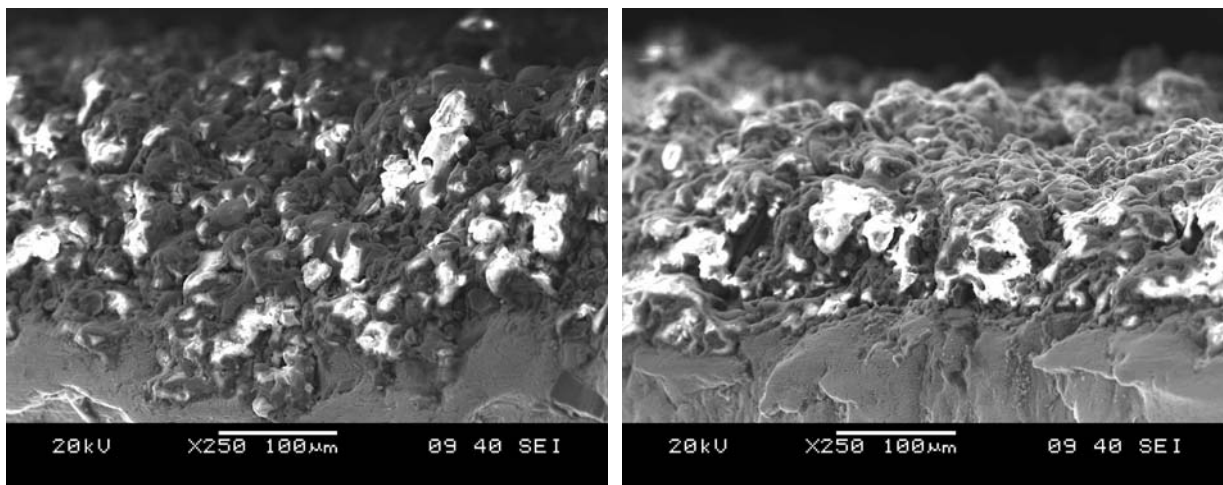
Figure 4.3 Surface morphology of fly ash+quartz+illmenite coatings deposited on mild steel Substrates, at (a) 11kW (b) 15kW (c) 18 kW (d) 21kW power level.

The coating deposited at 11kW power level (Fig 4.3(a)) on Mild Steel substrate, shows a uniform distribution molten/semi molten particle, which have agglomerated to form laths. More amount of cavitations observed at this lower power level. Some open pores are found on the inter particle boundaries and at triple particle/ grain junctions. These may have originated due to the inadequate flow of molten particles during their solidification [152]. The coating deposited at

15kW and 18kW (Fig 4.3(b) &(c)), forms a different morphology i.e. some spheroidal splats are found, indicative of complete melting of particles during in-flight traverse through plasma jet. Less cavitation is observed in inter-granular boundaries. In case of coating made at 21 kW power level (Fig 4.3(d)); the particles get more thermal energy, so during solidification from molten state, they agglomerate to form splats i.e. flattened region. Here very less amount of cavitations is observed. This may be the reason for better interface adhesion of the coating onto the substrate, leading to increase of adhesion strength. This morphology also shows a uniform distribution of molten/semi molten particles; hence no more increase in adhesion strength.

Interface Morphology:

The surface morphology of the coatings cannot predict how will be the interior (layer deposition) structures. So, the polished cross-sections of the samples were examined under scanning electron microscopy and are shown in Fig 4.4. From these micrographs approximate better result can be found. Fig 4.4(a) shows the coating deposited at 11 kW. Here it is found that lamellar structure present with cavitations at the coating-substrate interface. Very small diameter splats are found with inter-splat voids. Some semi-molten powder particles found. So here, there is no expectation for good adhesion strength. Fig 4.4(b) shows the coating at 15 kW power level. Less number of voids are present than that of 11 kW deposition. Here, Splats are globular, larger in dimension and equi-axed type. Fig 4.4(c) shows deposition at 18kW power level. Here there is a negligible amount of voids, which are not easily visible. Here better inter-particle boundary match leads to better bond strength throughout the length of coating. In Fig 4.4(d), 21kW power level used for coating deposition, in which spheroidal particles observed with larger diameter splat. Here inter-layer gaps are found. This is due to more vapourization of molten particle during spraying. Other than the mechanical interlocking of the sprayed coating with the metal substrate, some metallurgical bonding might have occurred at the interface which is evident from the presence of some inter-diffusion zones [153].



(a)

(b)

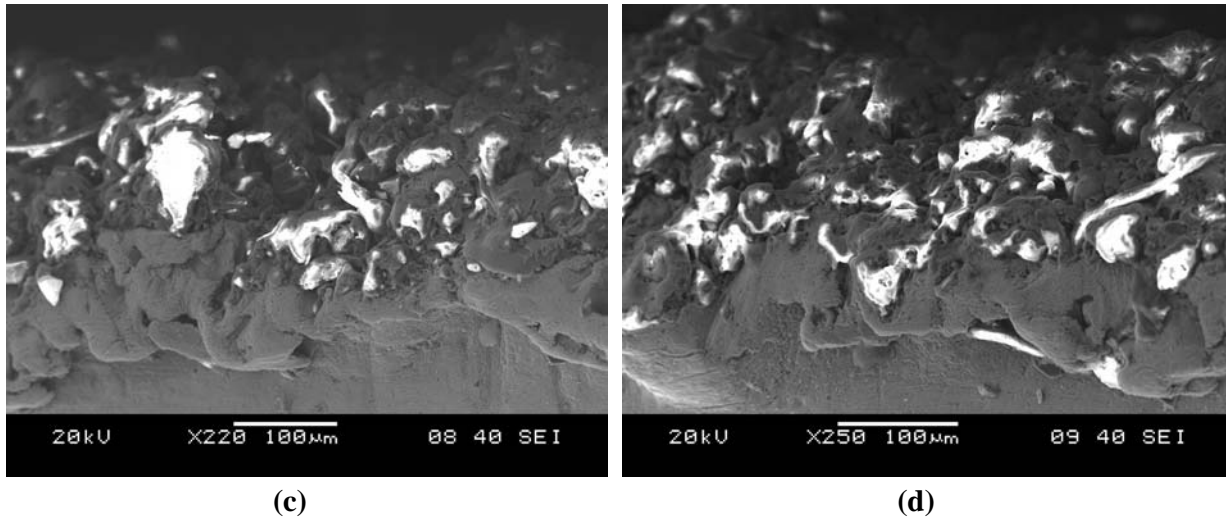


Figure 4.4 Interface morphology of fly ash+quartz+illmenite coatings deposited on mild steel Substrates, at (a) 11kW (b) 15kW (c) 18 kW (d) 21kW power level.

4.3.2 XRD ANALYSIS

Microstructural observations of the surface/interface shows optically different regions present on different places of the coating cross sections. Therefore, to ascertain the phases present and phase changes taking place during plasma spraying, X-ray diffractograms are taken for the raw material and for coatings using a Philips X-Ray Diffractometer with $\text{CuK}\alpha$ radiation. The XRD results are shown in Fig 4.5. Fig 4.5; presents XRD analysis of coating raw powder, where major phases are SiO_2 , TiO_2 , FeTiO_3 , Al_2O_3 and NiMn_2O_4 . Major peaks of the different phase are assigned in the figure. Fig 4.6 presents XRD analysis to examine the presence of various phases in the resulting fly-ash+quartz+illmenite composite coatings at 11kW power level. Major metal oxide phases present are SiO_2 , TiO_2 , Ti_3O_5 , Ti_4O_7 , FeTiO_3 , Fe_2TiO_5 , Fe_3O_4 , Fe_2O_3 , Al_2SiO_5 , $\text{Fe}_2\text{MnTi}_3\text{O}_{10}$, NiMn_2O_4 . XRD of 15kW power level deposition is shown in Fig 4.7, which reveals distinct peaks of the metal oxide phases present are: SiO_2 , TiO_2 , FeTiO_3 , Fe_2TiO_5 , Al_2O_3 , Al_2SiO_5 , $\text{Al}_6\text{SiO}_{13}$, $\text{Fe}_2\text{MnTi}_3\text{O}_{10}$. Fig 4.8 shows XRD analysis at 18 kW deposition and major oxide phases found are: SiO_2 , TiO_2 , Ti_3O_5 , FeTiO_3 , Fe_3O_4 , Al_2O_3 , FeSiO , NiMn_2O_4 and MnAl_2O_4 . In Fig 4.9, XRD analysis of 21kW deposition is presented. Here SiO_2 , TiO_2 , TiO , FeTiO_3 , Fe_2TiO_5 , Fe_3O_4 , Al_2O_3 , $\text{Fe}_2\text{MnTi}_3\text{O}_{10}$ and NiMn_2O_4 are the major phases. In this study it is found that some of intermetallic compounds are present in the coating product. When there is increase in power level from 11kW to 21kW, there is an occurrence of some phase change, which suggests that, due to the availability of high temperature and high enthalpy, some element combined with other element or transformed to its higher stable state. Different phase are formed depending on enthalpy/environment and transformation conditions during plasma spraying [124].

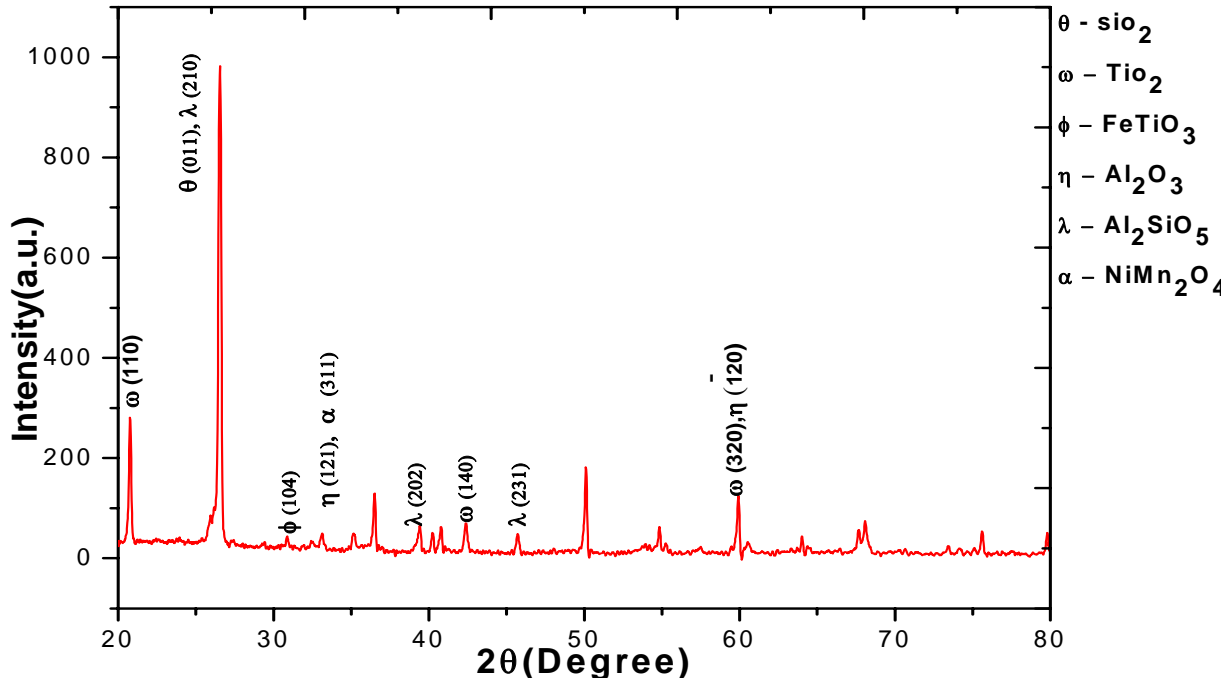


Figure 4.5 X-Ray diffractogram of fly ash+quartz+illmenite feedstock.

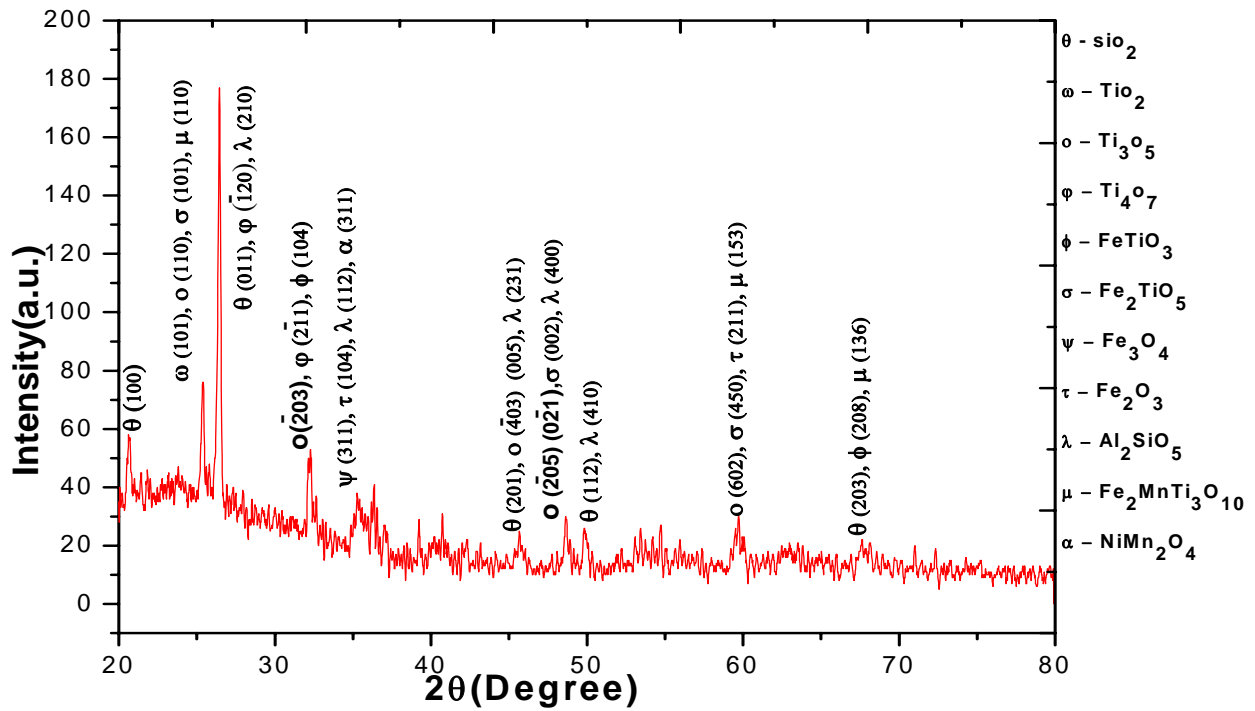


Figure 4.6 X-Ray diffractogram of fly ash+quartz+illmenite coating deposited at 11kW.

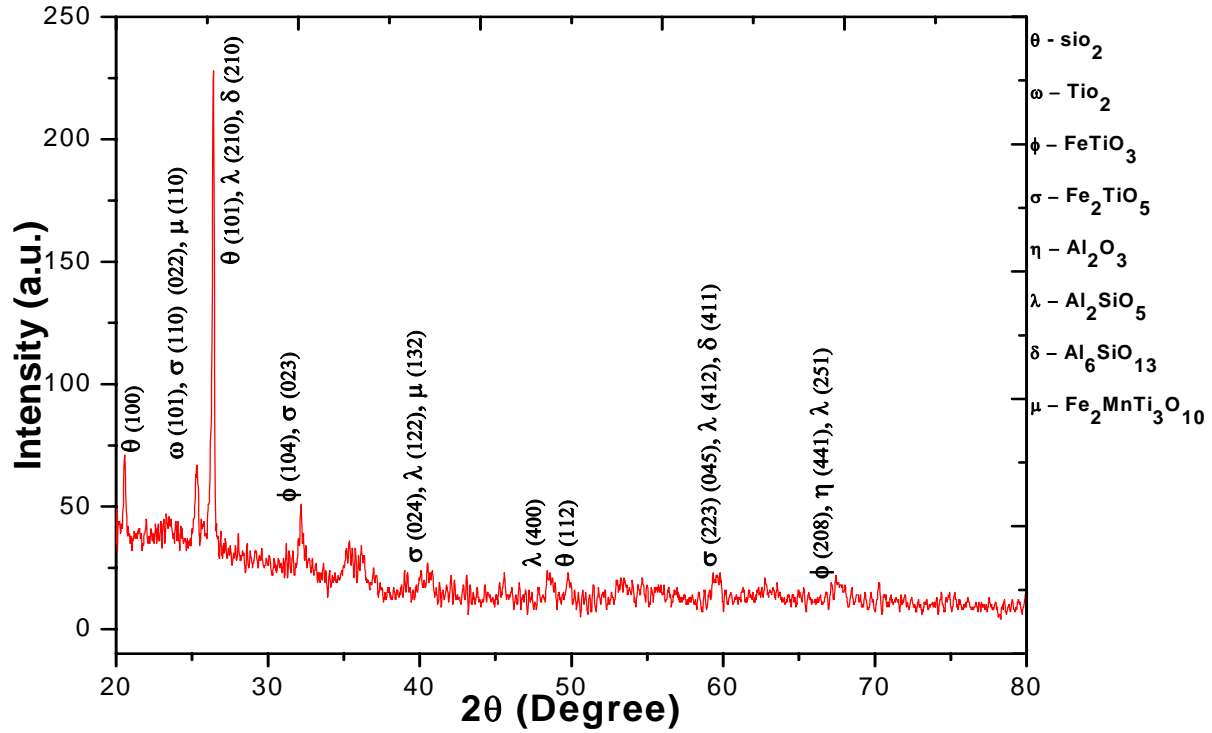


Figure 4.7 X-Ray diffractogram of fly ash+quartz+illmenite coating deposited at 15kW.

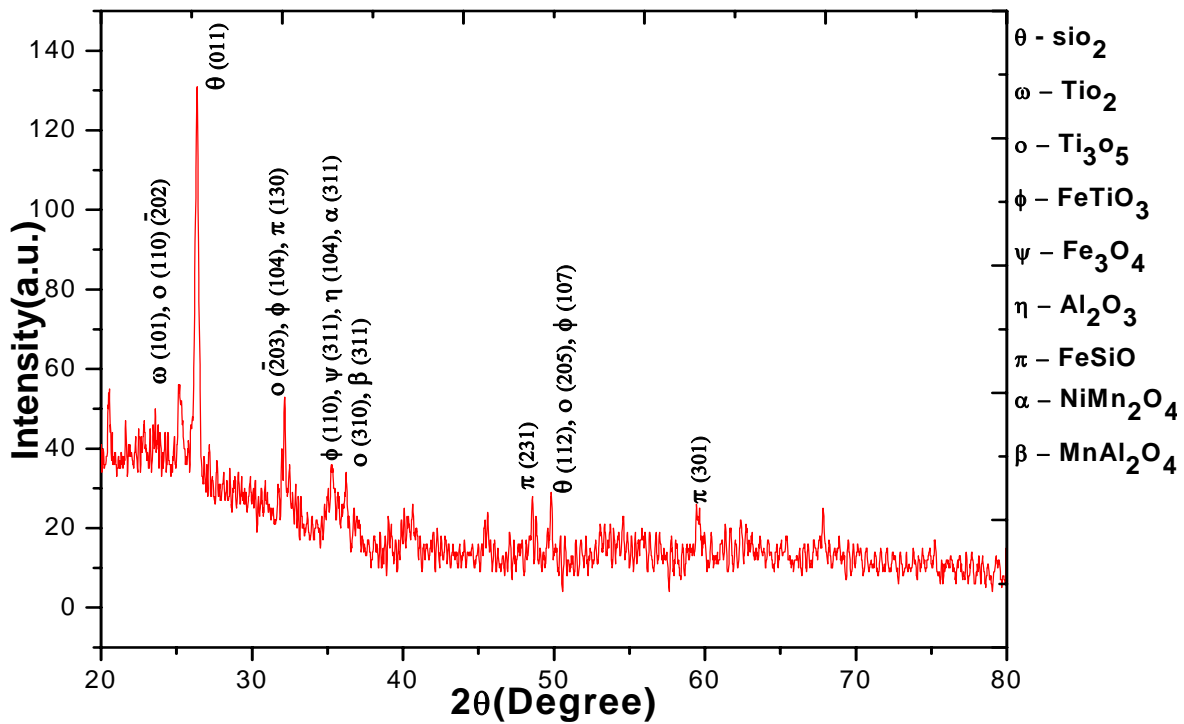


Figure 4.8 X-Ray diffractogram of fly ash+quartz+illmenite coating deposited at 18kW.

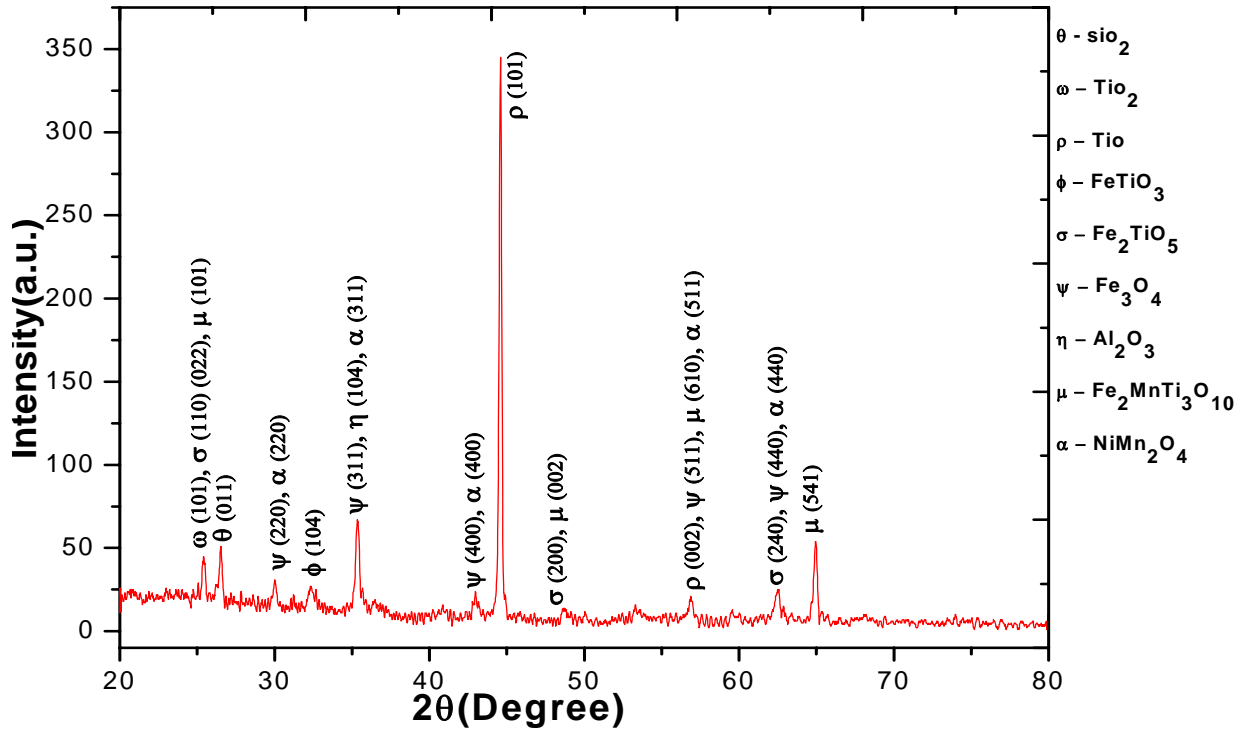


Figure 4.9 X-Ray diffractogram of fly ash+quartz+illmenite coating deposited at 21kW.

4.3.5 Coating Adhesion Strength

Coating adhesion tests have been carried out by many investigators with various coatings [154]. The fracture mode is adhesive if it takes place at the coating-substrate interface and that the measured adhesion value is the value of practical adhesion, which is strictly an interface property and depending exclusively on the surface characteristics of the adhering phase and the substrate surface condition [155, 156]. From the microscopic point of view, adhesion is due to physicochemical surface forces (i.e. Vander-walls, Covalent, ionic etc.), which are established at the coating-substrate interface [157]. In the present investigation, evaluation of coating interface bond strength is done using coating pull out method confirming to ASTM C-633. The variation of adhesion strength with operating power level for Mild Steel and Copper substrate is shown in Fig 4.10. Each data point is the average of five tests. It is found that, with increase in operating power level there is an increase in adhesion strength up to a certain level of operating power of the torch. It is found that for different type of substrate, the magnitude of adhesion strength differs. For Mild Steel the strength has varied from 3.5MPa to 6.56MPa, the maximum of 6.56MPa at 21kW power level. For Copper substrate this value ranges from 3.00MPa to 6.32MPa. Deposition efficiency improves to a certain extent with increase in arc power, since it is associated with an enhanced particle melting and hence the adhesion strength [158]. This might be due to the fact that, when the operating power level is increased, larger fraction of particles attain molten state as well as the velocity of the particles also increase. Therefore there is better probability for splat formation i.e. forms a lamellar structure and hence better mechanical inter-locking of molten particles/splats on the substrate leading to increase in

adhesion strength [159]. But with increase in torch input power, fragmentation and vaporization of the particles increases. There is also a greater chance to fly off of smaller particles and results almost no further increase in adhesion strength of the coatings [160].

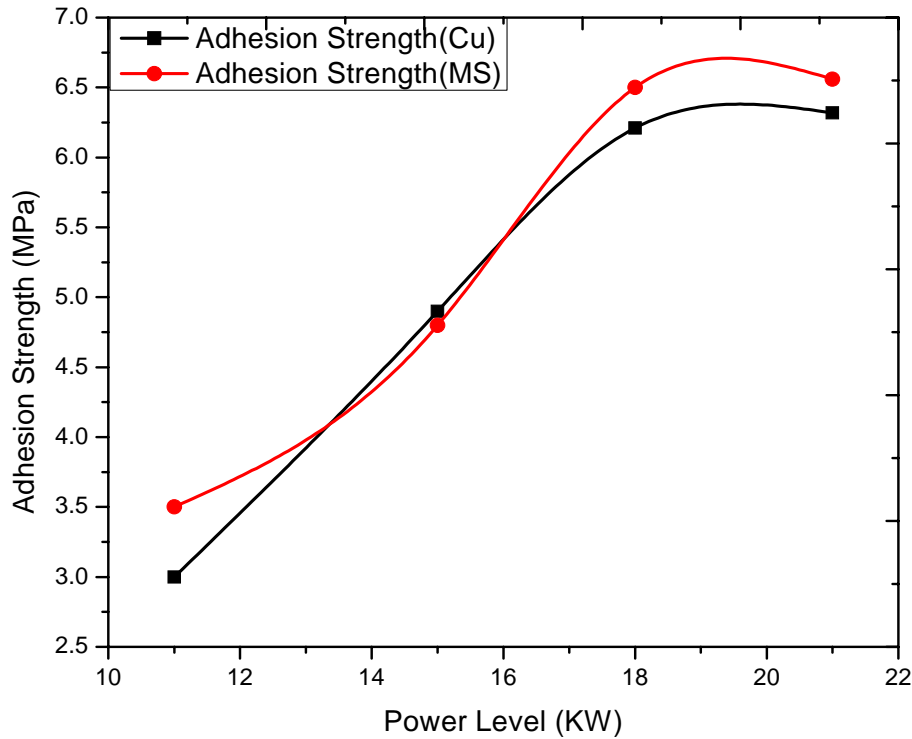


Figure 4.10 Comparison of adhesion strength of mild steel and copper with respect to power level.

Again by comparing adhesion strength of Mild Steel against Copper (Fig 4.10), it is found that at 11kW, 18 kW and 21kW power level adhesion strength of Mild Steel is greater. Coating made after 21 kW power level, the adhesion strength i.e. Mild Steel and Copper substrates tends to decrease. The low values of adhesion strength may be due to difference in coefficient of thermal expansion of substrate and coating material and/or formation of pores, cracks, voids in the coating and along coating-substrate interfaces [161-165].

4.3.1 Coating Deposition Efficiency

Coating deposition efficiency is defined as the ratio of the weight of coating deposited on the substrate to the weight of the expended feedstock. Weighing method is accepted widely to measure this [166]. It can be described by the following equation

$$\eta = \left(\frac{G_c}{G_p} \right) \times 100 \% \text{----- (4.1)}$$

Where, η is the deposition efficiency.

G_c is the weight of coating deposited on the substrate.

G_p is the weight-expended feedstock.

The deposition efficiency is a measure of the fraction of the powder that is deposited on the substrate. Deposition efficiency depends on many factors that include the input power to the plasma torch, material properties, such as melting point, particle size range, heat capacity of the powder being sprayed and standoff distance (torch to substrate distance) etc. For a given standoff distance and given material with specific particle size, torch input power appears to be an important factor for the deposition efficiency. Deposition efficiency values of fly ash+quartz+illmenite coating made at different operating power levels on mild steel and copper substrates are given in Table 4.2.

Table 4.2 Deposition efficiency of fly-ash+quartz+illmenite coatings.

Substrate Type	Coating Material	Power level(kW)	Deposition efficiency (%)
Mild Steel	Fly-ash+quartz+illmenite	11	25
Mild Steel	-do-	15	35
Mild Steel	-do-	18	45
Mild Steel	-do-	21	48
Copper	-do-	11	25
Copper	-do-	15	30
Copper	-do-	18	40
Copper	-do-	21	43

The variation of deposition efficiency of fly-ash+quartz+illmenite coatings with operating power level on mild steel substrate is shown in Fig 4.11. The deposition efficiency is increased in a sigmoidal fashion with the torch input power. Plasma spray deposition efficiency of a given material depends on its melting point, thermal heat capacity, rate of dissipation of heat at substrate and particle size of the sprayed powder etc. The coating deposition efficiency is significantly influenced by the input power to the torch.

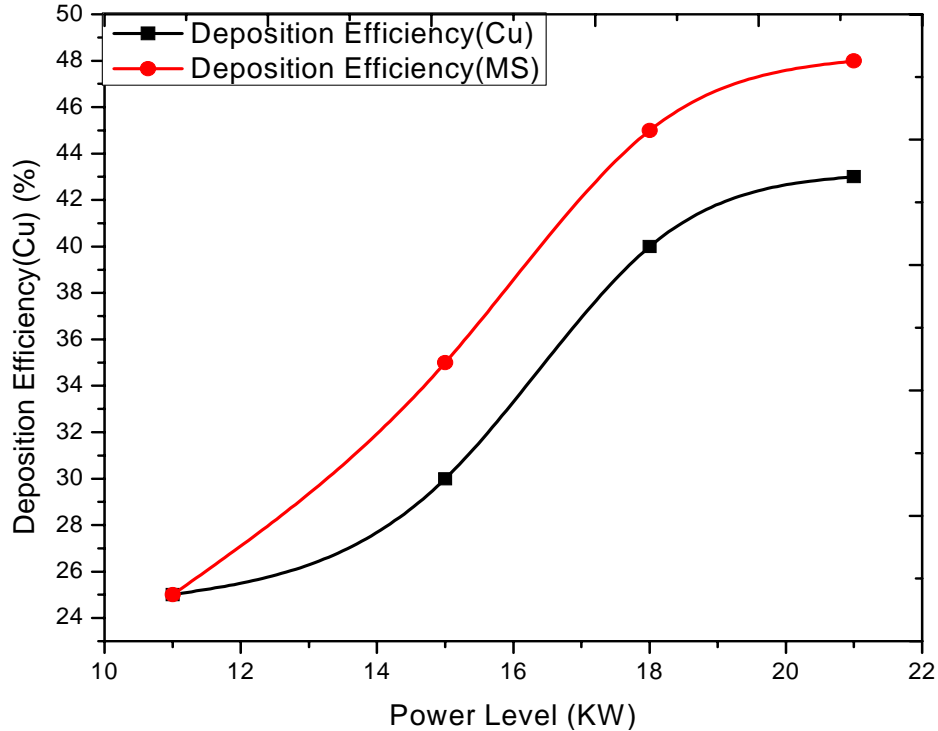


Figure 4.11 Variation of deposition efficiency of fly-ash+quartz+illmenite coatings at different power levels.

At lower power level, the plasma jet temperature is not high enough to melt the entire feed powder that enters the plasma jet. As the power level is increased, plasma temperature and enthalpy increases, thus melting a larger fraction of the feed powder. The spray efficiency therefore increases with increase in input power to the plasma torch. However, beyond a certain power level of the torch, temperature of the plasma becomes high enough leading to vaporization/dissociation of the feedstock. Thus there is not much increase in deposition efficiency. Because molten particle form a vaporized layer just before impact on the substrate surface which leads to formation of inter-layer voids [167].

4.3.2 Coating Thickness

Coating thickness of fly-ash+quartz+illmenite was measured on the polished cross-sections of the samples, using an optical microscope. The thickness values obtained for coatings deposited at different power levels for Mild steel and copper substrates are presented in Table 4.3. Each data point on the curves is the average of at least four readings. From the above data, it is found that maximum thickness of 300 μm found for mild steel. For copper maximum thickness is 350 μm , which is greater than mild steel substrate, may be due to difference in thermal conductivity of the substrates.

Table 4.3 Thickness values of fly ash+quartz+illmenite coatings on mild steel substrates.

Substrate Type	Coating Material	Power level (kW)	Coating Thickness (μm)
Mild Steel	Fly-ash+quartz+illmenite	11	250
Mild Steel	-do-	15	300
Mild Steel	-do-	18	280
Mild Steel	-do-	21	250
Copper	-do-	11	300
Copper	-do-	15	350
Copper	-do-	18	290
Copper	-do-	21	280

The variation of thickness values with torch input power for Mild steel and copper substrates is presented in Fig 4.12. From this figure it is observed that maximum coating thickness of $\sim 300 \mu\text{m}$ is obtained at 15 kW power level on mild steel substrates which decreases gradually with the increase in input power to the plasma torch. Similar situation obtained for copper substrate and the maximum coating thickness of $\sim 350 \mu\text{m}$ at 15 kW power level. In case of thermal spray of oxide coatings developed by APS technique, particle deposition is influenced by the input power to the plasma torch. With the increase in power level, the plasma density increases leading to rise in enthalpy and thereby the particle temperature. Hence more number of particles gets melted during in-flight traverse through the plasma jet. When these molten species hit the substrate, get flattened and adhere to the surface forming big splats. If the inter-lamellar bonding between these splats is strong and the area of contact between the lamellae is more, leads to less amount of porosity. Hence, although there is decrease in coating thickness but a dense coating is formed.

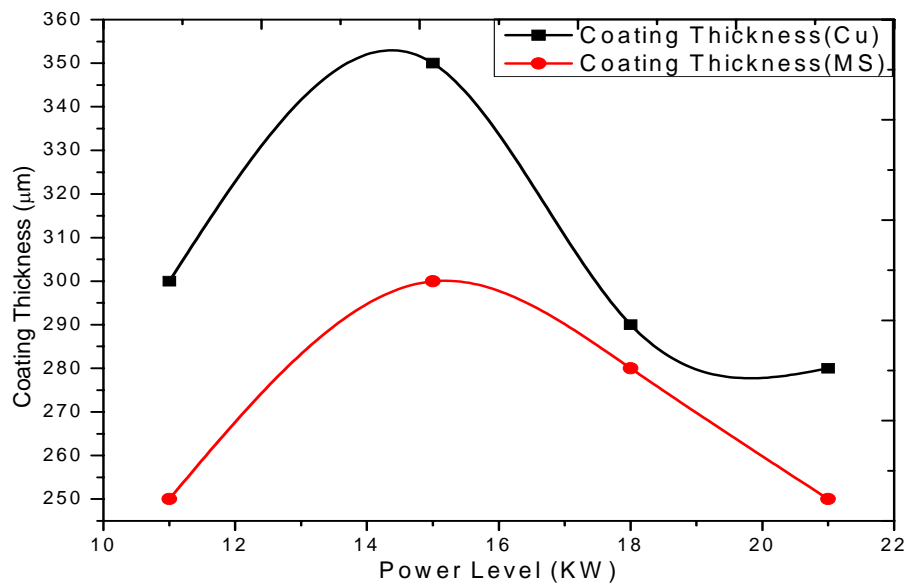


Figure 4.12 Variation of coating thickness of fly ash+quartz+illmenite coatings at different power levels.

4.3.3 Hardness of the Coatings

To measure hardness of the coating, microscopic observation of the polished cross section of the coatings under optical microscope is taken. Coating hardness measurement is carried out with Leitz Micro-Hardness Tester using 50Pa (0.419N) load, are summarized in Table 4.4. Each data point is the average of four observations. From this table, it is observed that there is an increase in coating hardness with the increase in plasma power level. This may be due to the formation/transformation of compounds viz. silica and alumina etc. to their allotropic forms and their compositional variations during spray deposition with the increase in input power to the plasma torch. Variation of coating hardness with respect to power level is given in Fig 4.13.

Table 4.4 Hardness on the coating cross section for the coatings deposited at different power levels.

Substrate Type	Coating Material	Power level(kW)	Avg. Hardness (H _v)
Mild Steel	Fly-ash+quartz+illmenite	11	534.09
Mild Steel	-do-	15	576.51
Mild Steel	-do-	18	642.94
Mild Steel	-do-	21	590.75
Copper	-do-	11	532.77
Copper	-do-	15	566.25
Copper	-do-	18	653.99
Copper	-do-	21	590.66

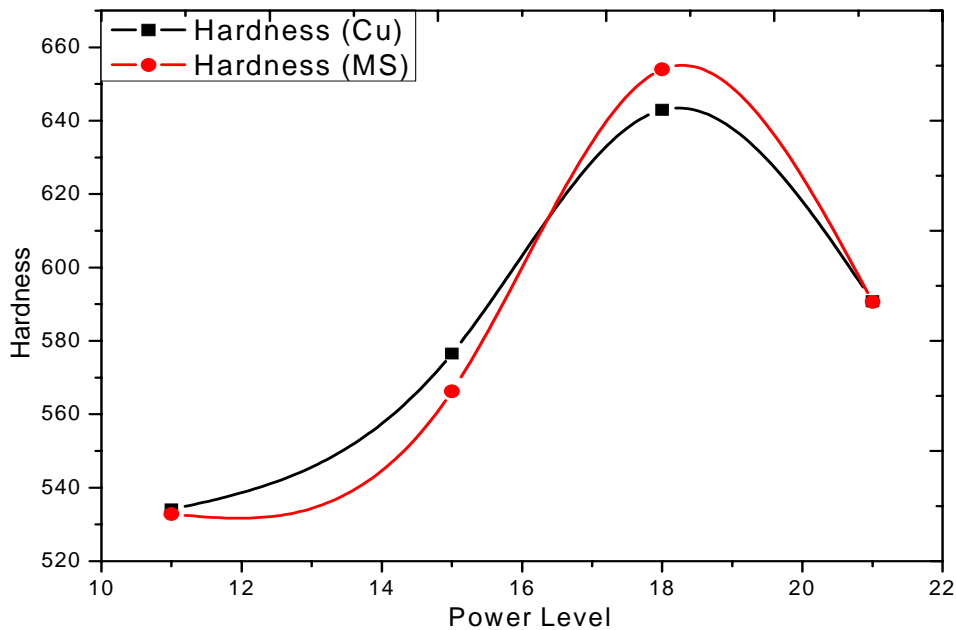


Figure 4.13 Variation of coating hardness of fly ash+quartz+illmenite coatings at different power levels.

4.3.4 Coating Porosity

Coating porosity measurement was done using the image analysis technique. The polished interfaces of various coatings are studied under optical microscope equipped with a CCD camera. From the digitized image obtained by this system, coating porosity was determined using VOIS image analysis software. The results are tabulated in Table 4.5.

Table 4.5 Coating porosity of mild steel and copper at different power levels.

Substrate Type	Coating Material	Power level(kW)	Coating Porosity (%)
Mild Steel	Fly-ash+quartz+illmenite	11	20
Mild Steel	-do-	15	18
Mild Steel	-do-	18	15
Mild Steel	-do-	21	15
Copper	-do-	11	22
Copper	-do-	15	28
Copper	-do-	18	23
Copper	-do-	21	18

Variation of coating porosity of fly ash+quartz+illmenite with torch input power is shown in Fig 4.14. It is observed that porosity volume fraction of these coatings lie in the range of from ~15 % to ~28%. The amount of surface porosity is more in the case of coatings made at lower (11kW) and gradually decreases as increase in power level. However porosity is minimum at 18kW for the coatings under this study. The increased value of porosity may be the reason for low adhesion strength and higher thickness [168] of the coatings deposited at low and at high power levels.

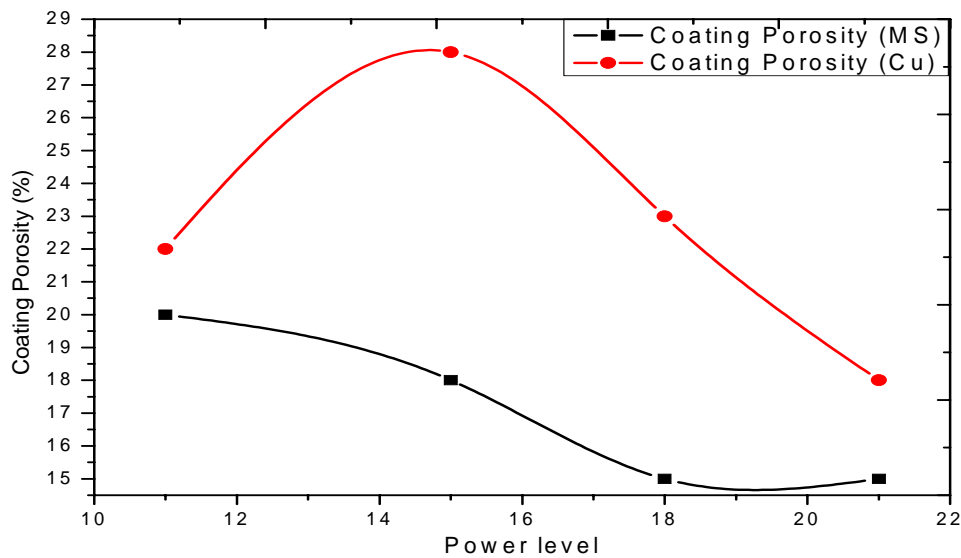


Figure 4.14 Variation of coating porosity of fly ash+quartz+illmenite coating with torch power.

4.3.4 Surface Roughness

In Table 4.6, the surface roughness of mild steel and copper at different power level are given. Surface roughness has varied from 5.2 – 11.7Ra incase of coatings made on mild steel substrate and that from 12.4 – 14.33 Ra incase of copper substrate. It is found that, in case of mild steel, the surface roughness increase as increase the power level from 11 to 18 KW and then decreases at higher power level. But in case of copper, gradual decrease in surface roughness occurs from 11KW to 18KW and then increases at higher power level. At higher power level, more is the energy transfer to molten powder and more is the chance of pore formation due to vaporization. Variation of surface roughness of mild steel and copper with respect to power level are given in Fig 4.15.

Table 4.6 Surface Roughness of mild steel and copper at different power levels.

Substrate Type	Coating Material	Power level(kW)	Surface roughness (Ra)
Mild Steel	Fly-ash+quartz+illmenite	11	11.73
Mild Steel	-do-	15	13
Mild Steel	-do-	18	13.26
Mild Steel	-do-	21	5.2
Copper	-do-	11	14.33
Copper	-do-	15	12.4
Copper	-do-	18	12.4
Copper	-do-	21	14.06

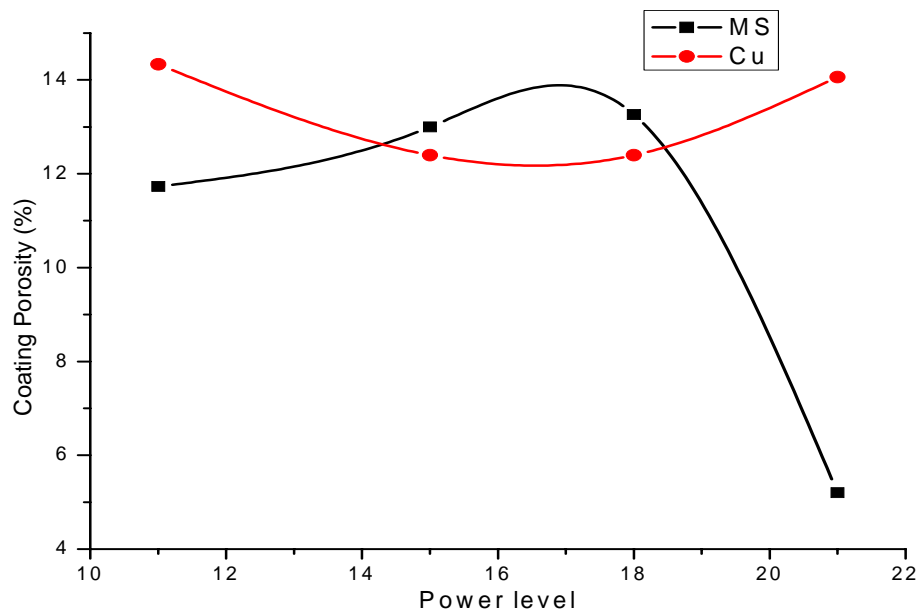


Figure 4.15 Variation of Surface Roughness of fly ash+quartz+illmenite coating with torch power.

4.3.6 ANN Prediction of Adhesion Strength

Artificial Neural Network analysis (ANN) is software package [169], which copies the functional principle of the human brain. ANNs are a comparatively new modeling technique composed of large number of inter-related elements operating in parallel. They can be used to solve problems that are difficult for conventional techniques or for human reasoning [170-173]. ANN calculation is also faster than other finite element modeling [174, 175]. In this process, the parameters are connected by means of weights which are numbers, translating the strength of neuron connections. Input variables are taken as number fluxes which feed the network structure and are obtaining the output pattern. ANN is based on a training procedure to decrease the error between ANN response and experimental response for a given set of input variables by considering neuron number and weight updates [176]. ANN bibliography is very rich with learning models, like the popular back propagation and the quick propagation, the Hebbian algorithm, the ADALINE model or the Kohonen learning rule and among the other models [177-182]. Plasma spraying is considered as a non-linear problem with respect to its variables: either materials or operating conditions. To obtain functional coatings exhibiting selected in-service properties, combinations of processing parameters have to be planned. These combinations differ by their influence on the coating properties and characteristics. In order to control the spraying process, one of the challenges nowadays is to recognize parameter interdependencies, correlations and individual effects on coating characteristics. To optimize these interrelated effects, a robust method i.e. ANN is used. Different ANN structures (I-H-O) (shown in Fig 4.16) with varying number of neurons in the hidden layer are tested at constant cycles, learning rate, error tolerance, momentum parameter, noise factor and slope parameter. Based on least error criterion, one structure, shown in Table 4.7, is selected for training of the input-output data. The learning rate is varied upto 0.002 during the training of the input-output data. Neuron number in the hidden layer is varied and in the optimized structure of the network, this number is found to be 8 for adhesion strength. The number of cycles selected during training is high enough so that the ANN models could be rigorously trained.

Table 4.7 Input parameters selected for training (Coating adhesion strength).

Input Parameters for Training	Values
Error tolerance	0.003
Learning parameter(β)	0.002
Momentum parameter(α)	0.002
Noise factor (NF)	0.001
Maximum cycles for simulations	1,00,00,000
Slope parameter (ξ)	0.6
Number of hidden layer neuron	8
Number of input layer neuron (I)	5
Number of output layer neuron (O)	1

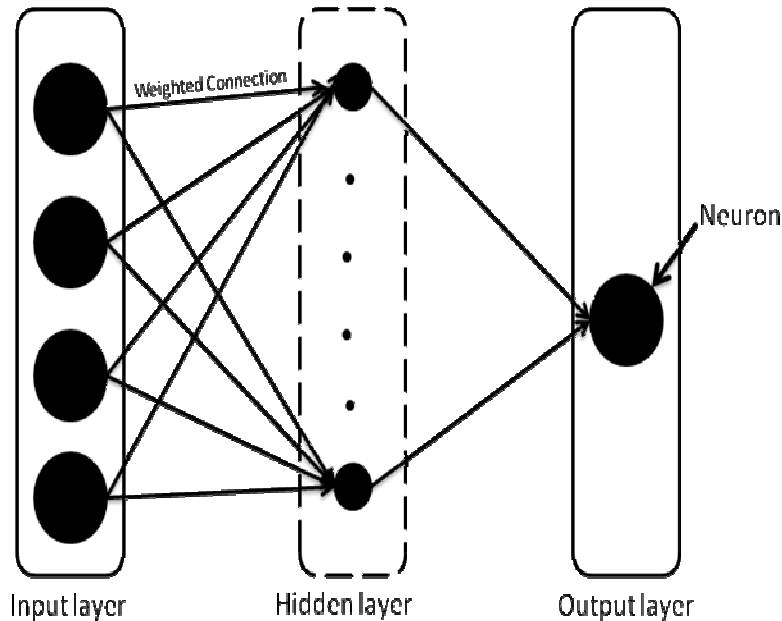


Figure 4.16 The three layer neural network for adhesion strength.

Predicted adhesion strength compare with experimental results based on different feed rate

The prediction value of neural network was tested with 12 data sets from the original process data. Each data set contained inputs such as torch input current and an output value i.e. Adhesion strength was returned by the network. Fig 4.17 presents the comparison of predicted output values for coating adhesion strength with those obtained experimentally for both copper and Mild Steel substrate, which is done at constant 12 gm/mm powder feed rate and 100mm torch to base distance with change in power level. The predicted results show good agreement with experimental observations, which assure to find out the adhesion strength by taking different parameters for future work. Here it is clearly observed that the predicted plot goes in the same way as that of experimental i.e. by increasing power level the adhesion strength increases up to a certain limit and no increase in adhesion strength with further increasing power level. Again for conformation by changing feed rate to 18 gm/min and torch to base distance 140 mm, the plot for both Copper and Mild Steel changed (shown in Fig 4.18) with good agreement between predicted value and experimental value.

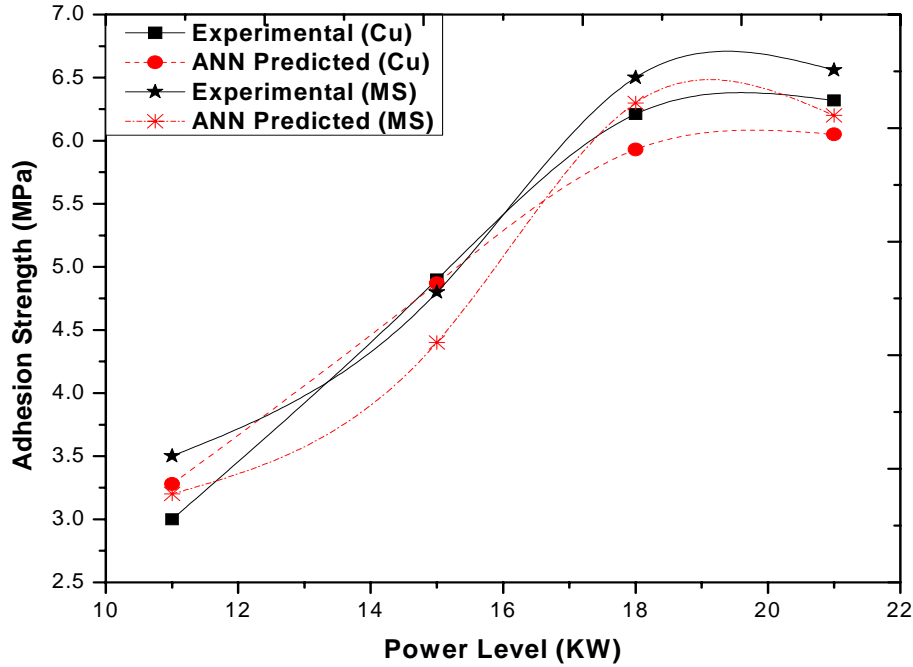


Figure 4.17 Comparative plot of experimental and ANN predicted values of adhesion strength of fly-ash+quartz+illuminite on Copper & Mild Steel substrate (Plasma spray at 12 gm/min feed rate and 100 mm torch to base distance).

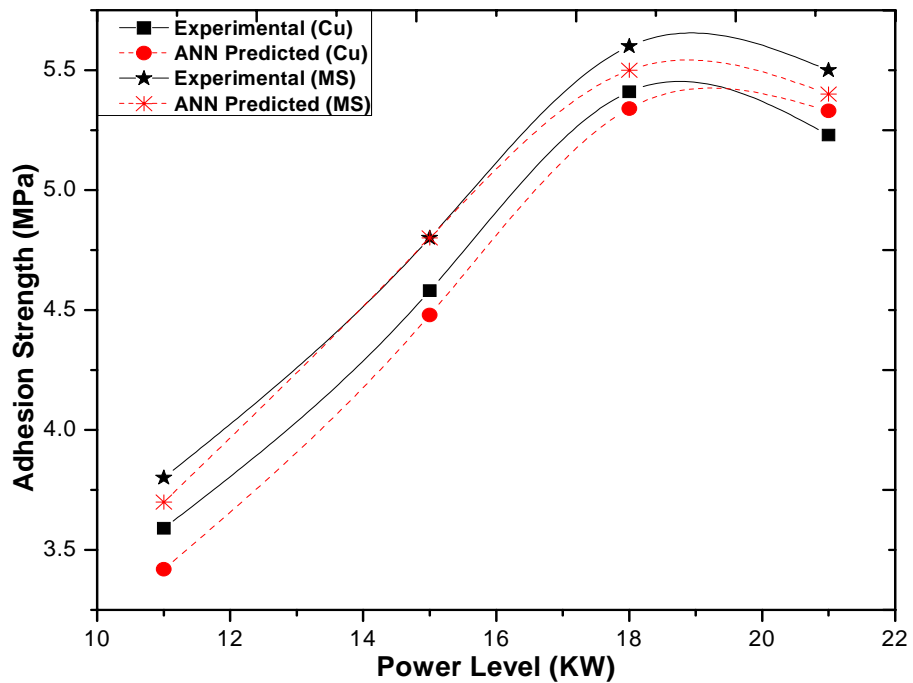


Figure 4.18 Comparative plot of experimental and ANN predicted values of adhesion strength of fly-ash+quartz+illuminite on Copper & Mild Steel substrate (Plasma spray at 18 gm/min feed rate and 140 mm torch to base distance).

comparison between mild steel & copper substrate in account of ANN Predicted adhesion strength results

In the Fig 4.19, it is clear that the adhesion strength increases with respect to power level from 10kW to 18 kW and further increase in power level there is no change in adhesion strength. It reveals that for 12 gm/min feed rate with 40µm powder size and 100mm torch to base distance, one should choose ~18kW power level for better spray coating. If greater than 18kW power level choose, then there will be loss of process efficiency [183]. Here it can know that, there is decrease in adhesion strength, by increasing power level to 21kW. The reason is due to higher thermal energy at 21kW, there is more vaporization of powder generate for which splats are connected before deposited at the surface of the substrate and there are many cavity formed at interlayer space. But it is found that the surface roughness at 21kW is very less as comparison to 18kW, because some particles are deposited from their vaporized condition. From the prediction plot in fig 4.19, the adhesion strength of mild steel always greater than that of copper.

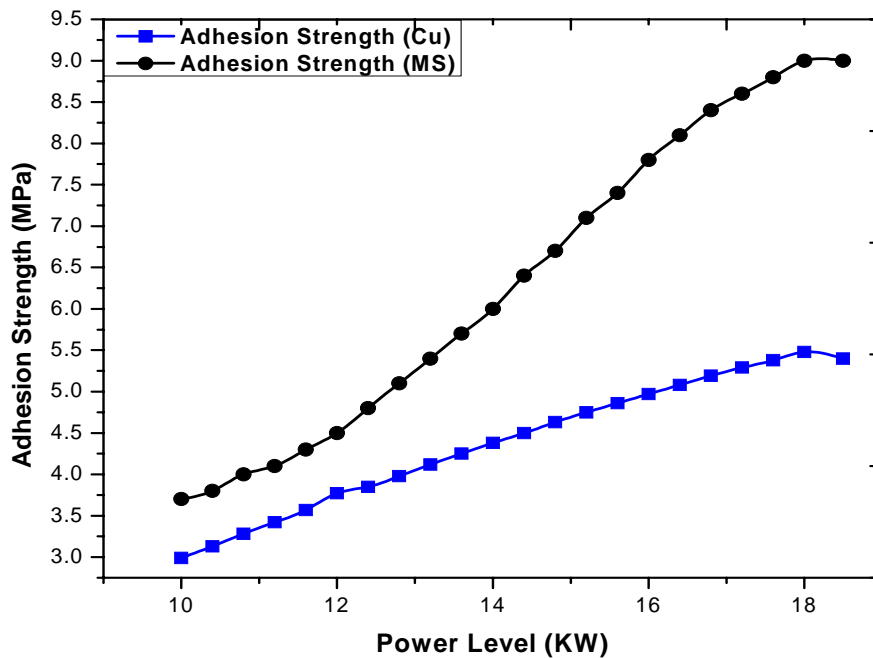


Figure 4.19 Predicted adhesion strength of Copper & Mild Steel substrate with respect to different power level (Plasma spray of fly-ash+quartz+illuminite at 12 gm/min feed rate and 40µm powder size, 100mm torch to base distance).

Prediction results based on powder particle size

In case of copper, at 12 gm/min feed rate and 100mm torch to base distance, it is observed from Fig 4.20 that, higher is the powder size, lower is the adhesion strength and there is nearly uniform increase in adhesion strength for each plot. From ANN calculation by choosing this set of parameter with 40µm powder size, the adhesion strength for copper substrate will be 5.48MPa at 21kW power level. But in case of Mild steel as shown in Fig 4.20, at 12 gm/min feed rate and 100mm torch to base distance, the increment value of adhesion strength is very low in between 10kW to 13kW and then uniformly increases up to 18kW power level. Higher adhesion

strength will be 9.00MPa for mild steel with 40 μ m powder size. From Fig 20 & 21 plots, it can be seen that the plasma spray will give better result at ~17kW to 18kW power level.

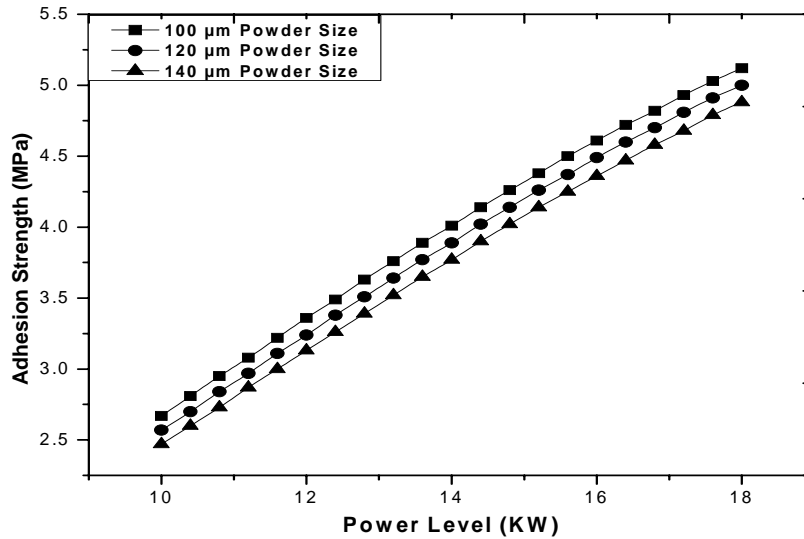


Figure 4.20 Predicted adhesion strength vs Power level for Copper by change in size of powder (Plasma spray of fly-ash+quartz+illuminite at 12 gm/min feed rate and 100 mm torch to base distance).

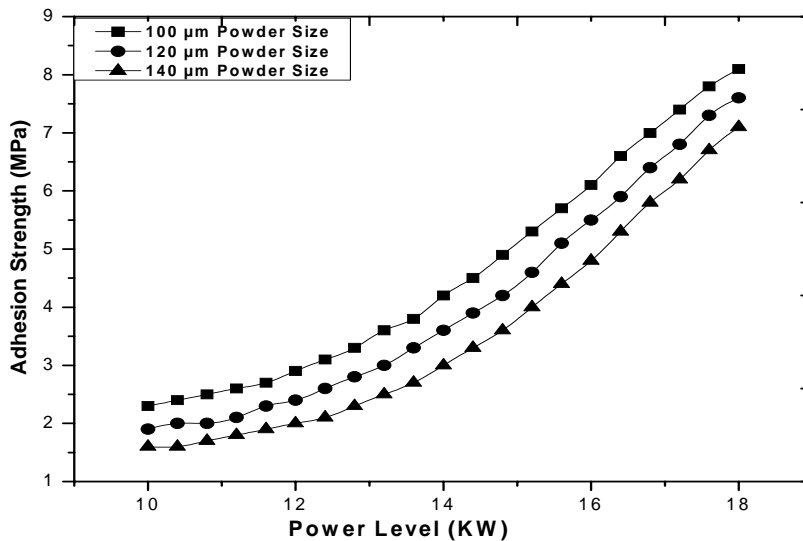


Figure 4.21 Predicted adhesion strength vs Power level for Mild Steel by change in size of powder (Plasma spray of fly-ash+quartz+illuminite at 12 gm/min feed rate and torch to base distance 100mm).

Prediction results based on torch to base distance

The adhesion strength decreases by increasing the torch to base distance, which is clearly observe in Fig 4.22. For smaller powder size (30 μ m), the adhesion strength is better than that of higher powder size (70 μ m, 90 μ m and 120 μ m), at 18kW power level and 12 gm/min feed rate.

In case of copper, for 50 μm powder size the highest adhesion strength 5.56 MPa will be achieved at 50mm torch to base distance. The Fig 4.23 (for mild steel) gives the same idea for coating by different particle size with respect to torch to base distance.

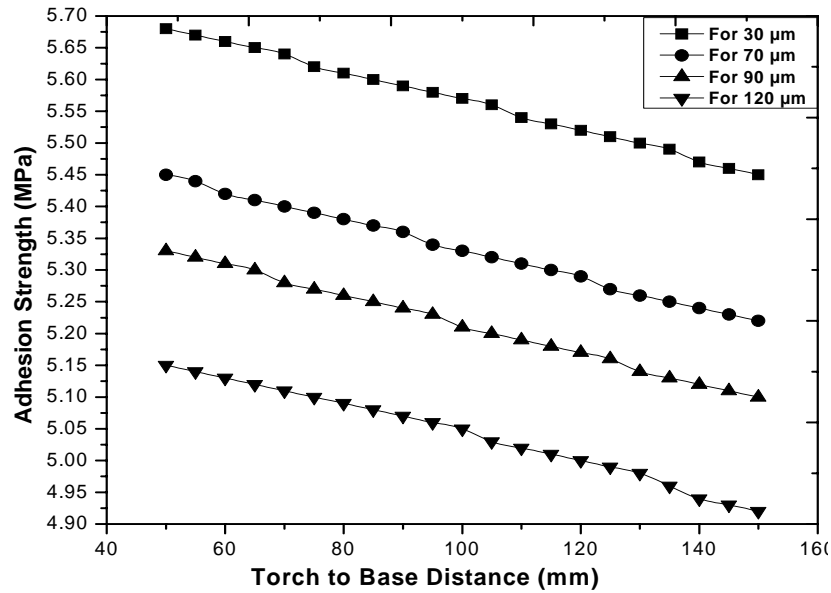


Figure 4.22 Predicted adhesion strength vs torch to base distance for Copper by change in size of powder (Plasma spray of fly-ash+quartz+illuminite at 18kW power level and 12 gm/min feed rate).

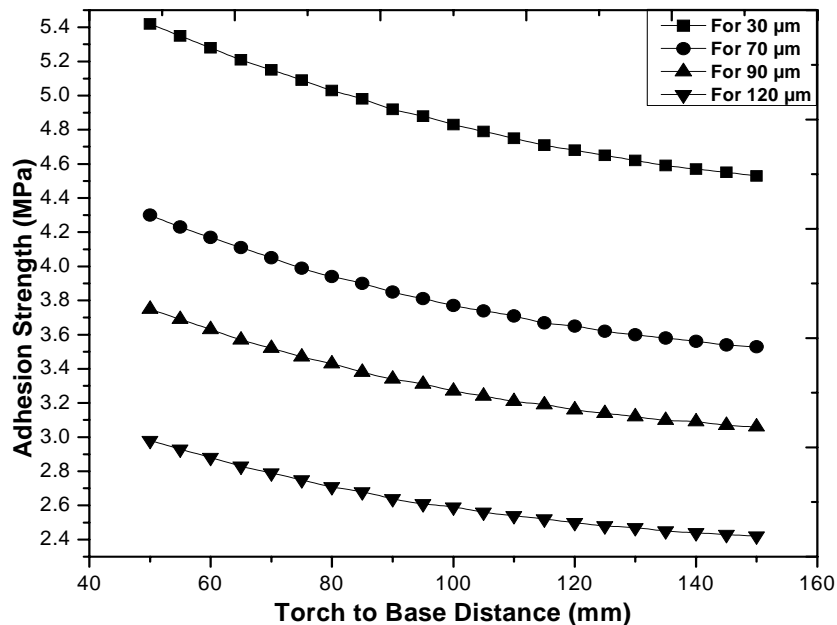


Figure 4.23 Predicted Adhesion strength vs torch to base distance for Mild Steel by change in size of powder (Plasma spray of fly-ash+quartz+illuminite at 15kW power level and 12 gm/min feed rate and).

4.4 EVALUATION OF COATING PERFORMANCE

4.4.1 Erosion Wear Behavior of Coatings

Erosion wear is a nonlinear process with respect to its variables: that are materials and operating conditions. To obtain the best functional output of coatings exhibiting selected in-service properties, the right combinations of operating parameters are to be known. These parameter combinations normally differ by their influence on the erosion wear rate i.e. coating mass loss. Statistical methods are commonly used to improve the quality of a product or process. Such methods enable the user to define and study the effect of every single condition possible in an experiment where numerous factors are involved. In case of plasma spray coatings encountering such situations, no specific model has been developed and thus the study of their erosion behavior has been mostly based on experimental data [184]. The less erosion wear rate is one the main requirements of the coatings developed by plasma spraying. In order to achieve certain values of erosion rate accurately and repeatedly, the influence parameters of the process have to be controlled accordingly. Since the number of such parameters in plasma spraying is too large and the parameter-property correlations are not always known, one of the statistical methods i.e. Taguchi method can be employed for precise identification of significant control parameters for process optimization. The Taguchi method consists of a plan of experiments with the objective of acquiring data in a controlled way, executing these experiments and analyzing data, in order to obtain information about the behavior of a given process. One of the advantages of the Taguchi method over the conventional experiment design methods is that optimum working conditions determined from the laboratory work can also be reproduced in the real production environment [185-189] and another advantage is, it minimizes the variability around the target when bringing the performance value to the target value in addition keeping the experimental cost at the minimum level.

4.4.2 Taguchi Experimental Design

There are three variant parameters i.e. power level, impact pressure and impingement angle with two constant parameter i.e. erodent size and standoff distance are considered in this study. In Table 4.8, each column represents a test parameter and a row gives a test condition that is nothing but combination of parameter levels. The experimental observations are transformed into a signal-to-noise (S/N) ratio. There are several S/N ratios available depending on the type of characteristics. The S/N ratio for minimum erosion rate coming under *smaller-is-better* characteristic, which can be calculated as logarithmic transformation of the loss function as shown below.

Smaller is the better characteristic:

$$\frac{S}{N} = -10 \log \left(\frac{1}{n} \right) (\sum y^2) \dots \dots \dots (4.2)$$

Where “n” the number of observations, and “y” the observed data. “Lower is better” (LB) characteristic, with the above S/N ratio transformation, is suitable for minimization of erosion rate. In Table 4.8, the last column represents S/N ratio of the erosion rate.

Table 4.8 Variables used in the experiment as per Taguchi L8 method.

Power level (kW)	Pressure (bar)	Angle(°)	Erosion rate*10 ⁻⁴	S/N Ratio
11	1.0	60	122.96	-41.7953
11	1.5	60	134.81	-42.5944
11	2.0	90	238.09	-47.5348
11	2.5	90	283.74	-49.0584
15	1.0	60	64.33	-36.1683
15	1.5	60	68.57	-36.7227
15	2.0	90	115.76	-41.2712
15	2.5	90	120	-41.5836
18	1.0	90	34.92	-30.8615
18	1.5	90	60.1	-35.5775
18	2.0	60	78.94	-37.9459
18	2.5	60	109.62	-40.7978
21	1.0	90	23.28	-27.3397
21	1.5	90	72.42	-37.1972
21	2.0	60	80.84	-38.1525
21	2.5	60	116.19	-41.3034

The analysis is made using the popular software specifically used for design of experiment applications known as MINITAB 14. The Residual plots for mean shown in Fig 4.24, The Residual plots of S/N ratio response are given in Table 4.8, Main effect of plots for means on erosion rate are given in Table 4.15 and Main effect of plots for S/N ratios on erosion rate are given in Table 4.16; from which it can be concluded that among all the factors, impact angle & Impact velocity are the most significant factor followed by erodent size and standoff distance. It also leads to the conclusion that factor combination of power level=21kW, Impact pressure=1.0bar and angle=90° gives minimum erosion rate. In Fig 4.24 & 4.25, normal probability plot of the residuals shows that maximum experimental data sets are nearer to the mean line and the histogram of the residual looks like as a bell shape, which signifies better experimental result.

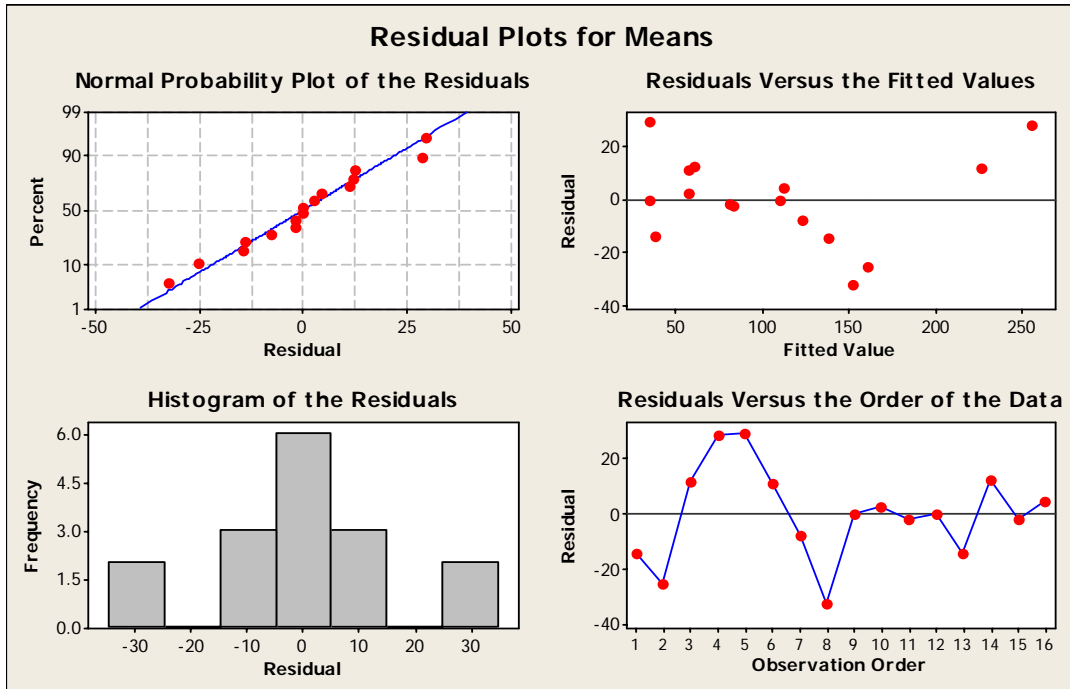


Figure 4.24 Residual plots for mean on erosion rate of fly-ash+quartz+illmenite coatings.

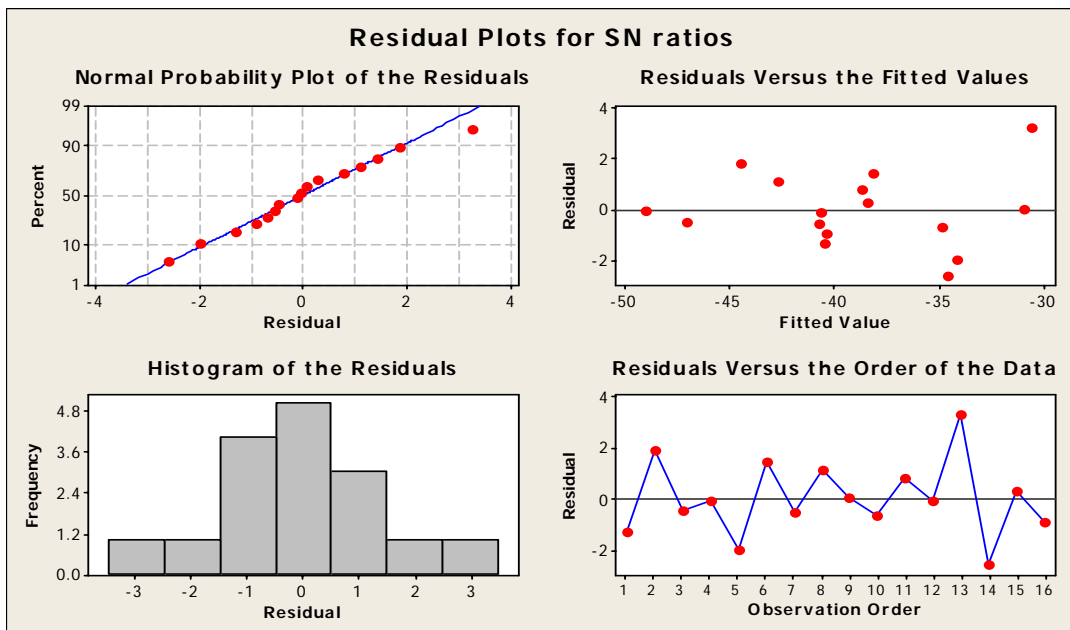


Figure 4.25 Residual plots for S/N ratio on erosion rate of fly-ash+quartz+illmenite coatings.

In Fig 4.26, main effects plot for mean are given. Here, it is observed that, erosion rate of the coating decrease by increasing the power level, decreasing the pressure and decreasing the impact angle of erodent. In Fig 4.27, Main effect of plots for S/N ratios are given. In case of lower is better Taguchi experiment, for S/N ratio value will be more, which is given in Fig 4.27.

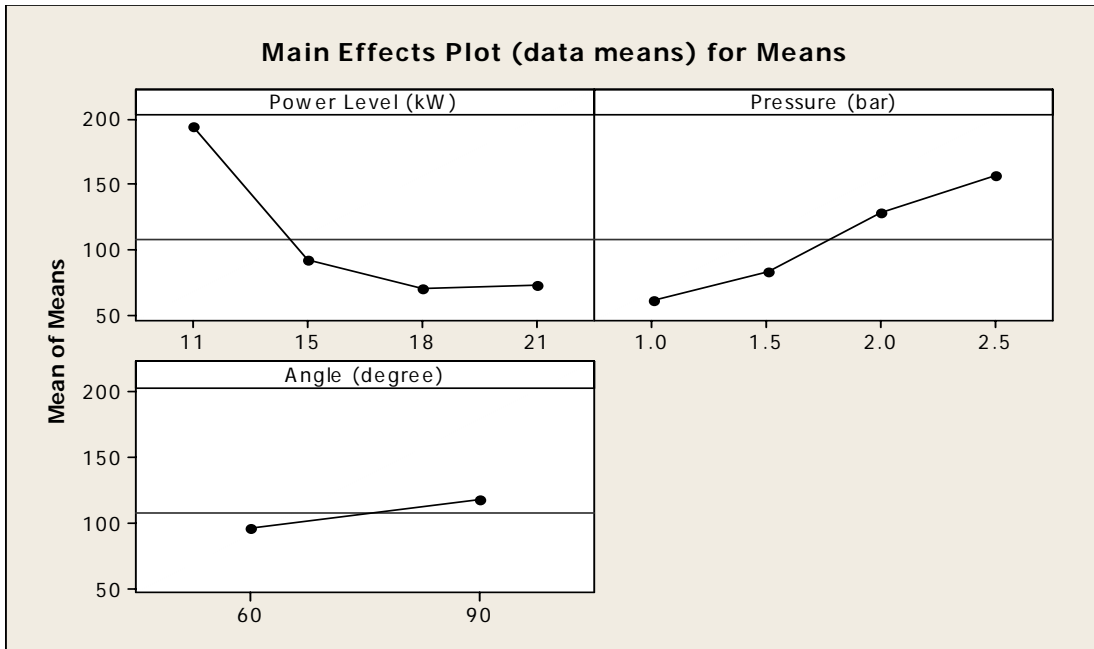


Figure 4.26 Main effect of plots for means on erosion rate of fly-ash+quartz+illmenite coatings.

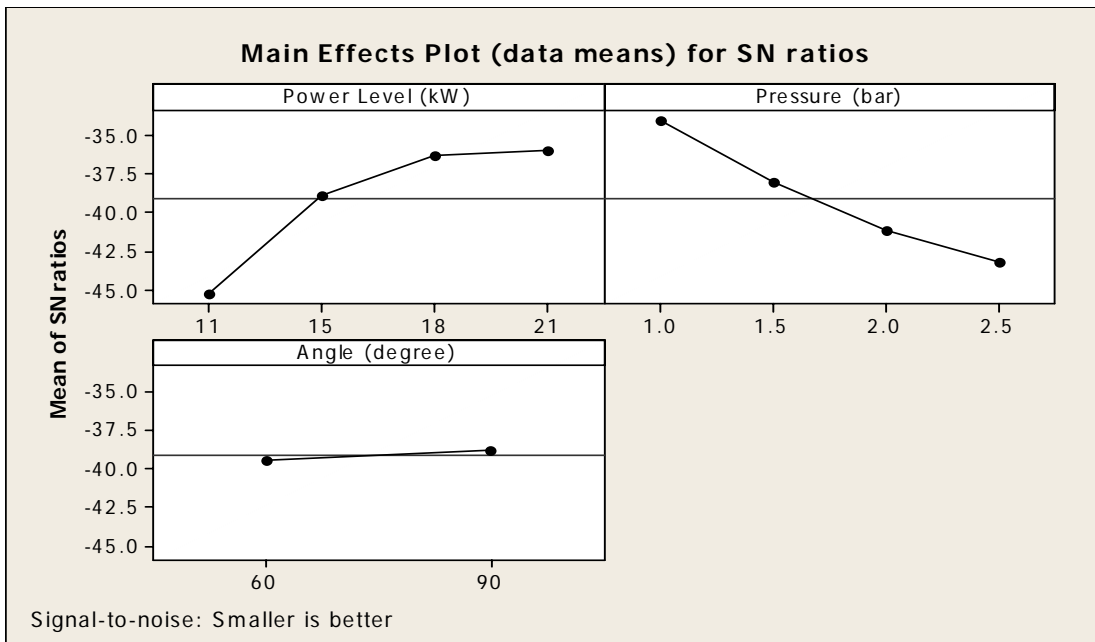


Figure 4.27 Main effects of plots for S/N ratios on erosion rate of fly-ash+quartz+illmenite coatings.

Based on the above findings, erosion tests were carried out, on plasma sprayed fly ash+quartz+illmenite coatings by a stream of silicon carbide particles of average size of ~200

μm ; at different impact angles (60° and 90°) with standoff distance of 65 mm and at a pressure 1.0 bar to 2.5 bar.

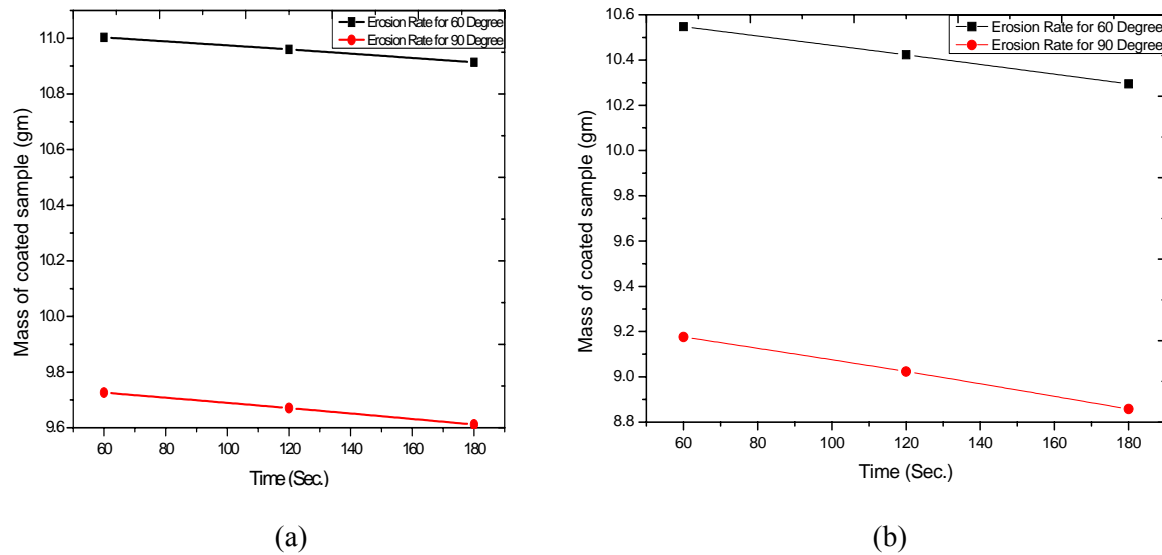


Figure 4.28 cumulative mass loss of coating vs time for 18kW coating substrate at erodent impact pressure of (a) 1 bar, (b) 2 bar.

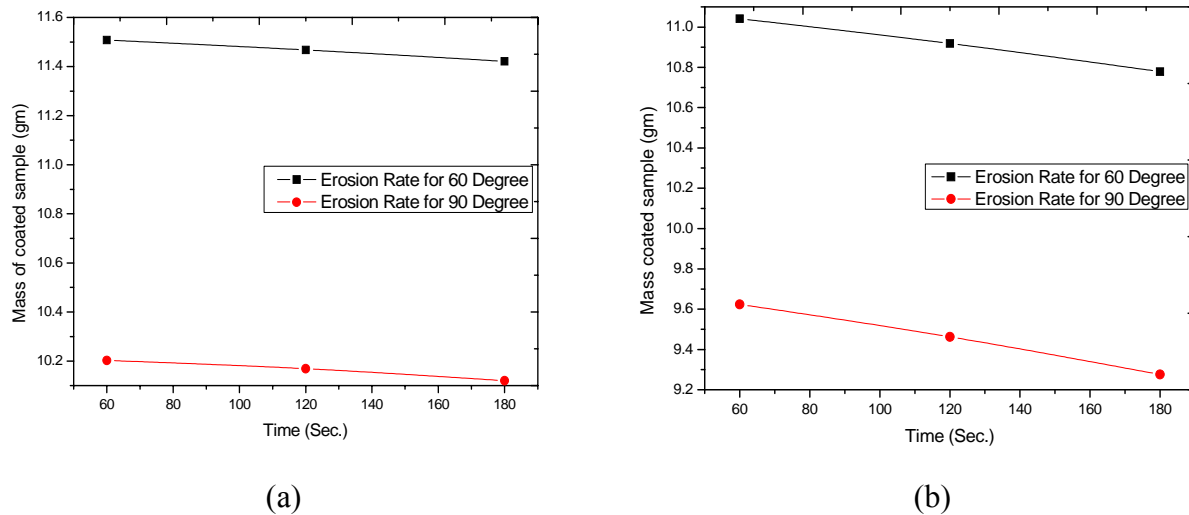


Figure 4.29 Cumulative mass loss of coating vs time for 21kW coating substrate at erodent impact pressure of (a) 1 bar, (b) 2 bar.

The variation of cumulative mass loss with time, in case of the coating eroded by SiC for 18kW are illustrated in Fig 4.28 and for 21kW illustrated in Fig 4.29. From the figures, it is seen that, the coating mass decreases with time period. The initial mass loss is high and it follows a steady state after certain time of exposure. Finnie [190] has explained that the drastic drop of erosion rates is due to transition of type of fracture mechanism i.e. from brittle to ductile behavior. Sparks and Huchtings [191] have also discussed this type of transition in detail using

models based on Hertzian fracture and lateral fracture. And such mechanisms are explained in the book edited by Ritter [192] also. So in our observation, sharp change/decrement in mass of the coatings may be due to brittle to ductile transition behavior, with increment in attack time. From the above figures, it is evident that the initial wear rate is high irrespective of the angle of impact. With increasing exposure time the rate of wear starts decreasing and in the transient regime, a steady state is attended. It is also found that, maximum erosion occurs at normal impact angle ($\alpha = 90^\circ$). This behavior is observed in case of brittle materials where the erosion rate continuously increases with increasing the impact angle and attains a maximum at 90° (normal impact), in addition under brittle erosion conditions the magnitude of erosion rate is determined only by normal component of impact velocity [193], where as in case of ductile materials; major amount of material removal is by plastic deformation and high rate of material removal is at shallow impact angles. According to the common rule of the erosion rate with the change of impact angle α , the erosion wear can be divided into ductile/plastic material wear and brittle material wear. The relationship between erosion rate and impact angle as predicted by Lishizhou [194] is as follows:

$$E = A \cos^2 \alpha \sin(m\alpha) + B \sin^2 \alpha \dots \dots \dots (4.3)$$

Where m, A, B are constants.

For typical brittle material, A is equal to zero and the erosion rate is largest at 90° impact angle. For typical plastic material, B is equal to zero and the erosion rate is largest at about 20° - 30° impact angle. The variation of erosion wear (Fig.4.19, 4.20) thus confirms that the angle at which the stream of solid particles impinges the coating surface influences the rate of material removal i.e. the degree of erosion. It further suggests that, this dependency is also influenced by the hardness of the erodent particles.

4.4.5 Microstructural Investigation of Erodants and Eroded Surfaces.

The morphology of the erodent (i.e. SiC) is shown in Fig 4.30. It can be visualized that silicon carbide particles are having multiple angular facets and sharp edges. This might be the cause of fast rate of removal of material through chipping/plowing of the surface when silicon carbide is used as erodent, thereby leading to higher amount of material loss (i.e. cumulative mass loss). Hence erosion rate is higher. So there is negligible crack initiation/formation and major chipping portions are observed on the eroded surfaces.

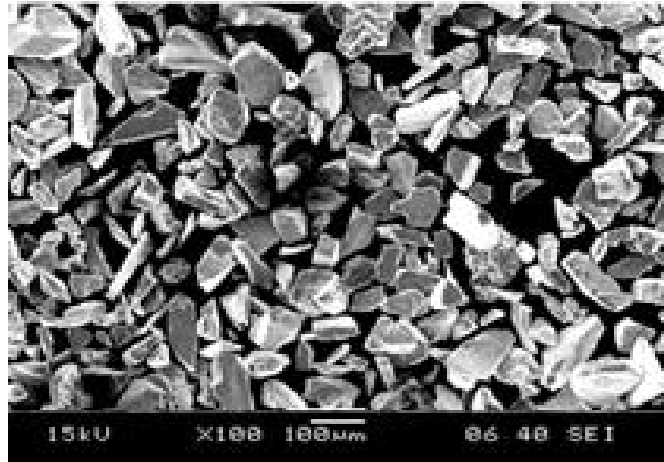
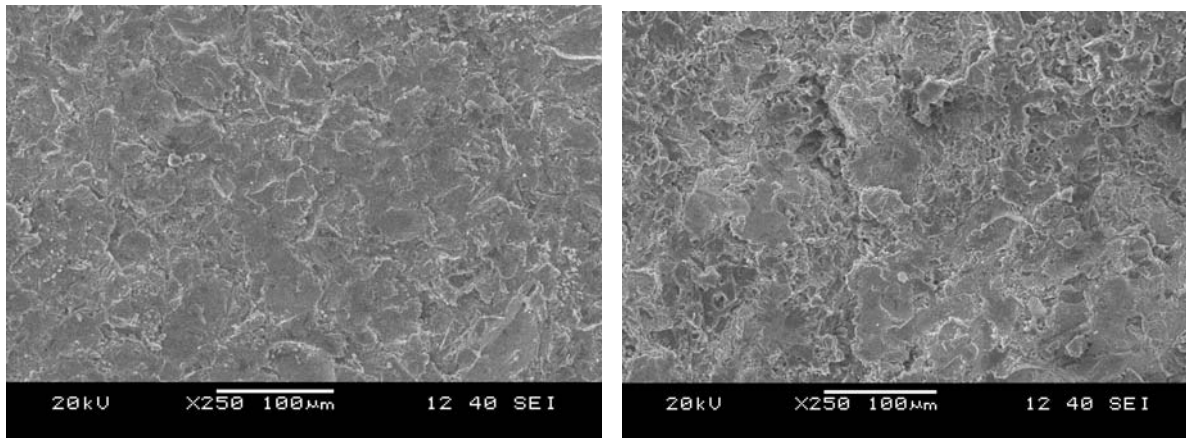


Figure 4.30 Surface morphology of SiC particles.

Morphology of Eroded Surfaces

Surface morphology of fly ash-quartz coating eroded with SiC erodent at different impact angles are shown in Fig 4.31.



(a)

(b)

Figure 4.31 SEM micrographs of eroded surfaces of coatings deposited at 18 kW at angle of impact (a) 60° and (b) 90° using SiC as the erodent.

Fig. 4.31 (a) and Fig 4.31 (b), show the surface morphology of worn surfaces, when the erodent is impacted at 60° and 90° respectively. Some small cracks are observed and spread along splats boundaries. At 60° angle of impact, there are many angular grooves occurs. At 90° angle of impact, sharp vertical grooves are seen which is due to dominating effect of perpendicular component of the force of impingement of the erodent. In general it can be stated that when hard and multifaceted erodent i.e. SiC is used, deeper groves are produced and plastically flow regions are found and also limit the surface crack propagation.

4.5 DISCUSSION

In this investigation, it is found that the adhesion strength increases up to a certain limit (i.e. up to 18kW) then further increasing in power level there is no significant change in adhesion strength. Same observation also seen in case of deposition efficiency. This is a measure of the amount of material deposited per unit surface area. It is observed that the coating thickness acquires a maximum at 15 kW input power and then decreases. The porosity in the coatings is also found to be maximum at nearly same input power level. The increased amount of porosity in case of low and high power levels may be the cause of low adhesion strength. Variation of coating hardness with power level reveals that, there might be formation/transformation of allotropic forms and their compositional variations during spray deposition, which is evident from the XRD compositional analysis. It is observed that, the surface roughness decreases with increasing in power level. To assess the suitability of these coatings for tribological applications, solid particle erosion wear behavior is studied. Taguchi statistical technique is used to identify the significant parameter affecting the wear rate of the coatings. Impingement angle followed by erodent size is identified as the important process parameter affecting the erosion of the coatings. With the increase in impact angle erosion wear increases and attains maximum at 90°. The angle of impact determines the relative magnitude of the two components of the impact velocity namely, the component normal to the surface and parallel to the surface. The normal component determines/is responsible for the lasting time of impact (i.e. contact time) and the load. The product of this contact time and the tangential (parallel) velocity component determines the amount of sliding that takes place. The tangential velocity component also provides a shear loading to the surface in addition to the normal load of the normal velocity component. Hence, as this angle changes the amount of sliding that takes place also changes as does the nature and magnitude of the stress system. Both of these aspects influence the way a coating/material wears. Statistical modeling/analysis techniques viz. ANN, Taguchi technique etc. can be very much useful to predict the experimental data with conducting least number of experiments; and also can predict experimental results beyond the parameter domains used in the experimentations.

Chapter 5

Conclusions

Chapter 5

Conclusions

The conclusions drawn from the present investigation are as follows:

- ❖ Fly ash, the waste generated from thermal power plants may be eminently coatable on metal substrates when mixed with quartz and illmenite, the low grade mineral ore, employing atmospheric plasma spraying technique.
- ❖ Such coatings possibly possess potential coating characteristics such as good adhesion strength, hardness, porosity etc.
- ❖ Operating power level of the plasma torch influences the coating adhesion strength, deposition efficiency and coating hardness to a great extent. The coating morphology is largely affected by the plasma input power.
- ❖ The microstructure of the coatings is also dependent on the physical characteristics such as porosity, phase transformations of the coating materials during spraying at different power levels.
- ❖ Adhesion strength of the coatings varied with the plasma power level and the kind of substrate on which coatings are deposited. Maximum adhesion strength of 6.56 MPa on mild steel substrate and 6.32 MPa on copper substrate are obtained.
- ❖ The coating-substrate interface (bond) strength increases with the input power to the torch up to a certain power level and further increase in input power there is no significant increase in adhesion strength. Coating adhesion is better in case of mild steel substrate than that of copper substrate.
- ❖ A maximum deposition efficiency of 48 % could be achieved for mild steel and 43% for copper substrates and the deposition efficiency has increased in a step up fashion with the increase in torch power input.
- ❖ Amount of porosity is more in case of coatings made at lower power level and at higher power level. However porosity is less for the coatings made 18 kW. More amount of

porosity may be the reason for low adhesion strength of the coatings deposited at low and high power levels.

- ❖ Due to phase transformations and inter-oxide formation during plasma spraying, changes in coating characteristics such as hardness etc. are observed.
- ❖ The coatings developed in this work are much harder than substrate metals on which they are deposited. Hence these coatings can be recommended for tribological applications.
- ❖ Factors such as erodent size, impact angle of the erodent, velocity of impact and standoff distance and hardness etc. affect the coating erosion wear rate. Taguchi experimental design has proved to be a useful tool for identifying the significant parameters in this case. It has been identified that, impact angle and erodent size are the most significant factors affecting the erosion wear rate of fly ash+quartz+illmenite coatings.
- ❖ Maximum erosion of the coatings took place at an impact angle of 90° .
- ❖ Microstructure of the eroded surfaces suggests that, when hard and multifaceted erodent i.e. SiC is used, deeper grooves are produced and plastically flow regions are found and also less amount of surface crack propagation.
- ❖ Erosion wear behavior is one of the main requirements of the coatings developed by plasma spraying for recommending specific application.
- ❖ The coating sustains erosion by solid particle impingement substantially and therefore fly ash+quartz+illmenite can be considered as a potential coating material suitable for various tribological applications.

SCOPE FOR FUTURE WORK

The present work opens up a wide area for future investigators to explore the possibility of development of new fly-ash composite materials to ascertain further improvement in coating properties with considering cost of coating material.

References

References

- [1] S.C. Mishra, “Analysis of Experimental Results of Plasma Spray Coatings Using Statistical Techniques”, BOOK: Advanced Plasma Spray Applications, Published by InTech, Printed in Croatia, 83-96, 2012, ISBN 978-953-51-0349-3.
- [2] P Fauchais, Topical Review: Understanding plasma spraying, Journal of Physics D: Applied Physics, 37, 2004, R86-R108.
- [3] Alok Satapathy, S.C. Mishra and D.K. Nath, P.V. Ananthapadmanabhan and K.P. Sreekumar, “Deposition of Redmud-Graphite Coating on Metals by Plasma Spraying, International Conference on Advances in Surface Treatment”, Research & Applications (ASTRA), 537-540, 2004.
- [4] Swapnil M.Kondawar & Mr. V.W.Khond “Fly Ash Utilization Technologies and Use as Thermal Composite Insulation”, Indian Streams Research Journal, Vol - II , ISSUE – III, 2012, <http://www.isrj.net/PublishArticles/647.aspx>.
- [5] S. C.Mishra and Alok satpathy, “Plasma spraying of red mud-fly ash mixture on metals: an experimental study”, Presented in National Conference on Materials and Related Technology, TIET, 2003, Patiala, India, <http://dspace.nitrkl.ac.in/dspace/bitstream/2080/315/1/ALOK-NCMRT+2003.pdf>.
- [6] C. N. Panagopoulos, E.P. Georgiou, A.G. Gavras, “Composite zinc-fly ash coating on mild steel”, Surface & Coatings Technology”, 204:37-41, 2009, doi:10.1016/j.surfcoat.2009.06.023.
- [7] S. C.Mishra, S.K.Acharya, “Weathering behavior of fly ash-jute-polymer composite”, Journal of Reinforced Plastics and Composite, vol.26, 1201-1202, 2007.
- [8] Jadambaa Temuujin, Amgalan Minjigmaa, William Rickard, Melissa Lee, Iestyn Williams, Arie van Riessen, “Fly ash based geopolymer thin coatings on metal substrates and its thermal evaluation”, Journal of Hazardous Materials, Vol. 180, 748-752, 2010.
- [9] S. Das, Thesis on: “Processing and Tribological Behaviour of Flyash-Illmenite Coating”, Department of Metallurgical & Materials Engineering National Institute of Technology, Rourkela, 2008.
- [10] S. Praharaj, “Processing and Characterization Of Fly Ash- Quartz Coatings”, Thesis Submitted for M.Tech Degree in Metallurgical & Materials Engineering , National Institute Of Technology, Rourkela , 2009.

- [11] Seiji Kuroda, Jin Kawakita, Makotowatanabe and Hiroshi Katanoda, "Warm Spraying- A Novel Coating Process Based on High-Velocity Impact of Solid Particles", *Science and Technology of Advancedmaterials*, 9: 033002, pp17, 2008, DOI:10.1088/1468-6996/9/3/033002.
- [12] C. M. Cotell and J.A. Sprague, "Preface: Surface Engineering", *ASM Handbook*, ASM International, Vol. 5, pp.5, 1994.
- [13] Joseph R. Davis, "Surface Engineering for Corrosion and Wear Resistance", ASM International, 2001, ISBN: 0-87170-700-4.
- [14] George E. Totten, Hong Liang, "Surface Modification And Mechanisms: Friction, Stress And Reaction Engineering", published by Taylor & Francis, ISBN 0-203-02154-10-203-02154-1
- [15] R. Edwards, "Cutting Tools", The Institute of Materials, UK, 1993.
- [16] K. G. Budinski, "Surface Engg. for Wear Resistance", N.J., USA, 1988.
- [17] O. Knotek, "Handbook of Hard Coatings: Deposition Technologies, Properties and Applications", U. S. A./William Andrew Publishing, LLC, Norwich, New York, 2001.
- [18] K. G. Budinski, "Engineering Materials, Properties and Selection", Pub. Prentice-Hall of India, New Delhi, India 1998.
- [19] Metco Plasma Spraying Manual, Metco, USA, 1993.
- [20] T. S. Sidhu, S. Prakash and R. D. Agrawal, "Studies on the properties of high-velocity oxy-fuel thermal spray coatings for higher temperature applications", *Materials Science*, Vol. 41, No. 6, 805-823, 2005, DOI: 10.1007/s11003-006-0047-z.
- [21] H. Singh, B. S. Sidhu, D. Puri, and S. Prakash, "Use of plasma spray technology for deposition of high temperature oxidation/corrosion resistant coatings- a review", *Materials and Corrosion*, 58, No. 2, 2007, DOI: 10.1002/maco.200603985.
- [22] Thorpe, M.L., "Thermal Spray. Industry in Transition", *Adv.Mater.Process.*, Vol. 143, No. 5, 50-61, 1993.
- [23] Yongxiong Chen, Xiubing Liang, Yan Liu, Jinyuan Bai, Binshi Xu, "Finite element modeling of coating formation and transient heat transfer in the electric arc spray process", *International Journal of Heat and Mass Transfer*, 53, 2012-2021, 2010.
- [24] L. F. Longo, "Thermal Spray Coatings", ASM, USA, 1985.
- [25] V. Meringolo, "Thermal Spray Coating", Tappi Press, Atlanta, USA, 1983.

- [26] Alok Satapathy, “ Thermal Spray Coating Of Red Mud On Metals”, A Thesis Submitted In Partial Fulfilment of The Requirement for The Degree Of Doctor of Philosophy in Mechanical Engineering, National Institute of Technology Rourkela, India November, 2005.
- [27] Alok Satpathy, S.C. Mishra, P.V.A Padmanabhan, K.P. Sree Kumar, “Development of Ceramic Coatings Using Red Mud- A Solid Waste of Alumina Plants”, Journal of Solid Waste Technology and Management, Vol. 33, No 2, 48-53, 2007.
- [28] P. Fauchais, M. Verdelle, A. Verdelle, L. Bianchi, “Plasma Spray: Study of Coating Generation”, Ceramic International, Vol. 22, 295-303, 1996.
- [29] B. Selvan¹, K. Ramachandran^{1a}, B. C. Pillai¹ and D. Subhakar, “Modelling of the plasma-substrate interaction and prediction of substrate temperature during the plasma heating”, Eur. Phys. J. D, Vol. 61, No 3, 663-675, 2011, <http://dx.doi.org/10.1140/epjd/e2010-10443-1>.
- [30] E. Pfender, “Fundamental Studies Associated with the Plasma Spray Process”, Surf. Coat. Technol., Vol. 34, pp.1, 1988.
- [31] P. Fauchais, A. Vardelle, M. Vardelle, “Modelling of Plasma Spraying of Ceramic Films and Coatings”, Ed. Vinezini, Pub. Elsevier State Publishers B.V, 1991.
- [32] National Materials Advisory Board, “Coatings for High-Temperature Structural Materials: Trends and Opportunities”, National Academy Press Washington D.C., <http://www.nap.edu/openbook/0309053811/html>, 1996.
- [33] A. W. Batchelor, L. N. Lam, M. Chandrasekaran,” Materials Degradation and its Control by Surface Engineering”, 2nd Edition, Imperial College Press, London 2003.
- [34] L. Leon, U. Shawa, Daniel Gobermana, Ruiming Rena, Maurice Gell, Stephen Jiangb, You Wangb, T. Danny Xiaob, Peter R. Strutt, “The dependency of microstructure and properties of nanostructured coatings on plasma spray conditions”, Surface and Coatings Technology 130, 1-8, 2000.
- [35] N. Venkatramani, “Industrial plasma torches and applications”, Current Science, Vol. 83, No. 3, 254-262, 2002.
- [36] Buta Singh Sidhu and S. Prakash, “Evaluation of the behavior of shrouded plasma spray coatings in the platen superheater of coal-fired boilers”, metallurgical and Materials Transactions A, Vol. 37, No 6, 1927-1936, 2006, DOI: 10.1007/s11661-006-0135-6.
- [37] P. Fauchais, J. F. Coudert, M. Vardelle, J. De Physique IV, 7, C 4–187, 1997.
- [38] P. Niranatlumpong, C. B. Ponton, H. E. Evans, Oxid. Met., 53, 241, 2000.

- [39] Wrigren, J., Surf. Coat. Tech. Vol. 45, pp. 263, 1991.
- [40] M. G. Nicholas and K. T. Scott, “Characterization of Grit Blasted Surfaces”, Surfacing Journal, Vol. 12, pp.5, 1981.
- [41] C.W. Kang, H.W. Ng, “Splat morphology and spreading behavior due to oblique impact of droplets onto substrates in plasma spray coating process”, Surface & Coatings Technology 200, 5462-5477, 2006, doi:10.1016/j.surfcoat.2005.07.067
- [42] B. Wielage, U. Hofmann, A. Steinhauser, G. Zimmerman, “Improving Wear and Corrosion Resistance of Thermal Spray Coatings”, Surface Engineering, Vol. 14, No.2, 136-138, 1998.
- [43] N. Y. Lee, D. P. Stinton, C. C. Brandt, F. Erdogan, Y. D. Lee, and Z. Mutasim, “Concept of Functionally Graded Materials for Advanced Thermal Barrier Coating Applications”, J.Am. Cer. Soc., Volume 79, No.12, 3003-3012, 1996.
- [44] Joseph R. Davis, “Handbook of Thermal Spray Technology”, ASM International. Thermal Spray Society Training Committee, 2004, ISBN 0-87170-795-0.
- [45] J. Tanya, BEng Levingstone, “Optimisation of Plasma Sprayed Hydroxyapatite Coatings”, Ph. D thesis, School of Mechanical and Manufacturing Engineering, Dublin City University, Ireland, 2008.
- [46] Christian Coddet, “Thermal Spray: Meeting the Challenges of the 21st Century, Proceedings of the 15th international thermal spray conference”, France, Vol. 1, 1998, ISBN 0-87170-659-8.
- [47] H. S. Ingham and A. J Fabel, Welding Journal, pp. 101, 1975.
- [48] B. Elvers, S. Hawkins and G. Schultz, Uhlmann’s Encyclopedia of Industrial Chemistry, Vol. 1/16, VCH, pp. 433, 1990.
- [49] Hennaut, J., Othmezouri, J. and Charlier, J., Mat. Sc and Tech., Vol.11, pp. 174, 1995.
- [50] R Mc Pherson, “A Review of Microstructure and Properties of Plasma Sprayed Ceramic Coatings”, Surface and Coatings Technology, Vol. 39, No. 40, 173-181, 1989.
- [51] H.W. Ng, Z. Gan, “A finite element analysis technique for predicting as-sprayed residual stresses generated by the plasma spray coating process”, Finite Elements in Analysis and Design 41, 1235-1254, 2005.
- [52] Mc Pherson, R., “The Relationship Between the Mechanism of Formation, Microstructure and Properties of Plasma Sprayed Coatings”, Thin Solid Films, Vol. 83, 297-310, 1981.

- [53] N. N Ault, "Characteristics of Refractory Oxide Coatings Produced by Flame Spraying", J.Am.Ceram.Soc., Vol. 40, 69-74, 1957.
- [54] R. Mc Pherson, "Formation of Metastable Phases in Flame and Plasma Sprayed Coatings", J.Mater.Sci., Vol. 8, pp. 851, 1973.
- [55] R. Mc Pherson, and B.V. Shafer, "Interlamellar Contact Within Plasma Sprayed Coatings", Thin Solid Films, Vol. 97, 201-204, 1982.
- [56] Saed Safai , Herbert Herman, "Microstructural Investigation of Plasma Sprayed Aluminium Coatings", Thin Solid Films, Vol. 45, 295-307, 1977.
- [57] N. A. Tape, E. A. Baker and B. C. Jackson, "Plating and Surface finishing", pp. 30, 1976.
- [58] An Introduction to Thermal Spray, Sulzer Metco , Sulzer, Issue 4 , 1-24, 2011.
- [59] S. Matthews and B. James, "Review of Thermal Spray Coating Applications in the Steel Industry: Part1- Hardware in Steel Making to the Continuous Annealing Process", Journal of Thermal Spray Technology, Vol. 19, No.6, 1267-1276, 2010, DOI: 10.1007/s11666-010-9518-8.
- [60] <http://www.progressivesurface.com/aerospace.php>
- [61] <http://www.asbindustries.com/industry-applications/industries/medical-coatings>
- [62] F. N. Longo, "Industrial guide- markets, materials, and applications for thermal-sprayed coatings", Journal Of Thermal Spray Technology, Vol.1, No.2, 143-145, 1992, DOI: 10.1007/BF02659014.
- [63] <http://www.thermalsprayindia.com/Gas-Turbine.php>
- [64] B. V. Tilak, A. C. Ramamurthy and B. E. Conway, "High performance electrode materials for the hydrogen evolution reaction from alkaline media", Journal Of Chemical Sciences, Vol. 97, NO. 3-4, 359-393, 1986, DOI: 10.1007/BF02849200.
- [65] Lynne M. Ernes, Richard C. Carlson, Kenneth L. Hardee, "Substrate of improved plasma sprayed surface morphology and its use as an electrode in an electrolytic cell", Patent 5324407 Issued on June 28, 1994, Filing date: Feb 26, 1993.
- [66] <http://www.edisonsa.co.za/thermalspraying.htm>
- [67] <http://www.ec21.com/product-details/Aluminium-Foil-Roll--6584377.html>
- [68] Pierre D'Ans, Jean Dille, Marc Degrez, "Thermal fatigue resistance of plasma sprayed yttria-stabilised zirconia onto borided hot work tool steel, bonded with a NiCrAlY coating:

Experiments and modeling”, Surface and Coatings Technology, Vol. 205, Issue 11, 3378-3386, 2011.

- [69] Robert B. Heimann, “Plasma-Spray Coating: Principles and Applications”, 1996, ISBN 3-527-29430-9
- [70] Ramnarayan Chattopadhyay, “Advanced Thermally Assisted Surface Engineering Processes”, 2004, ISBN 1-4020-7696-7.
- [71] <http://www.textiletoday.com.bd/magazine/printable.php?id=175>
- [72] <http://www.indiamart.com/plasmaapplication-processor-s/thermal-spraying.html>
- [73] http://nxedge.supremeserver23.com/is_glass_industry.php
- [74] R. Holm, “The Frictional Force Over the Real Area of Contact”, *Wiss. Vereoff. Siemens Werken*, Vol. 17, No. 4, 38-42, 1938.
- [75] S.S. Rajahrama, T.J. Harveya, J.C. Walkera, S.C. Wanga, R.J.K. Wooda, G. Lalev, “A study on the evolution of surface and subsurface wear of UNS S31603 during erosion-corrosion”, *Wear* 271, 1302-1313, 2011, doi:10.1016/j.wear.2010.11.018.
- [76] A. Nilsson, L. Kirkhorn, M. Andersson, J. E. Stahl, “Improved tool wear properties in sheet metal forming using Carbide Steel, a novel abrasion resistant cast material”, *Wear* 271, 1280-1287, 2011, doi:10.1016/j.wear.2011.01.083
- [77] Z. Kamdia, P.H. Shipwaya, K.T. Voiseya, A.J. Sturgeon, “Abrasive wear behaviour of conventional and large-particle tungsten carbide-based cermet coatings as a function of abrasive size and type”, *Wear* 271, 1264-1272, 2011, doi:10.1016/j.wear.2010.12.060
- [78] F. Cernuschia, L. Lorenzonia, S. Capelli, C. Guardamagnaa, M. Karger, R. Vaßenb, K. von Niessenc, N. Markocsand, J. Menueye, Carlo Giolli, “Solid particle erosion of thermal spray and physical vapour deposition thermal barrier coatings”, *Wear* 271, 2909-2918, 2011, doi:10.1016/j.wear.2011.06.013
- [79] M. Toparli, E. Celik, I. Birlik, E. Dokumaci & N. F. Ak Azem, “Tribological Properties of Electric Arc-Sprayed CuSn”, *Coating for Bearing Elements, Tribology Transactions*, 52: 389-394, 2009, doi: 10.1080/10402000802593122
- [80] Mustafa Ulutan A, M. Mustafa Yildirim B, Soner Buytoz C & Osman N. Çelik, “Microstructure and Wear Behavior of TIG Surface-Alloyed AISI 4140 Steel”, *Tribology Transactions*, 54: 67-79, 2011, doi: 10.1080/10402004.2010.519859

- [81] D. M. Mihut a , S. M. Aouadi b & S. L. Rohde, “Assessing Nanotribological Performance and Surface Energies of Inconel-ZrN, Cr-ZrN, Nb-ZrN, and ZrN Thin Films”, *Tribology Transactions*, 53: 881-887, 2010, doi: 10.1080/10402004.2010.501949
- [82] M. X. Wei a , S. Q. Wang a , X. H. Cui a & K. M. Chen, “Characteristics of Extrusive Wear and Transition of Wear Mechanisms in Elevated-Temperature Wear of a Carbon Steel”, *Tribology Transactions*, 53: 888-896, 2010, doi: 10.1080/10402004.2010.501950
- [83] Kuldeep K. Mistry, Ardian Morina, Anne Neville, “A tribochemical evaluation of a WC-DLC coating in EP lubrication conditions”, *Wear* 271, 1739-1744, 2011, doi:10.1016/j.wear.2011.01.071
- [84] Manoj Masanta, S.M. Shariff, A. Roy Choudhury, “A comparative study of the tribological performances of laser clad TiB₂-TiC-Al₂O₃ composite coatings on AISI 1020 and AISI 304 substrates”, *Wear* 271, 1124-1133, 2011, doi:10.1016/j.wear.2011.05.009
- [85] Chong Y. Wonga, Christopher Solnordalb, Anthony Swallowc, Steven Wangd, Lachlan Grahama, Jie Wu, “Predicting the material loss around a hole due to sand erosion”, *Wear* 276- 277, 1-15, 2012, doi:10.1016/j.wear.2011.11.005
- [86] Vinay Pratap Singh, Anjan Sil, R. Jayaganthan, “Tribological behavior of plasma sprayed Cr₂O₃-3%TiO₂ coatings”, *Wear* 272, 149-158, 2011, doi:10.1016/j.wear.2011.08.004
- [87] M. F. Ashby and S. C. Lim, “Wear-Mechanism Maps” *Scripta Metallurgical et Materialia*, Vol. 24, 805-810, 1990.
- [88] Y. Wang, T.C. Lei and C.Q. Gao, “Influence of Isothermal Hardening on the Sliding Wear Behaviour of 52100 Bearing Steel”, *Tribology International*, Vol. 23, No.1, 47-63, 1990.
- [89] N. Soda, “Wear of Some F.F.C metals During Unlubricated Sliding Part-1, Effects of Load, Velocity and Atmospheric Pressure on Wear”, *Wear*, Vol. 33, 1-16, 1975.
- [90] J.T. Burwell, “Survey of Possible Wear Mechanisms”, *Wear*, Vol. 1, 119-141, 1957/58.
- [91] K. H. Zumgahr, “Microstructure and Wear of Materials”, Amsterdam, 1987.
- [92] J. T. Burwell and C. D. Strang, “On the Empirical Law of Adhesive Wear”, *J. Appl. Phys.* 23, 18 (1952); <http://dx.doi.org/10.1063/1.1701970>
- [93] ASTM G40-99 Standard Terminology Relating to Wear and Erosion, doi: 10.1520/G0040-99.
- [94] A. V. Levy, “The Erosion-Corrosion Behaviour of Protective Coatings”, *Surface and Coatings technology*, Vol. 36, 381-406, 1988.

- [95] Iain. Finnie, "Some Reflections on the Past and Future of Erosion", *Wear*, Vol. 186, No. 187, 1-10, 1995.
- [96] T. H. Kosel, "Solid Particle Erosion", In: *ASM Handbook, Friction, Lubrication and Wear Technology*, ASM International, USA, Vol. 18, 199-213, 1992.
- [97] J. Hallings, "Principles of Tribology", London and Basingstoke, The Macmillan Press Ltd., pp. 401, 1975.
- [98] C. M. Hansson, "Cavitation Erosion", In: *ASM Handbook, Friction, Lubrication and Wear Technology*, ASM International, USA, Vol. 18, 214-220, 1992.
- [99] J. E. Miller, "Slurry Erosion", In: *ASM Handbook, Friction, Lubrication and Wear Technology*, ASM International USA, Vol. 18, 233-235, 1992.
- [100] J. F. Mc Cabe, Y. Wang, MJA Braem, "Surface contact fatigue and flexural fatigue of dental restorative materials", 2000, doi: 10.1002/(SICI)1097-4636(20000605)50:3<375::AID-JBM11>3.0.CO;2-R
- [101] H. Abd-El-Kader, S.M. El-Raghy, "Wear-corrosion mechanism of stainless steel in chloride media", *Corrosion Science*, Vol. 26, Issue 8, 647-653, 1986.
- [102] P.L. Ko, "Metallic Wear-A Review with Special References to Vibration-Induced Wear in Power Plant Components", *Tribology International*, Vol. 20, No. 1, 66-78, 1987.
- [103] L. S. Eyre, "Wear Characteristics of Metals", *Tribology International*, 203-212, 1976.
- [104] J. Blau, "Fifty Years of Research on the Wear of Metals." *Tribology International*, Vol. 30, No. 5, 321-331, 1997.
- [105] M. Cadenas, R. Vijendra, H.J. Montes and J.M. Sierra, "Wear Behaviour of Laser Cladded and Plasma Sprayed WC-Co Coatings", *Wear*, Vol. 212, 244-253, 1997.
- [106] Nolan, Mercer, P. and Samadi, M., *Surf. Engg.*, Vol. 21, pp.124, 1998.
- [107] Naerheim, Coddet, C. and Droit, P., *Surf. Engg.*, Vol. 11, pp. 66, 1995.
- [108] K. Hojmrle and M. Dorfman, *Mod. Dev. Powder. Met.*, Vol. 15, No.15, pp. 609, 1985.
- [109] O. Knotek, E. Lugschedar, H. Reiman, *J. Vac. Sc. Tech. A*, Vol. 12, No. 4, pp.75, 1975.
- [110] M.Mohanty, R.W.Smith, M. De Bonto, J.P. Celis, E. Lugscheder, "Sliding Wear Behaviour of Thermally Sprayed 75/25 Cr₃C₂/NiCr Wear Resistant Coatings", *Wear*, Vol. 198, 251-266, 1996.

- [111] Y. Liu, D.Y. Chen, "Protective coatings for Cr₂O₃-forming interconnects of solid oxide fuel cells", *International Journal of Hydrogen Energy*, Vol. 34, Issue 22, 9220-9226, 2009.
- [112] *Metals Handbook*, ASM Metals Park, Ohio, USA.
- [113] S. Atamert and J. Stekly, "Microstructure", *Surf. Engg.*, Vol 9, No. 3, pp.231, 1993.
- [114] M.G. Habsur and R.V. Miner, *Mat. Sc. Engg.*, Vol. 83, pp.239, 1986.
- [115] A. E Spear, "Diamond-Ceramic Coating of the Future", *J.Am.Cer.Soc.*, Vol. 72, 171-191, 1989.
- [116] A. Marakawa, "Surface Coatings of Super hard Materials for Tool Applications", *Mat. Sc. Forum*, Vol. 246, 1-28, 1997.
- [117] K. Okada, S. Komatsu, S. Matsumoto, Y. Moriyoshi, "Morphology of Diamonds Prepared in a Combustion Flame", *J. Mat. Sc.*, Vol. 26, 3081-3085, 1991.
- [118] W. Zhu, B.H. Tan, H.S. Tan, "Diamond Thin Films Synthesized by a Multinozzle Oxy-Acetylene Chemical Vapor Deposition Method", *Thin Solid Films*, Vol. 236, 106-110, 1993.
- [119] P. Hollman, A. Alhelisten, T. Bjorke, S. Hogmark, "CVD Diamond Coatings in Sliding Contact With Al, Al-17Si and Steel", *Wear*, Vol. 179, 11-16, 1994.
- [120] A. Alhelisten, "Abrasion of Hot Flame Deposited Diamond Coatings", *Wear*, Vol. 185, pp.213, 1995.
- [121] Dong, Yingchao, Feng, Xuyong, Feng, Xuefei, Ding, Yanwei, "Preparation of Low-cost Mullite Ceramics from Natural Bauxite and Industrial Waste Fly ash", *Journal of Alloys and Compounds*, Vol. 460, 559-606, 2008.
- [122] L.N. Satapathy, "A Study on the Mechanical, Abrasion and Microstructural Properties of Zirconia-Fly ash Material", *Ceramics International*, Vol. 26, 39-45, 2000.
- [123] S. Tiwari, M. Saxena, "Use of Fly ash in High Performance Industrial Coatings", *British Corrosion Journal*, Vol. 34, No. 3, 184-191, 1999.
- [124] S.C. Mishra, K.C. Rout, P.V.A. Padmanabhan & B. Mills, "Plasma spray coating of fly ash pre-mixed with aluminium powder deposited on metal substrates", *Journal of Materials Processing Technology*, 102, 9-13, 2000.
- [125] S. C. Mishra, Satyabati Das, Alok Satapathy and S. Sarkar, "Investigation on Composite Coating of Low Grade Minerals", *Journal of Reinforced Plastics and Composites*, Vol. 28, No. 24, 3061-3067, 2009, doi: 10.1177/0731684408094225.

- [126] S.C.Mishra, S.Praharaj, Alok Satpathy, "Evaluation of Erosion Wear of a Ceramic Coating With Taguchi Approach", Journal of Manufacturing Engineering, Vol.4, Issue.2, 241-246, 2009.
- [127] S. C. Mishra, Alok Satapathy and M. Chaithanya, "Wear Characteristics of Plasma Sprayed Nickel-Aluminum Composite Coatings", Journal of Reinforced Plastics and Composites, Vol. 28, No. 23, 2009, DOI: 10.1177/0731684408094067.
- [128] S.C.Mishra and Alok satpathy, "Plasma spraying of red mud-fly ash mixture on metals: an experimental study", Presented in National Conference on Materials and Related Technology, TIET, 2003, Patiala, India, <http://dSPACE.nitrkl.ac.in/dSPACE/bitstream/2080/315/1/ALOK-NCMRT+2003.pdf>.
- [129] Buta Singh Sidhu, Singh, Harpreet, D. Puri, S. Prakash, "Wear and Oxidation Behavior of Shrouded Plasma Sprayed Fly ash Coatings", Tribology International, Vol. 40, 800-808, 2007.
- [130] C. N. Panagopoulos, E.P. Georgiou, A.G Gavras, "Composite zinc-fly ash coating on mild steel", Surface & Coatings Technology, 204, 37-41, 2009, doi:10.1016/j.surfcoat.2009.06.023
- [131] J. Temuujin, A. Minjigmaa, W. Rickard, M. Lee, I. Williams, A. Riessen, "Fly ash based geopolymer thin coatings on metal substrates and its thermal evaluation" Journal of Hazardous Materials, Vol.180, 748-752, 2010.
- [132] Sangeeta Tiwari, Mohini Saxena, Sandeep Kumar Tiwari, "Mahua-Oil-Based Resins for the High-Temperature Curing of Fly Ash Coatings", Journal of Applied Polymer Science, Vol. 87, 110-120, 2003.
- [133] Julian Fasano, Eric E. Janz and Kevin Myers, Design Mixers to Minimize Effects of Erosion and Corrosion Erosion, International Journal of Chemical Engineering, Vol. 2012, Article ID 171838, pp. 8, 2012, doi:10.1155/2012/171838.
- [134] Zhang, Tiancheng , Luo, Yichun, Li, D.Y., "Erosion Behavior of Aluminide Coating Modified with Yttrium Addition Under Different Erosion Conditions", Surface and Coatings Technology, Vol. 126, 102-109, 2000.
- [135] Ajit Behera, S .C. Mishra , "Dependence of Adhesion Strength of Plasma Spray on Coating Surface Properties", Journal of Materials & Metallurgical Engineering, Vol. 2, Issue 1, 23-30, 2012.
- [136] H. Singh, D. Puri, S. Prakash and V. V. Rama Rao, On the high-temperature oxidation protection behavior of plasma-sprayed Stellite-6 coatings, Metallurgical and Materials Transactions A, Vol. 37, Number 10 (2006), 3047-3056, doi: 10.1007/s11661-006-0186-8

- [137] O. Knotek, In: Bhushah, R.F., (Ed.), “Handbook of Hard Coatings Deposition Technologies”, Properties and Applications, pp.92, 2001.
- [138] W. Tabakoff, “Erosion Resistance of Superalloys and Different Coatings Exposed to Particulate Flows at High Temperature”, Surf. Coat. Technol., Vol. 120-121, pp.542, 1999.
- [139] A.J. Ninham, A.V. Levy, “The Erosion of Carbide-Metal Composites”, Wear, Vol. 121, 347-361, 1988.
- [140] M.K. Lee, W.W. Kim, C.K. Rhee, W.J. Lee, “ Liquid Impact Erosion Mechanism and Theoretical Impact Stress Analysis in TiN- Coated Steam Turbine Blade Materials”, Metal. Mater. Trans., Vol. A, No. 30 961-968, 1999.
- [141] Maozhong, Yi, Baiyun, Huang and Jiawen, He, “Erosion Wear Behavior and Model of Abradable Seal Coating”, Wear, 252, 9-15, 2002.
- [142] Roberto, Jose, Branco, Tavares, Gansert, Robert , Sampath, Sanjay , Christopher, C. Berndt , Herman, Herbert “Solid Particle Erosion of Plasma Sprayed Ceramic Coatings”, Materials Research, Vol. 7, No.1., 147-153, 2004.
- [143] Paul E. Stutzxnan,Lilia Centeno, “Compositional Analysis of Beneficiated Fly Ashes”, NISTIR 5598, Building and Fire Research Laboratov National Institute of Standards and Technology, Gaithersburg, MD 20899, 1995.
- [144] Christopher C. Berndt, Tensile adhesion testing methodology for thermally sprayed coatings, Journal of Materials Engineering, Vol. 12, Number 2, 151-158, 1990, doi: 10.1007/BF02834068
- [145] Hao Du, Huang Chen, Byung Kyu Moom, Jae Heyg Shin and Soo Wohn Lee, “Effect of Plasma Spraying Condition on Deposition Efficiency, Microstructure And Microhardness of Ti”, doi : 10.2240/azojomo0131.
- [146] H. Chen, S.W.Lee, Hao Du, Ding, X. Chuan and Chu Cho Ho, “ Influence of Feed Stock and Spraying Parameters on the Deposition Efficiency and Microhardness of Plasma Sprayed Zirconia Coatings”, Materials Letter, Vol. 58, Issues 7-8, 241-1245, 2004.
- [147] Manuel F. M. Costa , “Image processing. Application to the characterization of thin films”, Journal of Physics: ConferenceSeries, IOP Publishing, 274 (2011) 012053, doi:10.1088/1742-6596/274/1/012053
- [148] ASTM G76 - 07 Standard Test Method for Conducting Erosion Tests by Solid Particle Impingement Using Gas Jets, <http://www.astm.org/Standards/G76.htm>.
- [149] H. A. Aglan and T. A. Chenock, “Erosion Damage Features of Polyimide Thermoset Composites”, SAMPEQ, 41-47, 1993.

- [150] S. B. Mishra, K. Chandra, S. Prakash, B. Venkataraman, "Characterisation and Erosion Behaviour of a Plasma Sprayed Ni3Al Coating on a Fe-Based Superalloy", *Materials Letters*, Vol. 59, 3694-3698, 2005.
- [151] J. R. Nicholls, M.J. Deakin, D.S. Rickerby, "A Comparison Between the Erosion Behaviour of Thermal Spray and Electron Beam Physical Vapor Deposition Thermal Barrier Coatings", *Wear*, Vol. 233-235, 352-361, 1999.
- [152] Ctibor P. et al "Plasma Sprayed Ceramic Coatings without and with Epoxy Resin Sealing Treatment and Their Wear Resistance", *wear*, Vol. 262, 1274-1280, 2007.
- [153] S. Brossard, P. R. Munroe, A. Tran and M. M. Hyland, "Study of the Splat-Substrate Interface for a NiCr Coating Plasma Sprayed onto Polished Aluminum and Stainless Steel Substrates", *Journal of Thermal Spray Technology*, Vol. 19, No. 1-2, 24-30, 2010, DOI: 10.1007/s11666-009-9419-x.
- [154] M. Jalali Azizpour, H.Mohammadi majd, Milad Jalali, H.Fasihi, "Adhesion Strength Evaluation Methods in Thermally Sprayed Coatings", *World Academy of Science, Engineering and Technology*, 61, 2012.
- [155] Lima C. R. C., Trevisan, R. E., "Graded Plasma Spraying of Premixed Metal Ceramic Powders on Metallic Substrates", *J.Themal Spray Tech.*, Vol. 62, 199-204, 1997.
- [156] Lalleman G. Tallaron, "Study of Microstructure and Adhesion of Spinelles Coatings Formed by Plasma Spraying", Ph. D. Thesis No. 96-58, 1996, E.C. Lyon, France.
- [157] Ramchandran K. et. al. "Microstructure, Adhesion, Microhardness, Abrasive Wear Resistance and Electrical Resistivity of Plasma Sprayed Alumina and Alumina-Titania Coatings", Vol. 315, 149-152, 1998.
- [158] Zhi Yu Zhao, Jian Cheng Fang, H. Wang, H.Y. Li, "Arc Spray Forming of Stainless Steel Mould", *Key Engineering Materials*, Vol. 291-292, doi: 10.4028/www.scientific.net/KEM.291-292.603, 603-608, 2005.
- [159] P. Fauchais, M. Fukumoto, A. Vardelle, and M. Vardelle, "Knowledge Concerning Splat Formation: An Invited Review", *Journal of Thermal Spray Technology* Vol. 13(3), 2004, doi: 10.1361/10599630419670.
- [160] Alok Satapathy, Suwendu Prasad Sahu, Debadutta Mishra, "Development of protective coatings using fly ash premixed with metal powder on aluminium substrates", *Waste Management & Research* 2009: 00: 1-7, doi: 10.1177/0734242X09348016.
- [161] M. Ivosevic, R. Knight, S. R. Kalidindi, G. R. Palmese and J. K. Sutter, "Adhesive/cohesive properties of thermally sprayed functionally graded coatings for

polymer matrix composites”, *Journal Of Thermal Spray Technology*, Vol. 14, No 1, 45-51, 2005, DOI: 10.1361/10599630522765

- [162] Guilmad, Y., Denape, J. and Patil, J. A., “Friction and Wear Thresholds of Alumina-Chromium Steel Pairs Sliding at High Speeds Under Dry and Wet Conditions”, *Trib. Int.* Volume 26, pp. 29, 1993.
- [163] Mohamed S. Morsi, Soha A. Abd El Gwad, Madiha. A. Shoeib, Khalid. F. Ahmed, “Effect of Air Plasma Sprays Parameters on Coating Performance in Zirconia-Based Thermal Barrier Coatings”, *Int. J. Electrochem. Sci.*, 7, 2811-2831, 2012.
- [164] N. Krishnamurthy¹, M.S. Murali², B. Venkataraman³ and P.G. Mukunda, “Erosion Behavior of Plasma Sprayed Alumina and Calcia-Stabilized Zirconia Coatings on Cast Iron Substrate, Ceramic Coatings” *Applications in Engineering*, 100-126, 2012.
- [165] Chen, H., Lee, S.W., Du, Hao, Ding, Chuan. X. and Cho, Chu.l Ho; “ Influence of Feed Stock and Spraying Parameters on the Deposition Efficiency and Microhardness of Plasma Sprayed Zirconia Coatings”, *Materials Letter*, Vol. 58, Issues 7-8, 241-245, 2004.
- [166] Zhijian Yin, Shunyan Tao, Xiaming Zhou, Chuanxian Ding, “Preparation and characterization of plasma-sprayed Al/Al₂O₃ composite coating”, *Materials Science and Engineering A* 480, 580-584, 2008, doi:10.1016/j.msea.2007.07.009.
- [167] Sarikaya Ozkan, “Effect of Some Parameters on Microstructure and Hardness of Alumina Coatings Prepared by Air Plasma Spraying Process”, *Surface and Coatings Technology*, Volume 190,388-393, 2005.
- [168] V. Rao and H. Rao, “C++ Neural Networks and Fuzzy Systems” BPB Publications, 2000.
- [169] S. Guessasma and C. Coddet, “Microstructure of APS Alumina-Titania Coatings Analyzed Using Artificial Neural Network,” *Acta Mater.*, 52 (17) 5157-64, 2004.
- [170] Q. Wen, H. Zhang, P. Zhang, and X. Jiang, “Improved Artificial Neural Network for Data Analysis and Property Prediction in Slag Glass-Ceramic,” *J. Am. Ceram. Soc.*, 88, 1765-1769, 2005.
- [171] M. D. Jean, C. D. Liu, and J. T.Wang, “Design and Development of Artificial Neural Networks for Depositing Powders in Coating Treatment,” *Appl. Surf. Sci.*, 245, 290-303 2005.
- [172] S. Guessasma, G. Montavon, and C. Coddet, “Modeling of the APS Plasma Spray Process Using Artificial Neural Networks: Basis, Requirements and an Example,” *Comput. Mater. Sci.*, 29 (3) 315-333, 2004.

- [173] H. Cetinel, H. A. Ozyigit, L. Ozsoyeller, "Artificial neural networks modeling of mechanical property and microstructure evolution in the tempcore process", *Comput. Struct.* 80 (3-4) 213-218, 2002.
- [174] H. Cetinel, M. Toparli, L. Ozsoyeller, "A finite element based prediction of the microstructural evolution of steels subjected to the tempcore process", *Mech. Mater.* 32 (6) 339-347, 2000.
- [175] Abdoul-Fatah Kanta, Ghislain Montavon, "Artificial Neural Networks vs. Fuzzy Logic: Simple Tools to Predict and Control Complex Processes-Application to Plasma Spray Processes", *JTTEE5* 17:365-376, 2008.
- [176] T. Kohonen, "Self-Organization and Associative Memory", Springer-Verlag, New York, NY, USA, 1984.
- [177] D. B. Parker, "Artificial neural networks, an overview", *Comput.* 6 (10), 1988.
- [178] P. J. Werbos, "Generalization of back propagation with application to recurrent gas market model", *Neural Networks* 1, 339, 1988.
- [179] D. O Hebb, "The Organization of Behavior", Wiley and Sons, New York, NY, USA, 1949.
- [180] Sofiane Guessasma, Ghislain Montavon, Christian Coddet, "Modeling of the APS plasma spray process using artificial neural networks: basis, requirements and an example" *Computational Materials Science* 29, 315-333, 2004.
- [181] B. Windrow, M.E. Hoff, "Adaptative switching circuits", *IRE Wescon Conv. Rec. (Part 4)*, 96, 1960.
- [182] Leonid Innokent. et al. "Coated metal: structure and properties of metal-coating compositions", 165-168, 2002.
- [183] Roberto, Jose, Branco, Tavares, Gansert, Robert, Sampath, Sanjay, Christopher, C. Berndt, Herman, Herbert- "Solid Particle Erosion of Plasma Sprayed Ceramic Coatings", *Materials Research*, Vol. 7, No.1, 147-153, 2004.
- [184] B. K. Prasad, S. Das, A.K Jha, O.P. Modi, R. Dasgupta, A.H. Yegneswaran, "Factors Controlling the Abrasive Wear Response of a Zinc Based Alloy Silicon Carbide Particle Composite", *Composites, Part A*; Vol. 28A, 301-308, 1997.
- [185] M. S. Chua, M. Rahman, Y.S. Wong, H.T. Loh, "Determination of Optimal Cutting Conditions Using Design of Experiments and Optimization Techniques", *Int. J. Mach Tools Manuf.*, Vol. 32, No. 2, 297-305, 1993.

- [186] G. Taguchi, "Introduction to quality engineering", Tokyo: Asian Productivity Organization, 1990.
- [187] W. H. Yang, Y.S. Tarn, "Design Optimization of Cutting Parameters for Turning Operations Based on the Taguchi Method", J. Mater. Process Technol., Vol. 84, 121-129, 1998.
- [188] M. S. Phadke, "Quality engineering using Robust design", AT&T, Bell Laboratories Report. New Jersey: Prentice-Hall International Editions, 1989.
- [189] Iain Finnie, "Some Reflections on the Past and Future of Erosion", Wear, Vol. 186, No. 187, 1-10, 1995.
- [190] A.J. Sparks, I.M. Hutchings, "Transitions in Erosive Wear Behaviour of Glass Ceramic", Wear, Vol. 149, 99-110, 1991.
- [191] J. E. Ritter, "Erosion of Ceramic Materials", Trans. Tech. Publications, Zurich, Switzerland, 1992.
- [192] G. Sundarajan, M. Roy and B. Venkataraman, "Erosion Efficiency- A New Parameter to Characterize the Dominant Erosion Micromechanism", Wear, Vol. 140, 369-381, 1990.
- [193] Manish Roy, K. K. Ray and G. Sundararajan, "Erosion-oxidation interaction in Ni and Ni-20Cr alloy", Metallurgical and Materials Transactions A Vol. 32, No. 6, 1431-1451, 2001, DOI: 10.1007/s11661-001-0232-5
- [194] Lishizhou, Dong, XiangLin, "Erosion wear and Fretting Wear of Materials", Publisher of Mechanical Industry, Beijing, 1987.

List of Publications

- **Ajit Behera***, S.C. Mishra, “Dependence of Adhesion Strength of Plasma Spray on Coating Surface Properties”, Journal of Materials & Metallurgical Engineering, Volume 2, Issue 1, April 2012, Pp 23-30.
- **Ajit Behera*** and S.C Mishra, “Prediction and analysis of Deposition Efficiency of Plasma Spray Coating using Artificial Intelligence Method”, open journal of composite materials, 2012, 2, 54-60 doi:10.4236/ojcm.2012.22008.
- **Ajit Behera*** and S.C Mishra, “Fly-ash+quartz+iluminite Composite coating on Copper Substrate”, International Journal of Current Research, Manuscript Number: 1882 (Accepted).
- **Ajit Behera***, Sudeep Behera, S.C Mishra, “Analysis and prediction of Surface Roughness of plasma sprayed Mild Steel by application of soft Computing”, International Journal of Recent Scientific Research, Manuscript No- IJRSR- 472 (Accepted).
- **Ajit Behera***, Jyoti Prakash Dhal and S.C Mishra, “Porosity of plasma sprayed Mild Steel Analysis by application of soft Computing”, International Journal of Applied Physics and Mathematics (Communicated).
- **Ajit Behera***, S.C Mishra, “Improvement of Mild Steel Property by Fly-Ash+Quartz+Illminite Composite Coating”, Journal of Materials & Metallurgical Engineering (Communicated).
- **Ajit Behera***, S.C Mishra, S.S Mishra” Application of Neural Network Analysis to correlate the properties of Plasma Spray Coating”, Journal of metallurgy (Communicated).
- **Ajit Behera***, S.C Mishra, “ANN Controlled Plasma Spray Process by using Industrial waste”, Indian Journal of Engineering & Materials Sciences, (Communicated).